2023

Dissecting polarity formation in the *Drosophila* oocyte

Ana Milas

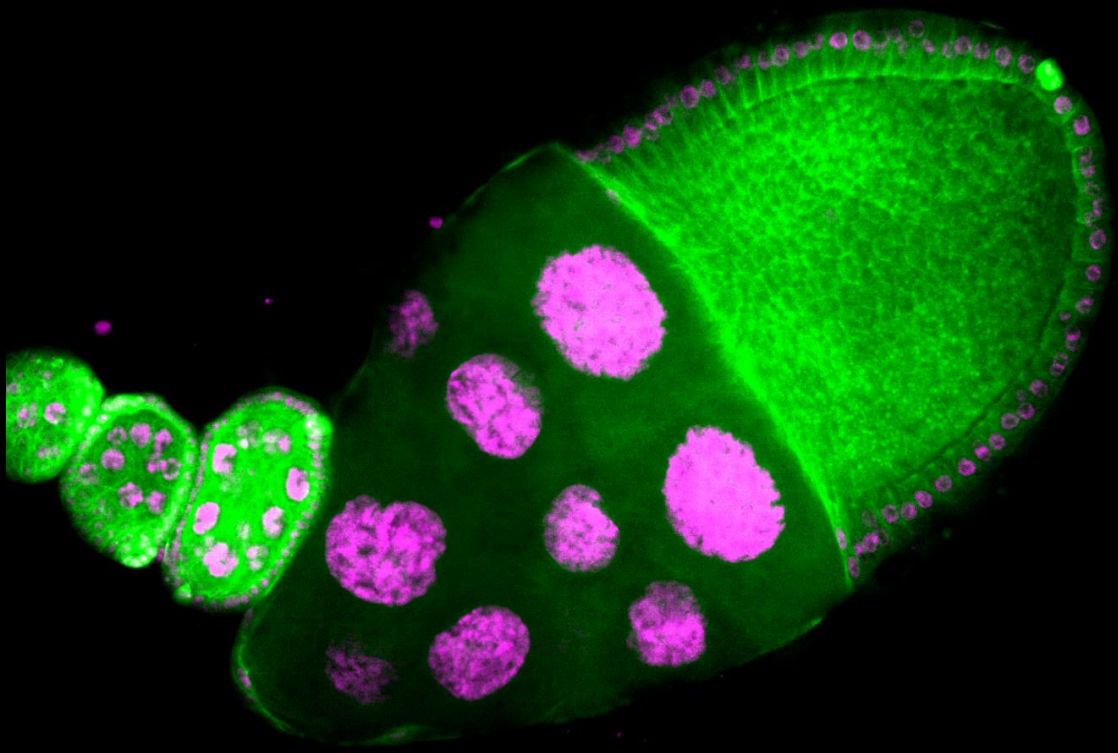

Dissertation presented to obtain the **Ph.D degree in Integrative Biology and Biomedicine**

Oeiras, January, 2023

INSTITUTO DE TECNOLOGIA QUÍMICA E BIOLÓGICA ANTÓNIO XAVIER | UNIVERSIDADE NOVA DE LISBOA

Dissecting polarity formation in the *Drosophila* oocyte

Ana Milas

Dissertation presented to obtain the Ph.D degree in Integrative Biology and Biomedicine

Instituto de Tecnologia Química e Biológica António Xavier | Universidade Nova de Lisboa

Research work coordinated by:

Oeiras, January, 2023

Financial support from Fundação para a Ciência e Tecnologia (FCT), through grant 2020.04666.BD awarded to Ana Milas, and Human Frontiers Science Program (HFSP), through grant RGY0083/2016 awarded to Ivo Telley.

Summary

The polarization of cells is a prerequisite for many fundamental biological processes, such as asymmetric cell division, neuronal polarization, and morphogenesis. In *Drosophila melanogaster*, both main body axes are established during oogenesis through polarization of the oocyte and as a result of crosstalk between the oocyte and surrounding cells.

According to the current view, the anterior-posterior body axis is established when posterior follicle cells (PFCs) send an unknown signal to the oocyte. This signal triggers asymmetry of the Par network in the oocyte: Par-1 and Lgl localize to the posterior, while Bazooka/Par-6/aPKC complex localizes to the anterolateral cortex. Par asymmetry induces reorganization of the microtubule cytoskeleton, which enables proper delivery of *bicoid* and *oskar* mRNAs to the opposite poles of the oocyte.

In recent years, the mechanisms of microtubule network polarization and mRNA transport have been well characterized using live imaging. However, our knowledge of upstream events - the triggering and maintenance of Par polarity - is mainly based on classical genetic experiments or inferred from the results in other model organisms and tissues. In the work presented in this thesis, we aimed to dissect the mechanisms of Par polarity establishment and maintenance in the oocyte using live imaging combined with physical manipulations and laser ablation.

In Chapter 2, we present an assay that enabled us to cut off the communication between the oocyte and its surrounding by ligating the egg chamber. By segregating the egg chamber into posterior and anterior compartments, we found that Bazooka localized to the posterior of the oocyte immediately following the ligation. However, rapid exclusion of the protein followed, thus re-establishing asymmetry in this compartment surrounded only by follicle cells. Interestingly, polar cells - a specialized

pair of PFCs - marked the center of exclusion. The posterior polarity protein, Par-1, was redistributed such that the signal's peak corresponded to the position of the polar cells. These results suggested that PFCs are involved in re-establishing the asymmetry following the perturbation. We hypothesized that PFCs maintain Par asymmetry in unperturbed oocytes throughout oogenesis.

In Chapter 3, we built upon this hypothesis and tested the maintenance role of PFCs by mechanically detaching PFCs from the oocyte. This perturbation caused premature posterior accumulation of Bazooka. In addition, we show that there is a tight cell contact between the oocyte and the PFCs until the late stages of oogenesis. In contrast, a visible intercellular gap exists between the oocyte and the follicle cells surrounding it on the lateral side. The posterior contact is lost during late oogenesis, followed by accumulation of Bazooka at the posterior of the oocyte. Furthermore, inhibition of posterior fate determination caused the gap to spread all around the oocyte cortex, disrupting the Par polarity in the oocyte. We conclude that contact of PFCs with the oocyte cortex maintains the Par polarity throughout oogenesis.

Finally, in Chapter 4, we used laser ablation to probe the maintenance role of PFCs further and test the current understanding of the interactions between Par proteins in mid-oogenesis. Laser ablation of PFCs resulted in the localization of Bazooka to the posterior membrane. However, the accumulation of Bazooka was limited to the membrane in contact with the ablated follicle cells, meaning that the intact PFCs maintained the ability to exclude Bazooka. Accumulation of Bazooka occurred before Par-1 removal, suggesting that the phosphorylation of Bazooka by Par-1 is insufficient to maintain Bazooka exclusion in the absence of PFC contact. Par-1 delocalized from the posterior after nucleation of Bazooka, followed by exclusion of *oskar* mRNA and local accumulation of microtubules. We conclude that the mutual antagonism between Par proteins is insufficient

to maintain the main body axis polarity in the oocyte. Instead, PFCs maintain both Bazooka exclusion and Par-1 enrichment at the posterior of the oocyte with a cell-size precision. This enables the anchoring of *oskar* mRNA to the posterior of the oocyte and the polarization of the microtubule network.

Sumário

A polarização das células é um pré-requisito para muitos processos biológicos fundamentais, tais como a divisão celular assimétrica, polarização neuronal e, morfogénese. Em *Drosophila melanogaster*, ambos os eixos corporais principais são estabelecidos durante a oogénese devido à polarização do oócito e como resultado do cruzamento de informação entre o oócito e as células circundantes.

De acordo com a visão atual, o eixo corporal anterior-posterior é estabelecido quando as células foliculares posteriores (PFC) enviam um sinal, desconhecido, para o oócito. Este sinal desencadeia a assimetria da rede de proteínas Par no oócito: Par-1 e Lgl localizam-se no polo posterior e o complexo Bazooka/Par-6/aPKC localiza-se no córtex ântero-lateral. Esta assimetria induz a reorganização do citoesqueleto de microtúbulos, permitindo o transporte e localização dos mRNA *bicoid* e *oskar* em polos opostos do oócito.

Nos últimos anos, os mecanismos de polarização da rede de microtúbulos e o transporte de mRNA têm sido bem caracterizados através do estudo e visualização de células vivas, em tempo real. No entanto, o nosso conhecimento dos eventos a montante - o desencadeamento e manutenção da polaridade Par - baseia-se principalmente em experiências de genética clássica ou inferidas a partir dos resultados obtidos noutros organismos e tecidos modelo. No trabalho apresentado nesta tese, o nosso objetivo era dissecar os mecanismos de estabelecimento e manutenção da polaridade Par no oócito através de imagens de células vivas, em tempo real, combinadas com manipulações físicas e ablação por laser.

No Capítulo 2, apresentamos um ensaio que nos permitiu anular a comunicação entre o oócito e a sua vizinhança laqueando a câmara do oócito. Ao segregar a câmara do oócito em compartimentos posterior e

anterior, verificou-se que a proteína Bazooka se localizou na parte posterior do oócito, imediatamente após a laqueação. No entanto, seguiu-se uma rápida exclusão da proteína, restabelecendo a assimetria neste compartimento rodeado apenas por células foliculares. Curiosamente, um par especializado de PFC- as células polares - marcaram o centro desta exclusão. A proteína de polaridade posterior, Par-1, foi redistribuída e a maior intensidade do sinal desta correspondeu à posição das células polares. Estes resultados sugeriram que as PFC estão envolvidas no restabelecimento da assimetria após a perturbação. Colocamos, então, a hipótese que as PFC mantêm a assimetria de Par em oócitos, não perturbados, durante a oogénese.

No Capítulo 3, baseámo-nos nesta hipótese e testámos o papel de manutenção das PFC, separando-as mecanicamente do oócito. Esta perturbação causou a acumulação prematura de Bazooka no pólo posterior. Além disso, mostramos que existe um contacto celular estreito entre o oócito e as PFC até às fases finais da oogénese. Em contraste, existe um hiato intercelular visível entre o oócito e as células foliculares que o rodeiam no lado lateral. O contacto posterior é perdido durante a oogénese tardia, seguido pela acumulação de Bazooka na parte posterior do oócito. Além disso, a inibição da determinação do polo posterior fez com que a fenda se espalhasse em redor do córtex do oócito, perturbando a polaridade Par no oócito. Concluímos que o contacto das PFC com o córtex do oócito mantém a polaridade Par durante a oogénese.

Finalmente, no Capítulo 4, utilizámos a ablação por laser para aprofundar o papel de manutenção das PFC e compreender as interações entre as proteínas Par na oogénese intermédia. A ablação a laser das PFC resultou na localização de Bazooka na membrana posterior. No entanto, a acumulação de Bazooka foi limitada à membrana em contacto com as células foliculares ablacionadas, o que significa que

as PFC intactas mantiveram a capacidade de excluir Bazooka. A acumulação de Bazooka ocorreu antes da remoção da Par-1, o que sugere que a fosforilação da Bazooka pela Par-1 é insuficiente para manter a exclusão da Bazooka na ausência do contacto com as PFC. A Par-1 é deslocalizada do polo posterior após a nucleação de Bazooka, seguido da exclusão do mRNA *oskar* e da acumulação local de microtúbulos. Concluímos que o antagonismo mútuo entre as proteínas Par é insuficiente para manter a polaridade do eixo corporal principal no oócito. Em vez disso, as PFC mantêm tanto a exclusão de Bazooka como o enriquecimento de Par-1 na parte posterior do oócito com elevada precisão. Isto permite a ancoragem do mRNA *oskar* ao polo posterior do oócito e a polarização da rede de microtúbulos.

Contents

1. Chapter 1: General introduction

Parts of this chapter are adapted from:

A. Milas, I. A. Telley. Polarity Events in the *Drosophila melanogaster* Oocyte. *Frontiers in Cell and Developmental Biology*, 10:1-13, 2022

1.1. Par proteins are key players in cell polarization

1.1.1 Par proteins are conserved across metazoa

Polarization of the cells is required for many fundamental biological processes, such as asymmetric cell division (Knoblich, 2008; Venkei and Yamashita, 2018), neuronal polarization (Schelski and Bradke, 2017), cell migration (Etienne-Manneville, 2008), morphogenesis (Veeman and McDonald, 2016; Macara and McCaffrey, 2013), and epithelial tissue formation (Cereijido et al., 2004; Roignot et al., 2013; Rodriguez-Boulan and Macara, 2014). A network of Partitioning-defective (Par) proteins establishes and controls cell polarity in all of these processes (Neumüller and Knoblich, 2009; Sunchu and Cabernard, 2020; Insolera et al., 2011; Goldstein and Macara, 2007; Lang and Munro, 2017). A common feature of Par networks in different contexts is the establishment of mutually exclusive domains when some of the Par proteins localize asymmetrically at the cell cortex (Figure 1.1).

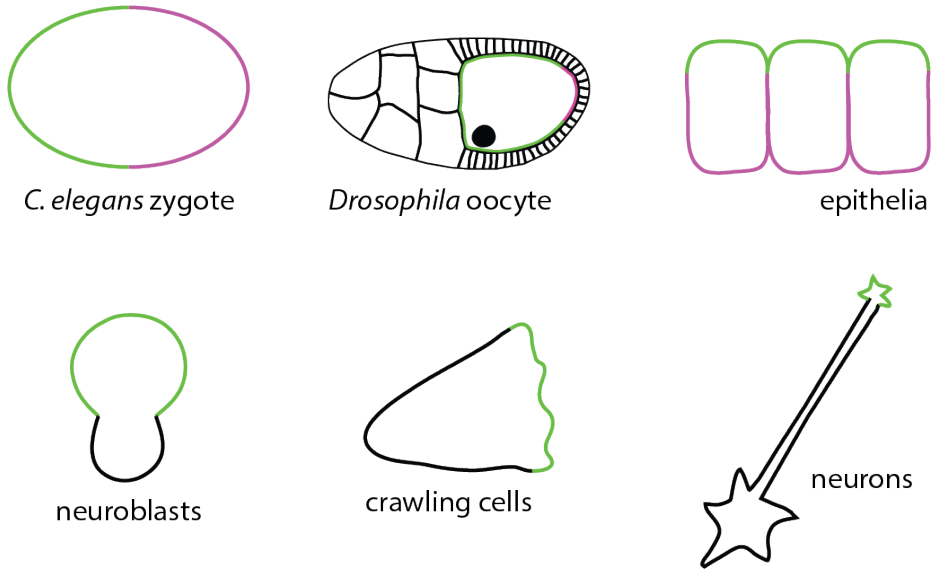

Figure 1.1. **Par proteins are key players in cell polarity in multiple systems.** A common feature of Par networks in all systems is asymmetric localization of some of the components of the network. Par-3 and/or Par-6 localize to the green-colored regions, while Par-1 and/or Par-2 localize to the magenta-colored regions. Adapted from (Goldstein and Macara, 2007)

The *par* genes were first identified in classical screening experiments for mutations that affect asymmetric cell division in *Caenorhabditis elegans* zygote (Kemphues et al., 1988). In total, six *par* genes were identified (Levitan et al., 1994; Etemad-Moghadam et al., 1995; Guo and Kemphues, 1995; Hung and Kemphues, 1999; Watts et al., 2000; Morton et al., 2002). In *C. elegans* zygote, asymmetry of the Par proteins is established following fertilization: the kinase Par-1 and the RING domain protein Par-2 localize to the posterior membrane, while the oligomeric scaffold Par-3 and the adaptor Par-6 localize to the anterior (Etemad-Moghadam et al., 1995; Guo and Kemphues, 1995; Boyd et al., 1996; Watts et al., 1996). The kinase Par-4 and the 14-3-3 protein Par-5 do not show polarized distribution, but their activity is important for the polarization of other Pars.

In addition to the six Par proteins that were identified in the initial

screens, several other proteins are necessary for the establishment and maintenance of the *C. elegans* zygote polarization. At the anterior, Par-3 and Par-6 form a complex with the protein kinase C (PKC-3) (Tabuse et al., 1998). Another highly conserved polarity protein, small GTPase Cdc-42, is also required at the anterior where it activates PKC-3 (Joberty et al., 2000). At the posterior, Cdc42-GTPase activating protein (CDC42-GAP), CHIN-1, and the tumor suppressor Lgl, are needed in addition to Par-1 and Par-2 (Beatty et al., 2010, 2013; Hoege et al., 2010; Kumfer et al., 2010).

The polarization of any cell happens in two phases - the establishment and the maintenance. Before the polarity of the *C. elegans* zygote is established, Par-3, Par-6, and PKC-3 are localized all around the cortex, while the posterior Pars are cytoplasmic (Etemad-Moghadam et al., 1995; Guo and Kemphues, 1995; Boyd et al., 1996; Watts et al., 1996; Beatty et al., 2013). The symmetry is broken following fertilization when the centrosome delivered by the sperm provides a biochemical signal that inhibits the actomyosin contractility and causes a local asymmetry in cortical flow. Since Par-3, Par-6, and PKC-3 are embedded within the cortex, they are displaced from the posterior by advection allowing Par-1, Par-2, and Lgl to accumulate from the cytoplasm (Munro et al., 2004; Goehring et al., 2011; Gan and Motegi, 2021).

Once established, the polarity is maintained through mutual phosphorylation of posterior and anterior Par proteins. At the posterior, Par-1 phosphorylates Par-3 to exclude it from the membrane. Since Par-3 is a scaffold protein that recruits Par-6 and PKC-3 to the membrane, the exclusion of Par-3 also removes Par-6 and PKC-3 from the posterior. At the anterior, PKC-3 phosphorylates and excludes Par-1, Par-2, and Lgl (Hao et al., 2006; Hoege et al., 2010; Motegi et al., 2011). During the maintenance phase, several new asymmetries appear - Cdc-42 becomes enriched at the anterior, and CHIN-1 at the posterior domain.

In the years following the discovery of *par* genes, Par proteins proved to be the key players in the polarization of many other cell types in the *C. elegans*, such as epithelial and migrating cells (Nance, 2005). In 1998, the first homolog of one of the Par proteins was identified in *Drosophila melanogaster*, when cell polarization gene *bazooka* was shown to encode the homolog of Par-3 (Kuchinke et al., 1998). The other Par proteins also turned out to be highly conserved across the metazoa. The only exception is Par-2, which does not have known homologs in mammals or insects, but might have functional analogs in some organisms (Goldstein and Macara, 2007; Lang and Munro, 2017).

1.1.2 Polarity networks in *Drosophila melanogaster*

The fruit fly, *Drosophila melanogaster*, has homologs of five out of six originally identified Par proteins: Par-1, Par-3 (Bazooka in *Drosophila*), Par-4 (Lkb1), Par-5 (14-3-3ϵ) and Par-6. In addition, fly homologs of PKC-3 (atypical protein kinase C - aPKC), Cdc-42, and Lgl have been identified.

In the fly, the Par network has been best studied in the contexts of anterior-posterior polarization of the oocyte, and apico-basal polarization of the epithelia (Figure 1.2). The oocyte polarization establishes the body axes of the future embryo (Riechmann and Ephrussi, 2001), while the formation of the apico-basal axis in epithelial cells is the foundation for compartmentalization, organ formation, and physical separation of the animal body from the environment (Cereijido et al., 2004).

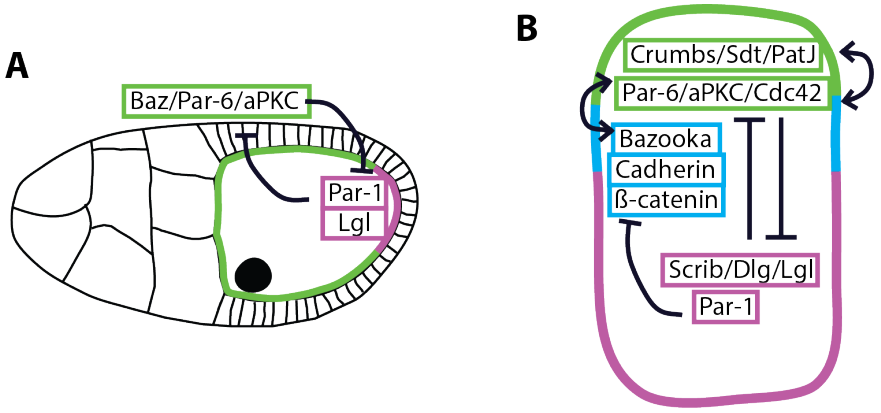

Figure 1.2. **Localization and interaction between polarity factors in *Drosophila* tissues. (A)** In the oocyte, the polarity is maintained through mutual antagonism between the anterolateral (green) and posterior (magenta) factors. **(B)** In the epithelia, there is positive feedback between the two apical modules (green). In addition, apical factors show mutually supportive interactions with the components of the adherens junction (blue). In contrast, there is mutual antagonism between the apical and basolateral (magenta) factors.

Anterior-posterior polarization of the oocyte

As will be described in detail in section 1.2, the Par polarity in the *Drosophila* oocyte is established in response to the unidentified signal that comes from the follicle cells at the posterior of the egg chamber (González-Reyes and St Johnston, 1994; González-Reyes et al., 1995; Roth et al., 1995). Once the polarity is established, two domains are distinguishable in the oocyte: Bazooka, Par-6, aPKC, and Cdc-42 localize to the anterolateral cortex (Benton and St Johnston, 2003; Doerflinger et al., 2010; Morais-de-Sá et al., 2014; Leibfried et al., 2013), while Par-1 and Lgl are found at the posterior (Shulman et al., 2000; Tomancak et al., 2000; Tian and Deng, 2008; Doerflinger et al., 2010) (Figure 1.2A).

Bazooka probably binds directly to the membrane, and recruits aPKC and Par-6. Phosphorylation of Bazooka by Par-1 reduces its affinity to the membrane, which removes the Bazooka/aPKC/Par-6 complex from the

posterior cortex. On the other hand, aPKC phosphorylates both Par-1 and Lgl to remove them from the anterolateral cortex (St Johnston and Ahringer, 2010). The role of Lgl in the polarity of the oocyte is not completely understood, it seems to contribute to the exclusion of Bazooka from the posterior, but the mechanism of its action is not clear (Tian and Deng, 2008; Morais-de-Sá et al., 2014). Similarly, the role of Cdc-42 in oocyte polarization has not been thoroughly studied, but, based on its localization and homology with *C. elegans* Cdc-42, it has been suggested that it activates aPKC (Leibfried et al., 2013).

Apico-basal polarization of the epithelia

In *Drosophila*, epithelial polarity is usually studied in embryonic epithelia, larval imaginal discs, and the follicle cells of the egg chamber. During polarization, the membrane of the epithelial cells is partitioned into the apical and basolateral domains. The apical membrane faces the external environment, the lateral membrane is in contact with the neighboring cells, while the basal membrane contacts the basement membrane. Cohesion between the cells is mediated by adherens junctions, which are located at the boundary between the apical and basolateral membrane (Laprise and Tepass, 2011).

The molecular circuitry that establishes and maintains the polarity in epithelia is much more complex than in *C. elegans* zygote or *Drosophila* oocyte. There are several distinct modules defining both apical and basolateral domains. These modules act somewhat redundantly to maintain mutual antagonism between the two domains during specific developmental stages or metabolic conditions (Laprise and Tepass, 2011). One of the apical modules consists of Par-6/aPKC and Cdc-42, which are also present in many other tissues (Laprise and Tepass, 2011; Suzuki and Ohno, 2006). The other consists of the Crumbs complex, which is composed of Crumbs, Stardust, and PatJ (Bulgakova and Knust,

2009). In contrast to the Par proteins, which contribute to polarity in many cell types, the Crumbs complex is specific to epithelia. However, like Par proteins, it is highly conserved in both invertebrates and vertebrates (Bachmann et al., 2001; Hong et al., 2001; Shin et al., 2005; Bulgakova and Knust, 2009). The basolateral domain of epithelia is enriched in Par-1 (Doerflinger et al., 2003; Vaccari et al., 2005) and the Scribble complex which consists of Scribble, Discs Large, and Lgl (Bilder and Perrimon, 2000; Bilder et al., 2003). Finally, Bazooka localizes to the adherens junctions and established the boundary between the apical and basolateral domain (Harris and Peifer, 2005) (Figure 1.2B).

The first step in the polarization of the epithelia is the localization of Bazooka to the future boundary between the apical and basolateral membrane through the interaction with E-cadherin and β-catenin (Wei et al., 2005; McGill et al., 2009). Bazooka then recruits the components of the adherens junction, as well as the apical polarity regulators to facilitate their accumulation to the apical membrane (Achilleos et al., 2010; Franz and Riechmann, 2010; Harris and Peifer, 2005; Krahn et al., 2010a; McKinley et al., 2012).

While the processes of polarity establishment and maintenance differ in many details between the epithelia and the oocyte, the basic phosphorylation events that are at the core of the mutual antagonism are preserved. Like in the oocyte, Par-1 phosphorylates Bazooka to exclude it from the basolateral membrane (Bayraktar et al., 2006; Benton and St Johnston, 2003; McKinley et al., 2012), while aPKC phosphorylates basolateral polarity regulators (Gamblin et al., 2014; Suzuki and Ohno, 2006). As opposed to the egg or the oocyte, Bazooka does not co-localize with Par-6/aPKC in the fully polarized epithelia (Harris and Peifer, 2005). Interestingly, apical exclusion of Bazooka is facilitated by its phosphorylation by aPKC, which reduces their mutual affinity. This mechanism of Bazooka exclusion is dependent on Crumbs, which makes

it specific to the epithelia (Morais-de-Sá et al., 2010; Walther and Pichaud, 2010). In addition to Par-1, the components of the Scribble module are involved in excluding the apical factors from the basolateral membrane (Bilder and Perrimon, 2000; Bilder et al., 2003; Tanentzapf and Tepass, 2003)

1.1.3 The molecular basis of cell polarity

For polarity proteins to be able to define domains of the polarized cell, they have to be targeted to the membrane.

One way in which polarity proteins accomplish this is by binding transmembrane proteins that are embedded in the membrane. Examples of the transmembrane proteins that are involved in polarization are Crumbs and E-cadherin which play a role in epithelial polarization.

More recently, it has become evident that lipids do not play only a passive role as building blocks of membranes, but can engage in interactions with components of polarity networks. Membrane phospholipids can themselves be asymmetrically distributed in the plasma membrane, thereby directly specifying membrane domains. This is the mode in which Cdc-42 asymmetry is established in yeast (Fairn et al., 2011) and mammalian epithelia (Martin-Belmonte et al., 2007). More often, phospholipids are evenly distributed in the membrane, while asymmetry is maintained by a local change in the charge of polarity proteins through phosphorylation.

Membrane targeting of polarity proteins through interaction with membrane lipids occurs either indirectly through effector proteins that bind phospholipids, or by direct interaction with phospholipids. The current evidence suggests that Par-1, Par-3, and Lgl can all directly bind the membrane lipids (Hammond and Hong, 2018).

The main lipids involved in the membrane targeting of polarity proteins are phosphoinositides, which also regulate numerous other cellular

processes, such as gating of ion channels, regulation of cellular adhesion, motility, and cytokinesis (Shewan et al., 2011; Balla, 2013). These lipids are derived through phosphorylation of one or more of the three hydroxylated carbons in phosphatidylinositol by various lipid kinases. Phosphorylation increases negative charge enabling positively charged domains of polarity proteins to interact with lipids through electrostatic interactions.

The most abundant phosphoinositide in the plasma membrane and the one that is primarily involved in the polarization of cells is phosphatidylinositol 4,5-bisphosphate (PI(4,5)P2). PI(4,5)P2 can be derived either by phosphorylation of PI4P (phosphatidylinositol 4-phosphate) by PIP5K (phosphatidylinositol-4-phosphate 5-kinase), or by phosphorylation of PI5P (phosphatidylinositol 5-phosphate) by PIP4K (phosphatidylinositol-5-phosphate 4-kinase) (Balla, 2013; Hammond and Hong, 2018).

Membrane targeting of Lgl

Polarity proteins can bind phosphoinositides in several ways. One way is through positively charged polybasic domains. This mode of membrane targeting has been shown for Lgl in *Drosophila* epithelia (Dong et al., 2015) as well as in both mammalian and *Drosophila* cell culture (Bailey and Prehoda, 2015; Dong et al., 2015). Lgl primarily binds PI(4,5)P2 through the polybasic domain that contains all the phosphorylatable serines in Lgl. Membrane targeting is regulated through phosphorylation of these residues by aPKC which neutralizes the positive charges required to bind phosphoinositides (Figure 1.3) (Almagor et al., 2019; Betschinger et al., 2003; Plant et al., 2003; Hutterer et al., 2004). The exact mode of membrane targeting of Lgl in *Drosophila* oocyte remains to be elucidated. However, the mode is likely equivalent to the one described since the non-phosphorylatable form of Lgl localizes uniformly at the oocyte cortex

(Tian and Deng, 2008).

Miranda and Numb, two polarity proteins that orient asymmetric cell division of *Drosophila* neuroblasts, also bind phosphoinositides through polybasic domains, which are located near their amino terminus (Bailey and Prehoda, 2015; Dong et al., 2015). Phosphorylation by aPKC is needed to exclude both Miranda and Numb from the apical membrane (Atwood and Prehoda, 2009; Wirtz-Peitz et al., 2008). However, the precise mechanism of exclusion is not clear since most of the aPKC phosphorylation sites in both of the proteins lay outside of the polybasic domain (Atwood and Prehoda, 2009; Nishimura and Kaibuchi, 2007; Smith et al., 2007; Hammond and Hong, 2018).

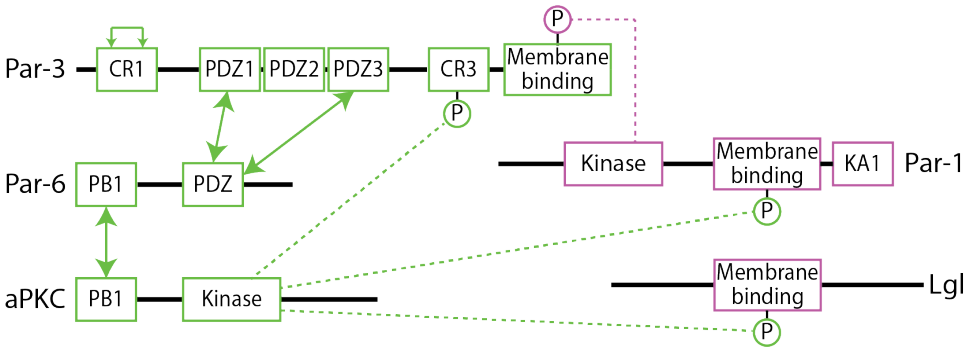

Figure 1.3. **Molecular interactions between polarity proteins.** Arrows indicate direct protein-protein interactions, while dotted lines indicate phosphorylation events. aPKC phosphorylates membrane binding domains of both Par-1 and Lgl, while Par-1 phosphorylates membrane binding domain of Par-3. Par-6 interacts with Par-3 through the binding between PDZ domains. Par-6 and aPKC bind through PB1 domains

Membrane targeting of Par-1

Contrary to Lgl, Miranda, and Numb; two Par proteins, Par-1 and Par-3/Bazooka, do not have polybasic domains. However, there is evidence

that both of these proteins can directly bind phosphoinositides.

Mammalian Par-1 binds membrane through its conserved KA1-domain, which binds a broad array of negatively charged phospholipids including phosphoinositides and phosphatidylserine (Moravcevic et al., 2010; Göransson et al., 2006). Phosphorylation of mammalian Par-1 by aPKC excludes it from the membrane (Hurov et al., 2004; Suzuki et al., 2004). Phosphorylation probably does not act by changing the charge of the KA1-domain, but by generating a 14-3-3 binding site, which is bound by Par-5 to mask the KA1-domain (Suzuki et al., 2004; Göransson et al., 2006).

In *Drosophila*, the N1S isoform of Par-1 was shown to be sufficient to maintain polarity in both oocyte and epithelia (Doerflinger et al., 2006). However, this isoform does not have a KA-1 domain (Shulman et al., 2000). Instead, the carboxyl terminus of the N1S isoform is necessary and sufficient for Par-1-N1S membrane localization (Figure 1.3)(Doerflinger et al., 2006; Vaccari et al., 2005). It is still unknown how this region facilitates interaction with the membrane, and how phosphorylation of Par-1 by aPKC (Doerflinger et al., 2010) disrupts this interaction.

Membrane targeting of Par-3/Bazooka

Mammalian and *Drosophila* Par-3 also seem to use different domains for membrane binding. Mammalian Par-3 binds to phosphoinositides through its second PDZ domain which contains conserved Arg and Lys residues (Wu et al., 2007). However, Bazooka does not require a PDZ domain for membrane binding. Instead, a conserved region in the C-terminal part is necessary and sufficient for membrane targeting of Bazooka in the oocyte, epithelia, neuroblasts, and S2 cells (Krahn et al., 2010b). This region binds PI(4,5)P2 liposomes *in vitro* (Krahn et al., 2010b). *In vivo*, PI(4,5)P2 is produced by PI4P5 kinase Skittles (SKTL), which is necessary for polarization of both oocyte and epithelia (Gervais

et al., 2008; Claret et al., 2014). The membrane-binding region of Bazooka contains Par-1 phosphorylation sites (Figure 1.3) (Krahn et al., 2010b). However, phosphorylation alone is not sufficient to prevent Bazooka from binding to the membrane. Instead, Par-1 phosphorylation generates 14-3-3 binding site that is recognized by Par-5 (Benton et al., 2002; Benton and St Johnston, 2003). By binding to Bazooka, Par-5 probably masks its phospholipid-binding region and sequesters it to the cytosol (Hammond and Hong, 2018).

Protein-protein interactions within Bazooka/aPKC/Par-6 complex

Par-6/aPKC complex does not bind the membrane directly, but through the interaction with other proteins. In these interactions, Par-6 acts as an adaptor that binds both aPKC and the membrane-binding protein. The interaction between Par-6 and aPKC in *Drosophila* complex is not completely resolved, but mammalian homologs of Par-6 and aPKC dimerize through their N-terminal PB1 (Phox and Bem1) domains (Figure 1.3) (Hirano et al., 2005).

In epithelia, the Par-6/aPKC complex primarily binds the transmembrane protein Crumbs through the PDZ domain of Par-6 (Hurd et al., 2003). In the oocyte, where there is no Crumbs, Par-6 binds to Bazooka. Recent structural analysis of the interaction between Bazooka and Par-6 in *Drosophila* identified PDZ domain-binding motif in Par-6, which can bind both PDZ1 and PDZ3 domains of Bazooka. This motif is essential for interaction *in vitro* and in *Drosophila* cell culture (Renschler et al., 2018).

1.2. Polarity in the context of *Drosophila* oogenesis

1.2.1 Architecture of the ovary and the timeline of oogeneisis

Drosophila Melanogaster oogenesis is a useful model to study many aspects of cell and developmental biology, such as cell cycle control, cell differentiation, migration, and polarization. This is because of the genetic tractability of *Drosophila*, as well as the practical aspects of oogenesis itself. The ovary is dispensable for survival, which makes it amenable to experimental manipulation. Additionally, it is the largest organ, while the oocyte is the largest cell of the fly (Bastock and St Johnston, 2008).

Each fly has two ovaries, which are composed of 16-20 ovarioles. Ovarioles are structures composed of the germarium at the anterior tip, and sequentially more mature egg chambers towards the posterior (Figure 1.4) (Spradling, 1993). Germarium hosts germline and somatic stem cells, which divide to give rise to a variety of cell types composing the egg chamber. Germline stem cells derive nurse cells and the oocyte, while somatic stem cells produce follicle cells. Each egg chamber contains one oocyte and 15 nurse cells surrounded by a layer of somatic follicle cells. Inside the ovariole, egg chambers are mutually connected by somatic stalk cells.

The germarium has been divided into 4 regions based on the developmental stage of the germline cyst - regions 1, 2a, 2b, and 3. After three days of development, the egg chamber buds from the germarium at region 3, marking stage 1 of the egg chamber development. During the next seven days of development, the egg chamber goes through 14 stages of maturation, which have been determined based on the morphology of the egg chamber (Spradling, 1993).

During oogenesis, both anterior-posterior and dorsal-ventral axes of the future embryo are determined. Several polarization steps need to happen in the course of oogenesis for a mature egg to have properly specified axes

(Figure 1.4). If one of these events fails, the system loses one or both axes of asymmetry (Roth and Lynch, 2009).

Oogenesis starts in region 1 of the germarium where germline stem cell divides to produce cystoblast. The cystoblast will divide four times to produce a 16-cell cyst, which will enter region 2a of the germarium. Starting at region 2b, one of the cells will start accumulating oocyte-specific markers showing clear differentiation into the oocyte. The selection of one of the cells in the cyst to become the oocyte is the first symmetry-breaking step of oogenesis. Although it is only in region 2b that differentiation of the oocyte becomes clear, there is evidence suggesting that oocyte selection occurs already at the first division of cystoblast, in region 1 (section 1.2.2).

In region 2b follicle cells start surrounding the cyst and play important role in the next polarization event: positioning of the oocyte to the posterior of the egg chamber (section 1.2.3). Positioning of the oocyte is accompanied by budding of the egg chamber from the germarium and first polarization of the oocyte in region 3 (section 1.2.4).

The next two polarization events happen during mid-oogenesis and require communication between the oocyte and follicle cells. First, the oocyte sends a signal to follicle cells at the posterior to induce posterior fate (section 1.2.5). Next, these cells send a signal back to the oocyte to induce the establishment of both body axes (section 1.2.6). The establishment of the anterior-posterior body axis is achieved through polarization of the Par network. Par network asymmetry will repolarize microtubule cytoskeleton, which will enable proper localization of *oskar* and *bicoid* mRNAs (section 1.2.8). Additionally, the signal from posterior follicle cells will induce migration of the oocyte nucleus, which will define the dorsal-ventral axis of the future embryo (section 1.2.7).

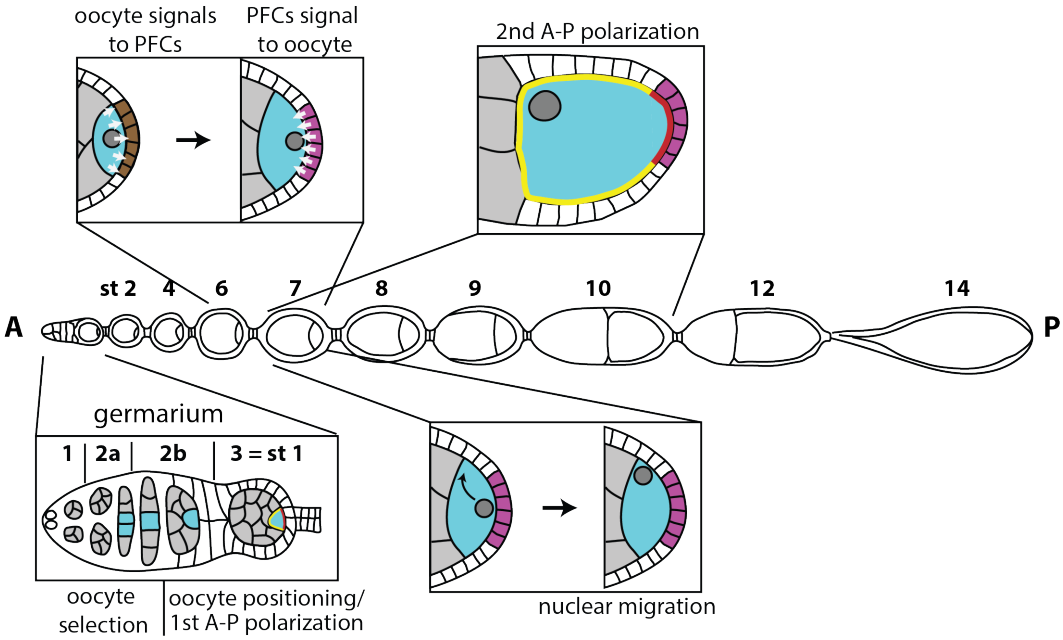

Figure 1.4. **Overview of polarization events during *Drosophila* oogenesis.** Oogenesis occurs inside ovarioles, structures composed of the germarium at the anterior tip (A), and sequentially more mature egg chambers towards the posterior (P). A first polarity event happens in the germarium when one of the cells in the germline cyst (grey) is selected to become the oocyte (blue). Next, the oocyte moves to the posterior of the germline cyst, and the egg chamber buds from the germarium, marking stage 1 of oogenesis. Around the same time, the oocyte cytoplasm becomes temporarily polarized, with defined anterior (yellow) and posterior (red) domains. At stage 6, the oocyte signals to the follicle cells at the posterior (brown), which causes them to adopt posterior follicle cell fate (magenta). At stage 7, posterior follicle cells (PFCs) signal back to the oocyte. This signal causes migration of the oocyte nucleus to the anterior of the oocyte at stage 7 and triggers a sequence of events that lead to anterior-posterior polarization of the oocyte between stages 7 and 10.

1.2.2 Oocyte selection

In region 1 of the germarium, germline stem cells divide asymmetrically to produce another stem cell and daughter cell called cystoblast (Fuller and

Spradling, 2007). This cell division is oriented perpendicular to the stem cell niche so that the daughter stem cell stays in the niche. Cystoblast will go through four rounds of incomplete cell divisions, giving rise to a cyst of 16 cells, which are called cystocytes. Due to these cell divisions being incomplete, cystocytes remain connected through cytoplasmic bridges called ring canals. Two cystocytes have four, two have three, four have two, and eight have one ring canal (Spradling, 1993). Two cells with four ring canals are called pro-oocytes, and one of them will differentiate into the oocyte. The other 15 cells in the cyst become nurse cells, which transport mRNAs, proteins, and nutrients to the oocyte through ring canals (Figure 1.5).

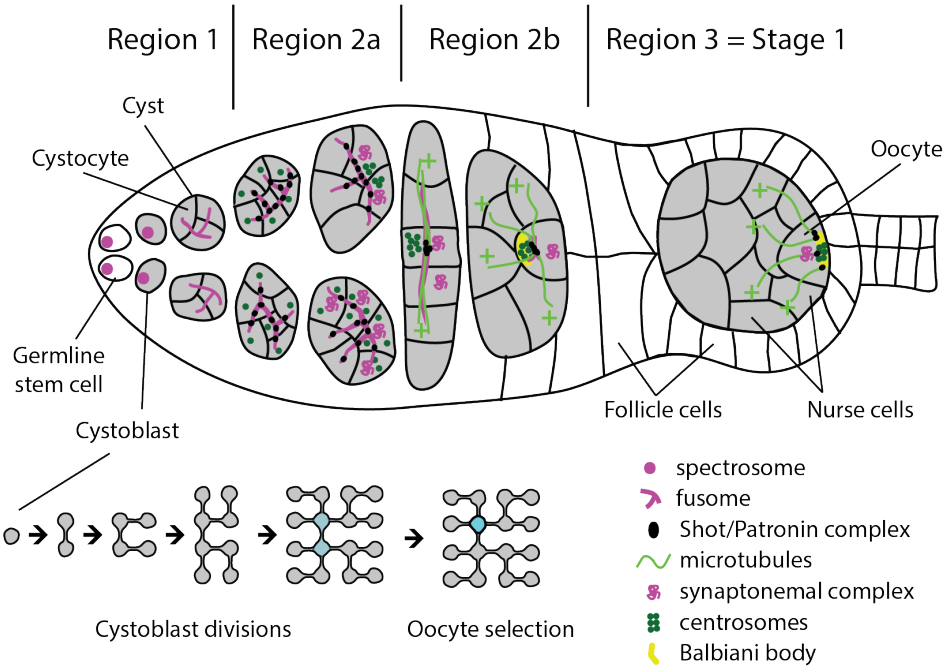

Figure 1.5. **Schematic of a germarium illustrating cellular configurations and polarity events in regions 1–3**. Germline stem cells divide asymmetrically and generate a cystoblast. Subsequent divisions occur with incomplete cytokinesis, leaving the cystocytes connected by ring canals.

continues on next page

Figure 1.5. *continued from previous page*

The two cystocytes with the most connections become pro-oocytes. Both pro-oocytes, as well as several cells with three ring canals, enter meiosis I and accumulate synaptonemal complex in region 2a. By the end of region 2b, only the oocyte remains in meiosis, while all other cells in the cyst start endoreplication and become nurse cells. Germline stem cells and cystoblasts contain spectrosome which develops into the fusome, connecting cells inside the cyst. At region 2a, the Shot/Patronin complex starts accumulating along the fusome and acts as a microtubule-organizing center (MTOC). The cell with the most fusome accumulates the most Shot/Patronin complex and the largest number of microtubule minus-ends. Oocyte determinants, including centrosomes and mRNAs, are preferentially delivered to this cell, causing it to adopt oocyte fate. In region 2b, oocyte determinants accumulate at the anterior of the oocyte and form the Balbiani body. At stage 3, MTOC and Balbiani body migrate from the anterior to the posterior of the oocyte to define the posterior cortical domain. Around the same time, the oocyte adheres to the follicle cells at the posterior of the germarium, which positions it to the posterior of the germline cyst.

The identity of the oocyte is established through both nuclear and cytoplasmic events. In the nucleus, the oocyte has to arrest in the prophase of meiosis I, while the other cystocytes exit meiosis and start the endoreplication cycle. In the cytoplasm, the microtubule network needs to be polarized so that minus ends of microtubules preferentially accumulate in one of the two pro-oocytes and form a noncentrosomal microtubule organizing center (ncMTOC) (Huynh and St Johnston, 2004; Theurkauf et al., 1993). This leads to the accumulation of oocyte-specific components in this pro-oocyte through dynein-dependent transport from other cystocytes (Suter and Steward, 1991; Mach and Lehmann, 1997; McGrail and Hays, 1997; Bolívar et al., 2001; Navarro et al., 2004; Nashchekin et al., 2021). Since all subsequent steps of oocyte polarization can be traced back to this event, the selection of one of the two pro-oocytes to become the oocyte is the symmetry-breaking step of

oogenesis (Roth and Lynch, 2009).

Initially, it was proposed that both pro-oocytes are equally competent to become the oocyte. This was based on the observation that cell cycle progression in two pro-oocytes is initially indistinguishable. Both pro-oocytes, as well as several cells with three ring canals, enter meiosis I and form synaptonemal complexes between homologous chromosomes (Figure 1.5). Only as the cyst develops, further progression through meiosis is first restricted to the two pro-oocytes in region 2b, and finally to the oocyte in region 3 of the germarium. All other cells start endocycling, thus becoming nurse cells (Carpenter, 1975, 1994; Roper and Brown, 2004; Nashchekin et al., 2021).

However, increasing evidence suggests that the symmetry-breaking event of oogenesis happens already during the first division (the cystoblast division) in region 1 of the germarium. This conclusion comes from the analysis of the formation and distribution of fusome (de Cuevas and Spradling, 1998). Fusome is a germline-specific membranous branched structure that runs through the ring canals and connects all cystocytes (Lin et al., 1994). The cystoblast inherits fusome from the germline stem cell. The inherited fusome then serves to orient the cell division of the cystoblast by anchoring one pole of the spindle. After division, only one cell will have the fusome, while the other will initially lack the fusome. During interphase, a new fusome will form in the ring canal. The two fusomes will migrate to each other and fuse, which will result in one cell having the original fusome inherited from the germline stem cell, plus half of the newly formed fusome, while the other will have only half of the newly formed fusome. This asymmetric distribution of fusome will continue during the next three divisions. As a result, the cell that inherited the original fusome in the first division will end up having the largest amount of fusome (Deng and Lin, 1997; Lin and Spradling, 1995; de Cuevas and Spradling, 1998).

After observation that microtubules form along the fusome, it has been suggested that polarization of the microtubule network is a direct consequence of fusome polarity (Grieder et al., 2000). In agreement with this idea, was the observation that the *Drosophila* homolog of Spectraplakin, Short Stop (Shot), a component of the fusome, is necessary for the oocyte specification, and appears to stabilize microtubules and link them to the fusome (Roper and Brown, 2004). Recent data further supported this model by showing that Shot stabilizes microtubules by recruiting microtubule minus-end stabilizing protein Patronin to the fusome and that Patronin is necessary for oocyte specification (Nashchekin et al., 2021). Patronin stabilizes most microtubule minus-ends in the cell with the largest portion of fusome, thereby establishing a weakly polarized microtubule network. This initial asymmetry is reinforced through a positive feedback loop since dynein transports Patronin-bound microtubules from other cells into the cell that already contains most Patronin. Finally, a now highly polarized microtubule network is utilized by dynein to transport oocyte determinants into this cell (Figure 1.5) (Nashchekin et al., 2021).

If this model is correct, the cell that inherits the original fusome in the cystoblast division also accumulates most of the Patronin and eventually becomes the oocyte. In support of this idea, it was shown that centrosomes and *oskar* and *orb* mRNAs preferentially accumulate in the cell with the most fusome (Cox and Spradling, 2003; Grieder et al., 2000).

1.2.3 Positioning of the oocyte to the posterior of the egg chamber

Oocyte determination and initial steps of oocyte differentiation do not depend on the layer of follicle cells that surround the germline cyst. However, subsequent steps of polarization depend on the communication of germline with soma. In fact, proper differentiation of follicle cells into distinct subpopulations is crucial for many aspects of egg chamber

development (Merkle et al., 2020). Here, I will focus on those steps of follicle cells patterning that are essential for the establishment of the body axes. For this, three canonical pathways must be activated in follicle cells: Notch, JAK-STAT, and EGFR. These pathways are activated either through signals received from the germline or through signaling between different types of follicle cells. Once follicle cells are properly differentiated they will signal back to the germline to specify both anterior-posterior and dorsal-ventral body axis.

The first round of signaling from the germline to the soma activates Notch and JAK-STAT pathways to induce differentiation of polar and stalk follicle cells. These cells are in turn required to position the oocyte to the posterior of the egg chamber.

Before this round of signaling, follicle cells separating region 2b cyst from region 3 cyst are undifferentiated precursors of stalk/polar cells (Tworoger et al., 1999). After germline cyst in region 3 of the germarium expresses Notch ligand Delta, Notch is activated in the surrounding follicle cells. This causes precursors of stalk/polar cells that are in direct contact with the cyst to differentiate into polar cells (Figure 1.6A) (Grammont and Irvine, 2001; López-Schier and St Johnston, 2001). These polar cells will then express Unpaired which will activate JAK-STAT signaling in more anterior stalk/polar precursors leading to their differentiation into stalk cells (Figure 1.6B). Unpaired is unable to activate JAK-STAT in cells that previously received high activation of Notch. Thus, it will not act on polar cells themselves, or on follicle cells surrounding the germline cyst in region 3 (Assa-Kunik et al., 2007; Roth and Lynch, 2009).

Newly differentiated stalk cells will form stalk which directly contacts younger germline cyst in region 2b. Both follicle cells and the oocyte express high levels of DE-cadherin, which causes the oocyte to adhere to stalk cells at the posterior thereby positioning the oocyte to the posterior of the egg chamber (Figure 1.6C) (Godt and Tepass, 1998;

González-Reyes and St Johnston, 1998a; Bécam et al., 2005). Thus, in this round of signaling information is transferred from older to younger cyst through a relay mechanism to properly position the oocyte to the posterior of the egg chamber (Torres et al., 2003). Stalk cells will also contribute to the establishment of the polar cells at the posterior pole of the oocyte (Torres et al., 2003; Assa-Kunik et al., 2007). These posterior polar cells, as well as the correct positioning of the oocyte, will be crucial in later stages of oogenesis when the new round of signaling between the oocyte and posterior follicle cells takes place to establish both anterior-posterior and dorsal-ventral axis (see sections 1.2.5 and 1.2.6).

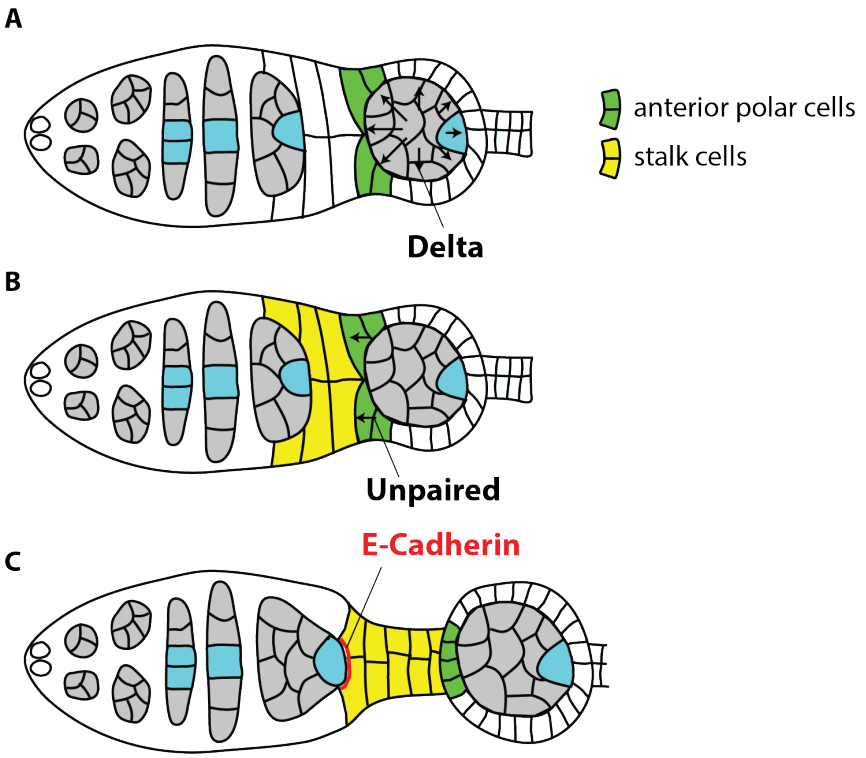

Figure 1.6. **Schematics of signaling events and cell-cell interactions required for positioning of the oocyte to the posterior of the egg chamber. (A)** Germline cyst in region 3 expresses Notch ligand Delta to induce differentiation of the anterior polar cells (green). **(B)** The polar cells express Unpaired, leading to differentiation of stalk cells (yellow). **(C)** Both follicle cells and the oocyte upregulate DE-cadherin to increase mutual adhesion and position the oocyte to the posterior of the egg chamber. Adapted from (Torres et al., 2003).

1.2.4 First round of oocyte anterior-posterior polarization

Positioning of the oocyte to the posterior of the egg chamber is accompanied by changes in the oocyte cytoplasm. At this time, components that were transported to the oocyte in the previous stage, such as centrosomes, Orb, BicD, and Egl protein, *oskar* and *orb* mRNAs, are located at the anterior of the oocyte and form a structure called Balbiani body (Cox and Spradling, 2003). Minus-ends of microtubules,

which facilitated the transport of Balbiani body components to the oocyte, are as well accumulated at the anterior. When the oocyte moves through region 3, the microtubule network is reorganized so that minus-ends move to the posterior. This is followed by the relocalization of Balbiani body components to the posterior of the oocyte where they form a tight crescent to define the posterior oocyte cortex (Figure 1.7). If this step fails, the oocyte loses its fate and becomes a nurse cell by exiting meiosis and becoming polyploid(Huynh et al., 2001b).

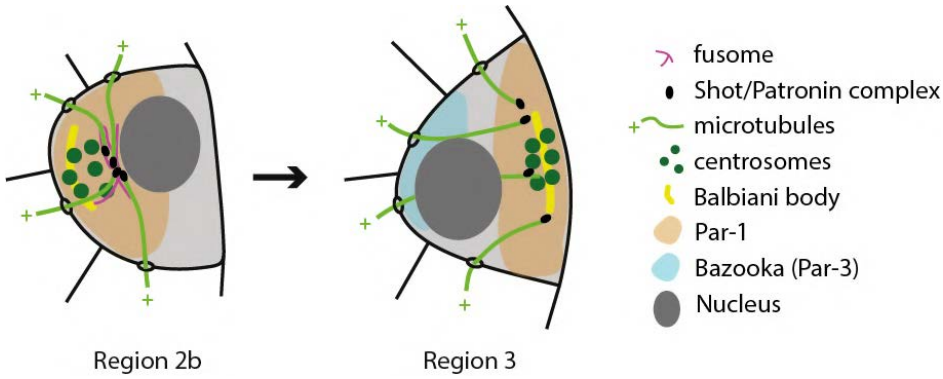

Figure 1.7. **Schematics of the first anterior-posterior polarization of the oocyte.** The microtubule cytoskeleton reorganizes in the transition from Region 2b to Region 3 so that their nucleation sites (Shot/Patronin) are now at the posterior end. This causes the Balbiani body to reposition from the anterior to the posterior. Similarly, Par-1 localization changes from anterior to posterior, while Bazooka (Par-3) shows antagonistic localization in Region 3.

Mechanisms involved in early oocyte polarization are not well understood. However, it is clear that it depends on all *Drosophila* homologs of *par* genes, as well as aPKC. When any of these genes are lacking, the oocyte de-differentiates into a nurse cell. (Huynh et al., 2001b; Cox et al., 2001a; Vaccari and Ephrussi, 2002; Huynh et al., 2001a; Cox et al., 2001b; Benton et al., 2002; Martin and St Johnston, 2003).

Initial efforts to determine the localization of Par proteins in early oogenesis showed that Bazooka and aPKC localize to the adherens

junctions that form around the ring canals (Cox et al., 2001b), while Par-1 localizes to the fusome (Cox et al., 2001a; Huynh et al., 2001b). This work also suggested that Bazooka, aPKC, and Par-1 do not depend on each other for their localization (Huynh et al., 2001a; Cox et al., 2001b). However, using isoform-specific antibodies, Vaccari and Ephrussi detected Bazooka at the anterior, and Par-1 at the posterior pole of the oocyte (Vaccari and Ephrussi, 2002). They also showed that Bazooka extends to the posterior in *par-1* mutants, while Par-1 remains anterior in *baz* mutants. This suggests that Par polarity in the early oocyte could be maintained through mutual antagonism between Baz/Par6/aPKC complex and Par-1. It is not clear what causes Par-1 relocalization to the posterior of the oocyte. But, since this event coincides with adhesive interactions between follicle cells and the oocyte, it has been suggested that a signal from follicle cells might play a role (Huynh and St Johnston, 2004; Roth and Lynch, 2009). This view has been supported by the finding that extracellular matrix receptor dystroglycan is required in the germline to polarize the oocyte at this stage (Deng et al., 2003).

It is not clear how *par* genes maintain oocyte fate, or how they are involved in the relocalization of the Balbiani body. It is also not clear if the Par network needs to be polarized at this stage to maintain oocyte fate. The microtubule network is likely a downstream target of Par polarity. This is based on the finding that microtubule minus-ends do not relocalize to the posterior cortex in any of the *par* mutants (Huynh et al., 2001b; Benton et al., 2002; Martin et al., 2003; Cox et al., 2001b; Vaccari and Ephrussi, 2002). However, Par-1 was later shown to inhibit microtubule nucleation at the posterior in later stages of oogenesis (Nashchekin et al., 2016; Parton et al., 2011) (see section 1.3.2). Therefore, it is not clear how Par-1 localization at the posterior could induce localization of minus ends at the posterior in earlier stages. In addition, posterior localization of Par-1 at this stage requires an intact microtubule network, suggesting

that microtubule polarity and Par protein localization are interdependent (Vaccari and Ephrussi, 2002).

Another possible target of the Par network is the actin cytoskeleton; *cdc42*, *apkc* and *baz* mutants show disrupted actin cytoskeleton, while treatment with Latrunculin A abolishes translocation of Orb from anterior to posterior of the oocyte (Leibfried et al., 2013). Additionally, components of the dynein/dynactin complex could also be targets of Par proteins (Huynh and St Johnston, 2004). This idea grew from the observation that translocation of proteins and centrosomes does not occur correctly in *Dhc*, *BicD* or *egl* mutants (Bolívar et al., 2001; Huynh and St Johnston, 2004; Vaccari and Ephrussi, 2002).

1.2.5 Signal from the oocyte specifies posterior follicle cells

A second round of signaling between the oocyte and follicle cells involves JAK-STAT and Notch pathways and occurs around stage 6 of oogenesis. At this point, Delta is once again upregulated in the germline and activates Notch signaling in the surrounding follicle cells (Figure 1.8) (López-Schier and St Johnston, 2001). The activation of Notch signaling has two main effects on follicle cells. First, it initiates a switch from the mitotic cycle to the endoreplication cycle, which stops the proliferation of follicle cells (López-Schier and St Johnston, 2001; Deng et al., 2001). Second, it provides competency to respond to JAK-STAT signaling that is activated by secretion of Unpaired from polar cells at the anterior and posterior ends of the egg chamber. This leads to the specification of terminal cell fate in around 200 epithelial cells at both the anterior and posterior end of the egg chamber (Xi et al., 2003).

At the anterior, Unpaired functions as a morphogen to specify three types of anterior follicle cells as a function of distance from the polar cells: border cells, stretched cells, and centripetal cells. Border cells receive the highest, and centripetal cells the lowest levels of Unpaired (Figure 1.8) (Xi

et al., 2003). Proper differentiation of anterior follicle cells is not necessary for the establishment of body axes but is important for other aspects of egg chamber development (Wu et al., 2008).

For posterior follicle cells (PFCs) to differentiate correctly, the EGF signaling pathway needs to be activated. If this does not happen, follicle cells at the posterior pole of the egg chamber will differentiate into the three types of anterior follicle cells (González-Reyes et al., 1995; Roth et al., 1995; González-Reyes and St Johnston, 1998b). EGFR in the follicle cells is activated by TGFα-like ligand Gurken (Neuman-Silberberg and Schupbach, 1993), which is secreted by the adjacent oocyte (Figure 1.8). EGFR activation leads to transcription of several target genes of EGF signaling such as *pointed* (Morimoto et al., 1996), *midline* and *H15* (Fregoso Lomas et al., 2013), with the final outcome of inducing posterior follicle cell fate. Importantly, Gurken can activate EGFR only in the layer of 200 cells that have previously received Notch and JAK-STAT signaling (Xi et al., 2003). Thus, all three pathways are needed for posterior follicle cells to correctly differentiate and be able to signal back to the oocyte to establish the anterior-posterior and dorsal-ventral body axes.

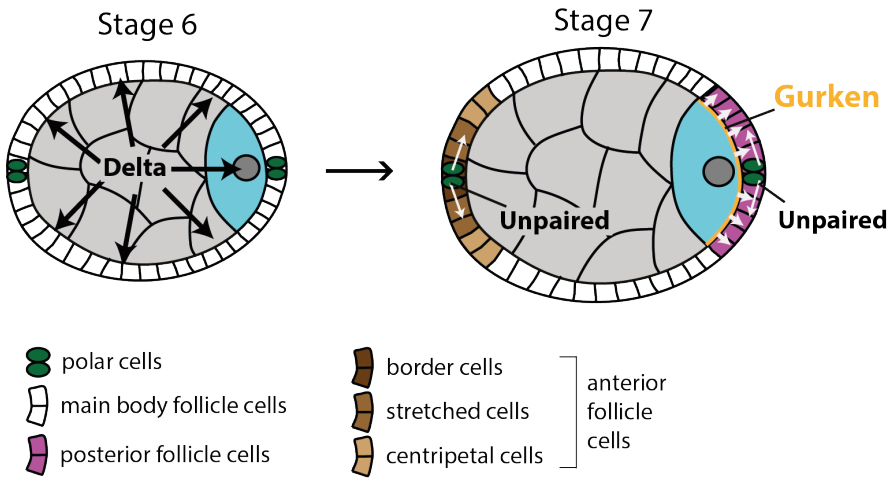

Figure 1.8. **Schematics of signaling events required for differentiation of anterior and posterior follicle cells.** At stage 6, the germline expresses Delta, which causes the surrounding layer of follicle cells to become competent to respond to JAK-STAT signaling. At stage 7, polar cells secrete Unpaired to activate the JAK-STAT pathway in surrounding follicle cells. At the anterior, Unpaired acts as a morphogen to specify three types of anterior follicle cells. At the posterior, the oocyte secretes Gurken to activate the EGF pathway in adjacent follicle cells. Activation of both JAK-STAT and EGF pathways causes these follicle cells to adopt a posterior fate.

1.2.6 Posterior follicle cells signal back to the oocyte

The role of the follicle cells in establishing anterior-posterior polarity of the oocyte has first been proposed in the early 1990s, based on the finding that *Notch* and *Delta* genes are required in follicle cells for proper localization of *oskar* and *bicoid* mRNAs in the oocyte (Ruohola et al., 1991; Ruohola-Baker et al., 1994). Next, González-Reyes and St Johnston showed that in a mutant where the oocyte is mispositioned to the center of the egg chamber, posterior follicle cells adopt anterior fate. This led them to propose a model according to which the oocyte signals to the follicle cells at the posterior to induce posterior fate, which in turn signal back to the oocyte to promote reorganization of the microtubule

cytoskeleton (González-Reyes and St Johnston, 1994). Soon after that, it was determined that the signal coming from the oocyte is Gurken, which activates EGF signaling pathway in the posterior follicle cells (González-Reyes et al., 1995; Roth et al., 1995). This work also confirmed the need for a signal coming from the posterior follicle cells, by showing that components of the EGFR network in follicle cells were necessary for proper localization of *oskar* and *bicoid* mRNA, organization of the microtubule cytoskeleton, and positioning of the nucleus (González-Reyes et al., 1995; Roth et al., 1995). However, more than 25 years after the signal coming from the oocyte has been elucidated, the molecular nature of the returning signal from the follicle cells which polarizes the oocyte remains unknown.

Several forward genetic screens for downstream targets of Notch, JAK-STAT, and EGFR in follicle cells have been performed with the aim of identifying the returning signal. However, they have not been successful in identifying the gene that encodes the signal molecule (Chen and Schüpbach, 2006; Pai et al., 2000; Sun et al., 2011; Wittes and Schüpbach, 2019). Evidence coming from the mosaic analysis of mutants in EGF and JAK-STAT signaling components suggests that the signal is transmitted in a local fashion. These studies looked at the localization of *oskar* mRNA and Staufen protein (an RNA-binding protein that can be used as a proxy for *oskar* mRNA localization (St Johnston et al., 1991)) in egg chambers in which mutant cell clones encompass only a subset of the PFCs. Both *oskar* mRNA and Staufen protein localize normally at the regions of the oocyte cortex that face wild-type PFCs, while mislocalization is observed only in regions facing mutant follicle cells (Frydman and Howard, 2001; Xi et al., 2003).

It is also unknown what the immediate target of the PFC signal is once it reaches the oocyte. The first sign of anterior-posterior polarity identified to date is the activation of non-muscle Myosin II at the posterior of the

oocyte, and this does not happen in *grk* mutants, in which PFCs do not differentiate correctly (Doerflinger et al., 2022). However, it is unclear if this change is the direct target of the signal. On the other hand, the oocyte nucleus has to migrate from the posterior to the anterior of the oocyte to define the dorsal side of the egg chamber. In *grk* mutants, the oocyte is not released from the posterior anchor and cannot migrate (Zhao et al., 2012). All the evidence suggests that a PFC signal is necessary to establish both the anterior-posterior and dorsal-ventral axis of the oocyte. However, the establishment of the two axes seems to be independent since the nucleus migrates normally in *par-1* mutants, which do not properly establish the anterior-posterior axis (Zhao et al., 2012). This also raises the possibility that the PFCs send two different signals to polarize the two main body axes.

1.2.7 Oocyte nucleus migrates to define dorsal-ventral axis

One of the downstream targets of the unidentified PFC signal is the movement of the nucleus from the posterior pole to the anterior at stage 7. Once it reaches the anterior, the nucleus is anchored to the oocyte membrane in contact with follicle cells. When the migration is completed, the nucleus accumulates high levels of *grk* mRNA and protein, and one more round of EGF signaling follows inducing dorsal fate in adjacent follicle cells (Schüpbach, 1987; Neuman-Silberberg and Schupbach, 1993; Roth et al., 1995).

In the mutants producing bi-nucleated oocytes due to a defect in cystoblast cytokinesis, both nuclei move to the anterior and induce dorsal fate in adjacent follicle cells. Additionally, both nuclei choose the position randomly with regard to each other (Roth et al., 1999). Thus, the nucleus can be localized at any point of the anterior margin, meaning that, prior to nuclear movement, the oocyte lacks any dorsal-ventral asymmetry. This makes the migration of the nucleus to the specific point of the margin a symmetry-breaking event.

The movement of the nucleus across the oocyte has been well characterized using live imaging (Zhao et al., 2012; Tissot et al., 2017). This work has shown that microtubules that nucleate at the posterior pole of the oocyte push the nucleus to the anterior. First, Zhao et al. showed that centrosomes, which are transported to the posterior at stage 1 of oogenesis, are the main nucleators of the microtubules (Zhao et al., 2012). However, a detailed 3D analysis of migratory paths showed that there are complementary mechanisms that can drive nuclear movement. While centrosomes control one migratory path, microtubule-associated protein Mud/NuMA, promotes a separate route (Tissot et al., 2017). This mechanistic redundancy provides robustness to the process of nuclear migration. In addition, it explains why centrosomes are not necessary for the correct positioning of the nucleus (Stevens et al., 2007). In the absence of centrosomes, nucleus movement is mediated either by the Mud/NuMA pathway (Tissot et al., 2017) or by acentrosomal microtubule-organizing centers that form behind the nucleus and provide the pushing force for nuclear migration (Zhao et al., 2012).

Although migration of the nucleus has been well described, it is not clear how the PFC signal triggers the movement of the nucleus. It has been suggested that the signal releases the nucleus from the posterior anchor (Zhao et al., 2012). This is based on the observation that active centrosomes are localized behind the nucleus already at stage 5 of oogenesis. These centrosomes nucleate microtubules, inducing indentation of the nucleus at the posterior. However, the nucleus is set in motion only following the PFC signal at stage 7. In *grk* mutants, the nucleus still maintains posterior indentation but fails to migrate since the pushing force remains countered by an anchor that keeps the nucleus in place (Zhao et al., 2012). Once the nucleus has reached its final position, it needs to be anchored (Guichet et al., 2001). If anchoring is omitted, the nucleus is found in the middle of the oocyte, which has been referred to as

a floating phenotype (Bernard et al., 2018). Not much is known about the mechanisms of the nucleus anchoring. However, microtubules play a role since a floating phenotype is observed when microtubules are depolymerized after the migration is completed (Januschke et al., 2006).

1.2.8 Second round of oocyte anterior-posterior polarization

As already mentioned, the signal from posterior follicle cells is necessary to establish the anterior-posterior axis of the egg chamber. This is achieved through the polarization of the oocyte. Since this thesis focuses on the establishment of the anterior-posterior axis of the egg chamber, this process will be covered in more detail in the following, separate chapter.

In short, asymmetry of the Par network is first established, with Par-1 at the posterior and Bazooka/Par6/aPKC complex at the anterior cortex. This is necessary to polarize the microtubule cytoskeleton through Par-1 dependent inhibition of microtubule nucleation at the posterior. A polarized microtubule network is then used by motor proteins to properly localize mRNAs.

1.3. Anterior-posterior polarity of the oocyte in midoogenesis

The final goal of establishing anterior-posterior polarity of the oocyte is the robust and precise delivery of anterior and posterior determinants, which will specify the poles of the future embryo. The anterior region will develop into the head while the posterior region will become the abdomen of the fly. The main posterior determinant is *oskar* mRNA (Lehmann and Nusslein-Volhard, 1986), and the anterior determinant is *bicoid* mRNA (Frohnhofer and Nusslein-Volhard, 1986). The process of anterior-posterior polarization of the oocyte occurs from stage 7 to stage 10 and can be divided into three steps (Figure 1.9). First, an asymmetry of the Par network is established, with Par-1 at the posterior and Bazooka/Par6/aPKC complex at the anterior cortex. Next, Par-1 inhibits microtubule nucleation at the posterior, which polarizes the microtubule cytoskeleton. Finally, motor protein-based transport of mRNAs on a polarized microtubule network leads to asymmetric mRNA localization.

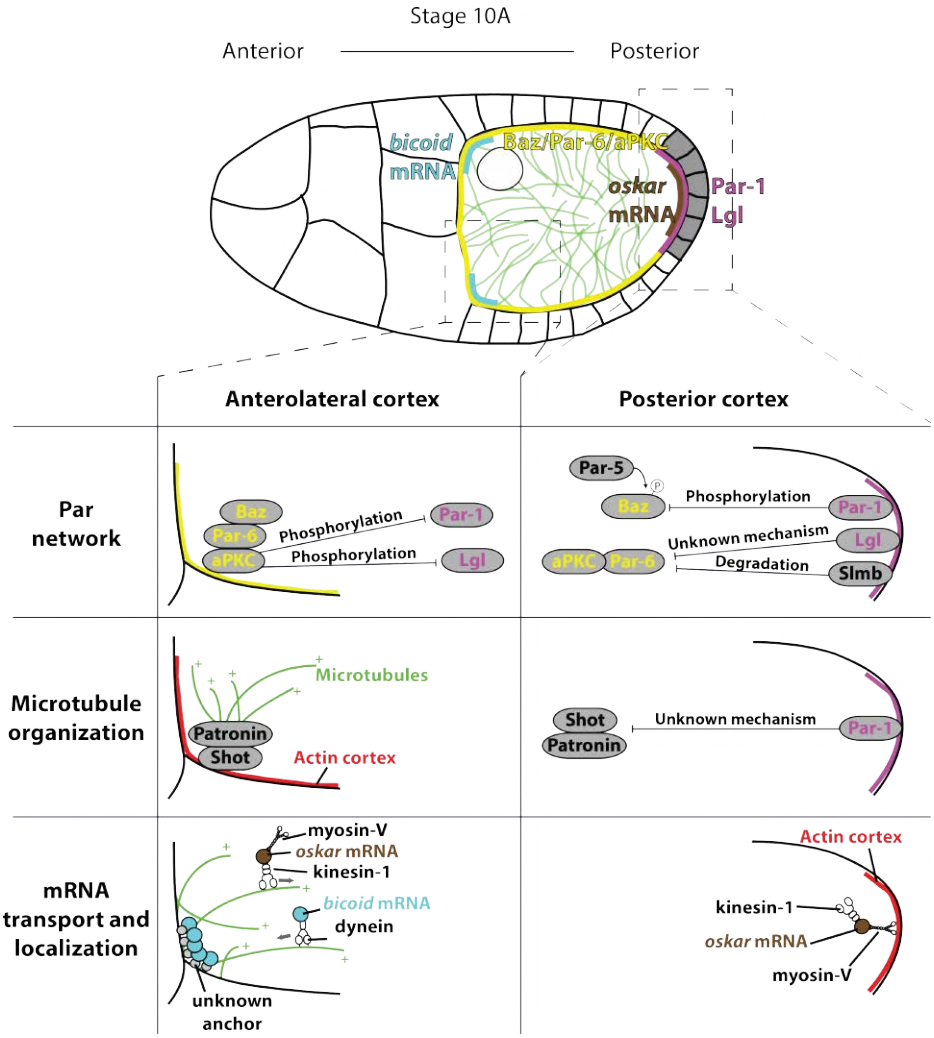

Figure 1.9. **Establishment of the anterior-posterior axis in the *Drosophila* oocyte.** Top: an overview of anterior-posterior polarization of the oocyte in mid-oogenesis. The signal from PFCs (grey) induces the establishment of posterior (magenta) and anterolateral (yellow) Par domains. Par polarity induces polarization of microtubule cytoskeleton (green) by inhibiting microtubule nucleation at the posterior. Polarized microtubule cytoskeleton directs delivery of *bicoid* mRNAs (blue) to the anterior and *oskar* mRNA (brown) to the posterior.

continues on next page

Figure 1.9. *continued from previous page*

Bottom: Detailed schematics showing three processes necessary for the oocyte polarization. **Par network polarity:** at the anterior, Bazooka/Par-6/aPKC complex binds to the membrane through interaction between Bazooka and membrane lipids. aPKC phosphorylates both Par-1 and Lgl to exclude them from the anterolateral membrane. At the posterior, Par-1 phosphorylates Bazooka, which is excluded from the posterior membrane following the binding by Par-5. In addition, Lgl and Slmb exclude aPKC/Par-6 complex from the posterior through not well-defined mechanisms. **Microtubule organization:** at the 488 anterior, Shot binds to actin and recruits Patronin. Patronin binds minus ends of existing microtubules, which template the growth of new microtubules. At the posterior, Par-1 excludes Shot/Patronin through an unknown mechanism to inhibit posterior nucleation of microtubules. **mRNA transport and localization:** at the anterior, dynein delivers *bicoid* mRNA to the cortex by moving towards the minus ends of the microtubules. *bicoid* is anchored only at the anterior of the oocyte by an unidentified linker. Kinesin-1 removes *oskar* mRNA from the anterolateral cortex by moving towards the plus ends of the microtubules. At the posterior, myosin-V anchors *oskar* mRNA to the cortical actin at the posterior of the oocyte, where the microtubule nucleation is inhibited.

1.3.1 Par polarity in midoogenesis

Localization of polarity proteins in mid-oogenesis

In *Drosophila* oocyte, Par proteins form mutually exclusive cortical domains. These domains are clearly discernible starting at late stage 9 of oogenesis. At this stage, Par-1 forms the posterior crescent (Shulman et al., 2000; Tomancak et al., 2000; Doerflinger et al., 2006), while Par-3/Bazooka, Par-6 and aPKC localize to the anterolateral cortex (Figure 1.9) (Benton and St Johnston, 2003; Doerflinger et al., 2010; Morais-de-Sá et al., 2014). Two other Par proteins, Par-4/LKB1 and Par-5/14-3-3ϵ, do not show polarized distribution. Par-4 is uniformly distributed around the cortex (Martin and St Johnston, 2003), while Par-5

is detected in the cytoplasm (Benton et al., 2002). In addition to Par proteins, tumor suppressor Lethal (2) giant larvae (Lgl) is required for the polarization of the oocyte. Lgl also shows the polarized distribution and localizes to the posterior of the oocyte (Tian and Deng, 2008; Doerflinger et al., 2010).

Described asymmetric distribution of Pars is established gradually. The first sign of polarization is the recruitment of Par-1 to the posterior at stage 7. Interestingly, at this stage Bazooka is also detected at the posterior, where it colocalizes with Par-1. During stages 8 and 9, the Par-1 crescent strengthens and expands, while Bazooka gradually disappears from the posterior, and relocalizes to the anterolateral cortex at late stage 9 (Doerflinger et al., 2010; Jouette et al., 2019). Par-6 disappears from the posterior before Bazooka. Already at stage 7, Par-6 is found all around the cortex, with slightly lower levels at the posterior. At stage 8, Par-6 completely disappears from the posterior and forms an anterolateral cortical domain (Doerflinger et al., 2010). Lgl localizes to the posterior later than Par-1, during late stage 8 and early stage 9 of oogenesis. It also extends more anteriorly than Par-1 (Doerflinger et al., 2010).

Phenotypes of polarity protein mutants in mid-oogenesis

The requirement of the Par proteins in the early stages of oogenesis makes it difficult to study their role during mid-oogenesis (see section 1.2.4). This was partially overcome either by using hypomorphic alleles of *par* genes that do not affect oocyte determination or by analyzing a few clones that escape early defects and continue to develop to later stages of oogenesis. Localization of mRNAs and Staufen, and organization of microtubule network are most commonly used as a readout for polarity defects.

Strong *par-1* hypomorphs show penetrant phenotype: depending on the combination of *par-1* alleles, *oskar* is mislocalized to the middle in

70-99% of the oocytes, and microtubules nucleate all around the cortex (Shulman et al., 2000; Tomancak et al., 2000; Doerflinger et al., 2006). Doerflinger et al. described *baz* allele that produces a penetrant polarity phenotype, with Staufen mislocalized in 98% of the oocytes, and uniform distribution of microtubules. This mutated gene gives rise to the truncated protein, lacking the C-terminal domain, which does not localize to the cortex (Doerflinger et al., 2010). Roles of Par-4 and Par-5 have been inferred from analysis of null mutants that escaped defects in oocyte differentiation and developed to stages 9-10. In *par-4* mutants, both Staufen protein and *oskar* mRNA are mislocalized in 80-90% of the oocytes (Martin and St Johnston, 2003). Analysis of *par-5* mutant escapers showed mislocalization of *oskar* mRNA in 31% of the oocytes (Benton et al., 2002).

The requirement for aPKC and Par-6 in the polarization of the oocyte in mid-oogenesis is controversial. By analyzing escapers of the strong *aPKC* mutant - $aPKC^{k06403}$ that developed to stage 9-10, Tian and Deng found mislocalization of Staufen in 47% of the oocytes (Tian and Deng, 2008). Conversely, Doerflinger et al. reported that these escapers develop a normal anterior-posterior axis at stage 9 (Doerflinger et al., 2006). Similarly, hypomorphic *aPKC* alleles, which lack either kinase activity or Par-6 binding site, do not cause polarity defects (Kim et al., 2009). To date, there have not been reports of weak alleles of *par6* that do not show defects in oocyte differentiation. However, Huynh et al. reported that *par-6* mutant egg chambers that escape the early arrest go on to produce normal eggs (Huynh et al., 2001a). Contrary to the Par proteins and aPKC, Lgl is not required in early oogenesis. At stage 9-10, *lgl* null mutants show defects in Staufen localization and microtubule organization in around 60% of the oocytes (Tian and Deng, 2008).

Mutal antagonism between anterior and posterior Pars maintains polarization

According to the current model, the Par polarity in the oocyte is maintained by mutual phosphorylation of posterior and anterior Par proteins. At the posterior, the main kinase is Par-1, which phosphorylates Bazooka to reduce its affinity for, and exclude it from, the membrane. Since Bazooka is a scaffold protein that recruits Par-6 and aPKC to the membrane, the exclusion of Bazooka also removes Par-6 and aPKC from the posterior. Additionally, Lgl binds to aPKC/Par-6 complex and inhibits aPKC activity. At the anterolateral cortex, aPKC phosphorylates both Par-1 and Lgl to exclude them from this domain (St Johnston and Ahringer, 2010). However, while evidence for some parts of this mechanism is strong, some have been inferred from other organisms and lack strong support in experiments using the *Drosophila* oocyte.

Evidence that Par-1 excludes Bazooka from the posterior is very strong. Phosphorylation of Bazooka by Par-1 has been shown both *in vitro*, by using biochemical assays; as well as *in vivo*, in both epithelia and the oocyte. Par-1 phosphorylates Bazooka on two conserved serines to generate a 14-3-3 binding site. Binding of 14-3-3ϵ/Par-5 to Bazooka disrupts its oligomerization and interaction with aPKC (Benton and St Johnston, 2003). In addition, in *par-1* mutants Bazooka is localized all around the oocyte cortex; and non-phosphorylatable form of Bazooka also shows uniform localization (Benton and St Johnston, 2003; Doerflinger et al., 2010). However, while phosphorylation of Bazooka by Par-1 is essential for its exclusion, it might not be sufficient. At stages 7 and 8, Par-1 and Bazooka co-localize at the posterior, and Bazooka exclusion is only observed at late stage 9 (Doerflinger et al., 2010; Jouette et al., 2019). Recent work has suggested the role of membrane trafficking and dynein-mediated transport in the maintenance of Bazooka asymmetry (Jouette et al., 2019).

While the requirement of Par-1 for Bazooka localization is clear, contradicting observations concerning how Bazooka influences Par-1 cortical recruitment have been made. One study reported a *baz* mutant in which Par-1 cortical localization is lost (Becalska and Gravis, 2010). Another study reported that Par-1 localizes all around the cortex in *baz* mutant (Doerflinger et al., 2010). Direct phosphorylation of Par-1 by aPKC has not been shown in *Drosophila*. However, aPKC phosphorylates conserved site in Par-1 in mammals, both *in vivo* and *in vitro* (Hurov et al., 2004; Suzuki et al., 2004). When the conserved aPKC phosphorylation site is mutated, Par-1 localizes all around the cortex (Doerflinger et al., 2010, 2006). Additionally, aPKC, as well as its binding partner Par-6, is excluded from posterior in mid-oogenesis (Morais-de-Sá et al., 2014; Doerflinger et al., 2010). From this, it has been inferred that aPKC phosphorylates Par-1 to exclude it from the anterolateral cortex (Doerflinger et al., 2010). However, as previously mentioned, the strong evidence for the requirement of aPKC and Par-6 in oocyte polarization is still lacking.

Drosophila homologue of Lgl is phosphorylated by aPKC on three sites *in vitro*, and this is important for asymmetric cell division of *Drosophila* neuroblasts. (Betschinger et al., 2003). Lgl binds directly to the aPKC/Par6 complex and inhibits aPKC activity in *Drosophila* neuroblasts (Wirtz-Peitz et al., 2008) and mammalian cells (Yamanaka et al., 2006). However, the role of Lgl in the polarization of the oocyte has been controversial. While one study found that *lgl* mutants show polarity phenotypes (Tian and Deng, 2008), other reported that almost all oocytes look normal and that Lgl activity is required in the posterior follicle cells for the proper polarization of the oocyte (Li et al., 2008).

During oogenesis, Lgl interacts with aPKC as shown by the pull-down assay. When three aPKC phosphorylation sites in Lgl are mutated, Lgl localizes all around the cortex. In addition, when a dominant-negative

form of aPKC is expressed, most of the egg chambers fail to show Lgl association with the oocyte cortex (Tian and Deng, 2008). Thus, there is strong evidence that aPKC restricts Lgl localization to the posterior of the oocyte through phosphorylation. Interestingly, expression of a non-phosphorylatable form of Lgl causes defects in the organization of the microtubule network and localization of *oskar* and Staufen that are more severe than the ones observed in *lgl* null mutant (Tian and Deng, 2008). Pull-down assay also showed that Lgl interacts with Par-1 during oogenesis (Tian and Deng, 2008), and Lgl and Par-1 seem to reinforce each other's posterior localization (Tian and Deng, 2008; Doerflinger et al., 2010). More recently, it has been reported that Slmb, the substrate specificity subunit of the SCF E3 ubiquitin ligase, excludes Par-6 and aPKC from the posterior by targeting them for degradation (Morais-de-Sá et al., 2014). Lgl overexpression partially rescues *slmb* phenotype, suggesting that it might play partially redundant role to *slmb* to inactivate aPKC/Par6 at the posterior (Morais-de-Sá et al., 2014).

The role of Par4/LKB1 in the polarization of the oocyte is not known. In mammals, LKB1 (STK11) phosphorylates the activation loop of Par-1 (MARK2) to turn on its kinase activity (Lizcano et al., 2004). Since *lkb1* mutants show similar polarity phenotype as *par-1* mutants (Martin and St Johnston, 2003), it is possible that LKB1 is needed to activate Par-1 in *Drosophila* oocyte.

1.3.2 Organization of microtubule cytoskeleton

While exact mechanisms of Par asymmetry establishment in mid-oogenesis remain unclear, much more is known about the downstream polarity event: the organization of the microtubule cytoskeleton (Figure 1.9). Initially, microtubule organization in the oocyte was inferred from final distributions of cargoes and motor proteins. This has led to a view that microtubules are highly polarized along the

anterior-posterior axis, with minus-ends at the anterior, and plus-ends at the posterior (Clark et al., 1994, 1997). Immunostaining of microtubules has led to the model of microtubules being nucleated from the anterior and the lateral cortex, but not at the posterior (Theurkauf et al., 1992; Cha et al., 2002; Serbus et al., 2005), while Januschke et al. proposed that nucleation occurs predominantly from the oocyte nucleus (Januschke et al., 2006).

Our current understanding of microtubule organization greatly benefited from the use of live imaging. First, live imaging showed that *oskar* mRNA is transported in all directions, with only a small bias towards the posterior (Zimyanin et al., 2008). This suggested that the microtubule network is not as highly polarized as previously thought. Next, Parton et al. used live imaging of microtubule plus end marker EB1-GFP to show that the microtubule network is highly dynamic, and only subtly polarized: around 60% of the microtubules grow towards the posterior, and 40% towards the anterior (Parton et al., 2011). 3D modeling of transport in the oocyte showed that this slight bias is sufficient to drive the asymmetric distribution of mRNAs (Khuc Trong et al., 2015). At the anterolateral cortex of the oocyte, microtubules are organized by noncentrosomal microtubules organizing centers (ncMTOCs). These ncMTOCs are composed of spectraplankin, Short stop (Shot), and microtubule minus-end binding protein, Patronin. Shot binds to the cortical actin and recruits Patronin to form cortical ncMTOC. Shot/Patronin complex does not nucleate microtubules, but captures existing microtubules minus ends, which template growth of new microtubules (Nashchekin et al., 2016).

There is strong evidence showing that Par-1 is a major effector of microtubule organization in the oocyte. In *par-1* mutants, the exclusion of Shot and Patronin from the posterior cortex is lost (Nashchekin et al., 2016), as is the suppression of microtubule nucleation at the posterior (Shulman et al., 2000; Parton et al., 2011). Expression of the

non-phosphorylatable form of Par-1, which localizes all around the cortex, causes the loss of all cortex-associated microtubules. In addition, when non-phosphorylatable forms of both Bazooka and Par-1 are co-expressed, the microtubule organization is the same as when only non-phosphorylatable Par-1 is expressed (Doerflinger et al., 2010). Whether Par-1 interacts directly with the Shot/Patronin complex to exclude it from the membrane or blocks its cortical recruitment through an indirect mechanism remains to be determined.

1.3.3 Localization of mRNAs in the oocyte

The final step of anterior-posterior polarization of the oocyte is the delivery of *oskar* mRNA to the posterior, and of bicoid mRNA to the anterior of the oocyte (Figure 1.9). It has been known for a long time that the localization of both mRNAs depends on microtubules (Clark et al., 1994; Pokrywka and Stephenson, 1991). These early results led to the model of mRNAs being transported towards the opposite poles by motor proteins moving in opposite directions on a highly polarized microtubule cytoskeleton. This idea was corroborated with the finding that correct *oskar* mRNA localization requires plus-end directed motor protein kinesin-1 (Brendza et al., 2000), while localization of *bicoid* mRNA is affected when the Dynein/Dynactin complex is disrupted (Duncan and Warrior, 2002; Januschke et al., 2002). However, as it became clear that the microtubule cytoskeleton is not as polarized as was initially assumed, novel mechanisms of mRNA transport and localization have been considered.

Once again, live imaging was essential for our current understanding of this process. First, Zimyanin et al. followed *oskar* mRNA particles in live oocytes and showed that *oskar* is transported in all directions, with only a slight bias toward the posterior (Zimyanin et al., 2008). Similarly, Trovisco et al. found that *bicoid* is randomly transported by dynein walking toward the minus-ends of the microtubules (Trovisco et al., 2016).

Computer simulations suggested that the existence of an anterior-posterior gradient of cortical microtubule nucleation is already sufficient to account for the localization of mRNAs (Khuc Trong et al., 2015). However, further experiments suggested that dynactin is necessary to protect the growing plus-ends of microtubules so that they are long enough for *oskar* to be delivered to the posterior (Nieuwburg et al., 2017). In addition, both *bicoid* and *oskar* mRNAs seem to require anchoring for stable localization. FRAP and photo-conversion experiments of fluorescently labeled *bicoid* mRNA showed a slow turnover of these particles suggesting that they are stably anchored (Trovisco et al., 2016). These observations led the authors to propose that dynein delivers *bicoid* mRNA to the broader anterolateral region by walking towards the minus-ends of the microtubules. *bicoid* is anchored by an unknown mechanism, which is active only at the anterior, but not at the lateral cortex. The molecular nature of this mechanism is not known, but it is independent of microtubule dynamics and polarization (Trovisco et al., 2016). Interestingly, *bicoid* mRNA that is injected into the oocyte localizes to the nearest region of the anterolateral cortex. However, when treated with the nurse cell cytoplasm prior to the injection, it properly localizes only at the anterior (Cha et al., 2001). A possible explanation is that some factors that are loaded on the mRNA in the nurse cells make it competent for the anterior anchoring (Trovisco et al., 2016). (Trovisco et al., 2016). A model that includes anchoring specifically at the anterior can explain why *bicoid* is not found at the lateral cortex. This model also predicts that the microtubule cytoskeleton does not need to be polarized for correct *bicoid* localization. Indeed, *bicoid* localizes correctly in the *shot* mutants, in which the microtubule cytoskeleton is not polarized (Trovisco et al., 2016). However, defects in *bicoid* mRNA localization occur in other mutants in which cytoskeleton polarization is compromised, such as *par-1*, *baz* and *grk* (Benton et al., 2002; Doerflinger et al., 2010;

González-Reyes et al., 1995).

The mechanism of *oskar* mRNA anchoring is clearer. First, it was shown that cortical localization of *oskar* is reduced upon F-actin fragmentation (Cha et al., 2002) and that it depends on actin motor, myosin-V (*didum* in *Drosophila*) (Krauss et al., 2009), which suggested that myosin-V might be involved in anchoring. However, since both myosin-V and actin are uniformly distributed throughout the oocyte cortex, it was not clear how they can anchor *oskar* mRNA specifically at the posterior. To elucidate the mechanism of *oskar* mRNA transport and anchoring, Lu et al. analyzed the localization of Staufen in different kinesin-1 and myosin-V mutants (Lu et al., 2020). Staufen is an RNA-binding protein that forms ribonucleoprotein particles with *oskar* mRNA (St Johnston et al., 1991), and is used as a proxy for *oskar* mRNA localization. According to their model, *oskar* mRNA is transported by kinesin-1 towards the plus ends of microtubules, followed by anchoring at the posterior by myosin-V. There is competition between kinesin-dependent removal of *oskar* mRNA from the cortex along microtubules and myosin-V anchoring. Since the density of the microtubules is high at the anterolateral cortex, kinesin removal wins there, while at the posterior, where nucleation of microtubules is suppressed, myosin-V wins (Lu et al., 2020). This model explains why posterior localization of *oskar* can be achieved by myosin-dependent anchoring, although myosin localization is not polarized. In addition, it explains why *oskar* localization critically depends on polarized microtubule network (Lu et al., 2020).

1.4. Bibliography

A. Achilleos, A. M. Wehman, and J. Nance. Par-3 mediates the initial clustering and apical localization of junction and polarity proteins during

c. elegans intestinal epithelial cell polarization. *Development*, 137:1833–1842, 2010.

L. Almagor, I. S. Ufimtsev, A. Ayer, J. Li, and W. I. Weis. Structural insights into the apkc regulatory switch mechanism of the human cell polarity protein lethal giant larvae 2. *PNAS*, 116(22):10804–10812, 2019.

E. Assa-Kunik, I. L. Torres, E. D. Schejter, D. St Johnston, and B.-Z. Shilo. Drosophila follicle cells are patterned by multiple levels of notch signaling and antagonism between the notch and jak/stat pathways. *Development*, 134(6):1161–1169, 2007.

S. X. Atwood and K. E. Prehoda. apkc phosphorylates miranda to polarize fate determinants during neuroblast asymmetric cell division. *Current Biology*, 19(9):723–729, 2009.

A. Bachmann, M. Schneider, E. Theilenberg, F. Grawe, and E. Knust. Drosophila stardust is a partner of crumbs in the control of epithelial cell polarity. *Nature*, 414(6864):638–643, 2001.

M. J. Bailey and K. E. Prehoda. Establishment of par-polarized cortical domains via phosphoregulated membrane motifs. *Developmental Cell*, 35:199–210, 2015.

T. Balla. Phosphoinositides: Tiny lipids with giant impact on cell regulation. *Physiological Reviews*, 93(3):1019–1137, 2013.

R. Bastock and D. St Johnston. Drosophila oogenesis. *Current Biology*, 18 (23):1082–1087, 2008.

J. Bayraktar, D. Zygmunt, and R. W. Carthew. Par-1 kinase establishes cell polarity and functions in notch signaling in the drosophila embryo. *Journal of Cell Science*, 119:711–721, 2006.

I. E. Bécam, G. Tanentzapf, J.-A. Lepesant, N. H. Brown, and J.-R. Huynh. Integrin-independent repression of cadherin transcription by talin during axis formation in drosophila. *Nautre Cell Biology*, 7(5):510–516, 2005.

A. Beatty, D. Morton, and K. Kemphues. The c. elegans homolog of drosophila lethal giant larvae functions redundantly with par-2 to maintain polarity in the early embryo. *Development*, 137:3995–4004, 2010.

A. Beatty, D. Morton, and K. Kemphues. Par-2, lgl-1 and the cdc-42 gap chin-1 act in distinct pathways to maintain polarity in the c. elegans embryo. *Development*, 140:2005–2014, 2013.

A. N. Becalska and E. R. Gravis. Bazooka regulates microtubule organization and spatial restriction of germ plasm assembly in the drosophila oocyte. *Developmental Biology*, 340:528–538, 2010.

R. Benton and D. St Johnston. Drosophila par-1 and 14-3-3 inhibit bazooka/par-3 to establish complementary cortical domains in polarized cells. *Cell*, 115:691–704, 2003.

R. Benton, I. M. Palacios, and D. St Johnston. Drosophila 14-3-3 / par-5 is an essential mediator of par-1 function in axis formation. *Developmental Cell*, 3:659–671, 2002.

F. Bernard, J.-A. Lepesant, and A. Guichet. Nucleus positioning within drosophila egg chamber. *Seminars in Cell and Developmental Biology*, 82:25–33, 2018.

J. Betschinger, K. Mechtler, and J. A. Knoblich. The par complex directs asymmetric cell division by phosphorylating the cytoskeletal protein lgl. *Nature*, 422(6929):326–330, 2003.

D. Bilder and N. Perrimon. Localization of apical epithelial determinants by the basolateral pdz protein scribble. *Nature*, 406:676–680, 2000.

D. Bilder, M. Schober, and N. Perrimon. Integrated activity of pdz protein complexes regulates epithelial polarity. *Nature Cell Biology*, 5:53–58, 2003.

J. Bolívar, J.-R. Huynh, H. López-Schier, C. González, D. S. Johnston, and A. González-Reyes. Centrosome migration into the drosophila oocyte is independent of bicd and egl, and of the organisation of the microtubule cytoskeleton. *Development*, 128:1889–1897, 2001.

L. Boyd, S. Guo, D. Levitan, D. T. Stinchcomb, and K. J. Kemphues. Par-2 is asymmetrically distributed and promotes association of p granules and par-1 with the cortex in c. elegans embryos. *Development*, 122: 3075–3084, 1996.

R. P. Brendza, L. R. Serbus, J. B. Duffy, and W. M. Saxton. A function for kinesin i in the posterior transport of oskar mrna and staufen protein. *Science*, 289:2120–2122, 2000.

N. A. Bulgakova and E. Knust. The crumbs complex: From epithelial-cell polarity to retinal degeneration. *Journal of Cell Science*, 122:2587–2596, 2009.

A. T. C. Carpenter. Electron microscopy of meiosis in drosophila melanogaster females - i. structure, arrangement, and temporal change of the synaptonemal complex in wild-type. *Chromosoma*, 51:157–182, 1975.

A. T. C. Carpenter. Egalitarian and the choice of cell fates in drosophila melanogaster oogenesis. *Ciba Foundation symposium*, 182:223–246, 1994.

M. Cereijido, R. G. Contreras, and L. Shoshani. Cell adhesion, polarity, and epithelia in the dawn of metazoans. *Physiological Reviews*, 84:1229–1262, 2004.

B.-J. Cha, B. S. Koppetsch, and W. E. Theurkauf. In vivo analysis of drosophila bicoid mrna localization reveals a novel microtubule-dependent axis specification pathway. *Cell*, 106:35–46, 2001.

B.-J. Cha, L. R. Serbus, B. S. Koppetsch, and W. E. Theurkauf. Kinesin i-dependent cortical exclusion restricts pole plasm to the oocyte posterior. *Nature Cell Biology*, 8:592–598, 2002.

Y. Chen and T. Schüpbach. The role of brinker in eggshell patterning. *Mechanisms of Development*, 123:395–406, 2006.

S. Claret, J. Jouette, B. Benoit, K. Legent, and A. Guichet. Membrane targeting of bazooka/par-3 is mediated by direct binding to phosphoinositide lipids. *Current Biology*, 24(10):1071–1079, 2014.

I. Clark, E. Giniger, H. Ruohola-Baker, L. Y. Jan, and Y. N. Jan. Transient posterior localization of a kinesin fusion protein reflects anteroposterior polarity of the drosophila oocyte. *Current Biology*, 4(4):289–300, 1994.

I. E. Clark, L. Y. Jan, and Y. N. Jan. Reciprocal localization of nod and kinesin fusion proteins indicates microtubule polarity in the drosophila oocyte, epithelium, neuron and muscle. *Development*, 124:461–470, 1997.

D. N. Cox, B. Lu, T.-Q. Sun, L. T. Williams, and Y. N. Jan. Drosophila par-1 is required for oocyte differentiation and microtubule organization. *Current Biology*, 11:75–87, 2001a.

D. N. Cox, S. A. Seyfried, L. Y. Jan, and Y. N. Jan. Bazooka and atypical protein kinase c are required to regulate oocyte differentiation in the drosophila ovary. *PNAS*, 98(25):14475–14480, 2001b.

R. T. Cox and A. C. Spradling. A balbiani body and the fusome mediate mitochondrial inheritance during drosophilaoogenesis. *Development*, 130:1579–1590, 2003.

M. de Cuevas and A. C. Spradling. Morphogenesis of the drosophila fusome and its implications for oocyte specification. *Development*, 125: 2781–2789, 1998.

W. Deng and H. Lin. Spectrosomes and fusomes anchor mitotic spindles during asymmetric germ cell divisions and facilitate the formation of a polarized microtubule array for oocyte specification in drosophila. *Developmental Biology*, 189:79–94, 1997.

W.-M. Deng, C. Althauser, and H. Ruohola-Baker. Notch-delta signaling induces a transition from mitotic cell cycle to endocycle in drosophila follicle cells. *Development*, 128(23):4737–4746, 2001.

W.-M. Deng, M. Schneider, R. Frock, C. Castillejo-Lopez, E. A. Gaman, S. Baumgartner, and H. Ruohola-Baker. Dystroglycan is required for polarizing the epithelial cells and the oocyte in drosophila. *Development*, 130:173–184, 2003.

H. Doerflinger, R. Benton, J. M. Shulman, and D. St Johnston. The role of par-1 in regulating the polarised microtubule cytoskeleton in the drosophila follicular epithelium. *Development*, 130:3965–3975, 2003.

H. Doerflinger, R. Benton, I. L. Torres, M. F. Zwart, and D. St Johnston. Drosophila anterior-posterior polarity requires actin-dependent par-1 recruitment to the oocyte posterior. *Current Biology*, 16:1090–1095, 2006.

H. Doerflinger, N. Vogt, I. L. Torres, V. Mirouse, I. Koch, C. Nüsslein-Volhard, and D. St Johnston. Bazooka is required for polarisation of the drosophila anterior-posterior axis. *Development*, 137:1765–1773, 2010.

H. Doerflinger, V. Zimyanin, and D. St Johnston. The drosophila anterior-posterior axis is polarized by asymmetric myosin activation. *Current Biology*, 32:374–385, 2022.

W. Dong, X. Zhang, W. Liu, Y. jiun Chen, J. Huang, E. Austin, A. M. Celotto, W. Z. Jiang, M. J. Palladino, Y. Jiang, G. R. Hammond, and Y. Hong. A conserved polybasic domain mediates plasma membrane targeting of lgl and its regulation by hypoxia. *Journal of Cell Biology*, 211(2):273–286, 2015.

J. E. Duncan and R. Warrior. The cytoplasmic dynein and kinesin motors have interdependent roles in patterning the drosophila oocyte. *Current Biology*, 12:1982–1991, 2002.

B. Etemad-Moghadam, S. Guo, and K. J. Kemphues. Asymmetrically distributed par-3 protein contributes to cell polarity and spindle alignment in early c. elegans embryos. *Cell*, 83:743–752, 1995.

S. Etienne-Manneville. Polarity proteins in migration and invasion. *Oncogene*, 27:6970–6980, 2008.

G. D. Fairn, M. Hermansson, P. Somerharju, and S. Grinstein. Phosphatidylserine is polarized and required for proper cdc42 localization and for development of cell polarity. *Nature Cell Biology*, 13(12):1424–1430, 2011.

A. Franz and V. Riechmann. Stepwise polarisation of the drosophila follicular epithelium. *Developmental Biology*, 338:136–147, 2010.

M. Fregoso Lomas, F. Hails, J.-F. Boisclair Lachance, and L. A. Nilson. Response to the dorsal anterior gradient of egfr signaling in drosophila oogenesis is prepatterned by earlier posterior egfr activation. *Cell Reports*, 4:791–802, 2013.

H. G. Frohnhofer and C. Nusslein-Volhard. Organization of anterior pattern in the drosophila embryo by the maternal gene bicoid. *Nature*, 324:120–125, 1986.

H. M. Frydman and A. C. S. Howard. The receptor-like tyrosine phosphatase lar is required for epithelial planar polarity and for axis determination within drosophila ovarian follicles. *Development*, 128: 3209–3220, 2001.

M. T. Fuller and A. C. Spradling. Male and female drosophila germline stem cells: Two versions of immortality. *Science*, 316(5823):402–404, 2007.

C. L. Gamblin, Émilie J.-L. Hardy, F. J.-M. Chartier, N. Bisson, and P. Laprise. A bidirectional antagonism between apkc and yurt regulates epithelial cell polarity. *Journal of Cell Biology*, 204:487–495, 2014.

W. J. Gan and F. Motegi. Mechanochemical control of symmetry breaking in the caenorhabditis elegans zygote. *Frontiers in Cell and Developmental Biology*, 8:1–11, 2021.

L. Gervais, S. Claret, J. Januschke, S. Roth, and A. Guichet. Pip5k-dependent production of pip2 sustains microtubule organization to establish polarized transport in the drosophila oocyte. *Devlopment*, 135: 3829–3838, 2008.

D. Godt and U. Tepass. Drosophila oocyte localization is mediated by differential cadherin-based adhesion. *Nature*, 395(6700):387–391, 1998.

N. W. Goehring, P. Khuc Trong, J. S. Bois, D. Chowdhury, E. M. Nicola, A. A. Hyman, and S. W. Grill. Polarization of par proteins by advective triggering of a pattern-forming system. *Science*, 334:1137–1141, 2011.

B. Goldstein and I. G. Macara. Review the par proteins: Fundamental players in animal cell polarization. *Developmental Cell*, 13:609–622, 2007.

A. González-Reyes and D. St Johnston. Role of oocyte position in establishment of anterior-posterior polarity in drosophila. *Science*, 266: 639–642, 1994.

A. González-Reyes and D. St Johnston. The drosophila ap axis is polarised by the cadherin-mediated positioning of the oocyte. *Development*, 125 (18):3635–3644, 1998a.

A. González-Reyes and D. St Johnston. Patterning of the follicle cell epithelium along the anterior-posterior axis during drosophila oogenesis. *Development*, 125(15):2837–2846, 1998b.

A. González-Reyes, H. Elliott, and D. St Johnston. Polarization of both major body axes in drosophila by gurken-torpedo signalling. *Nature*, 375: 645–658, 1995.

M. Grammont and K. D. Irvine. fringe and notch specify polar cell fate during drosophila oogenesis. *Development*, 128(12):2243–2253, 2001.

O. Göransson, M. Deak, S. Wullschleger, N. A. Morrice, A. R. Prescott, and D. R. Alessi. Regulation of the polarity kinases par-1/mark by 14-3-3 interaction and phosphorylation. *Journal of Cell Science*, 119(19): 4059–4070, 2006.

N. D. Grieder, M. de Cuevas, and A. C. Spradling. The fusome organizes the microtubule network during oocyte differentiation in drosophila. *Development*, 127:4253–4264, 2000.

A. Guichet, F. Peri, and S. Roth. Stable anterior anchoring of the oocyte nucleus is required to establish dorsoventral polarity of the drosophila egg. *Developmental Biology*, 237:93–106, 2001.

S. Guo and K. J. Kemphues. par-1, a gene required for establishing polarity in c. elegans embryos, encodes a putative ser/thr kinase that is asymmetrically distributed. *Cell*, 81:611–620, 1995.

G. R. Hammond and Y. Hong. Phosphoinositides and membrane targeting in cell polarity. *Cold Spring Harbor Perspectives in Biology*, 10(2):1–16, 2018.

Y. Hao, L. Boyd, and G. Seydoux. Stabilization of cell polarity by the c. elegans ring protein par-2. *Developmental Cell*, 10:199–208, 2006.

T. J. Harris and M. Peifer. The positioning and segregation of apical cues during epithelial polarity establishment in drosophila. *Journal of Cell Biology*, 170:813–823, 2005.

Y. Hirano, S. Yoshinaga, R. Takeya, N. N. Suzuki, M. Horiuchi, M. Kohjima, H. Sumimoto, and F. Inagaki. Structure of a cell polarity regulator, a complex between atypical pkc and par6 pb1 domains. *The Journal of Biological Cehmsitry*, 280(10):9653–9661, 2005.

C. Hoege, A.-T. Constantinescu, A. Schwager, N. W. Goehring, P. Kumar, and A. A. Hyman. Lgl can partition the cortex of one-cell caenorhabditis elegans embryos into two domains. *Current Biology*, 20:1296–1303, 2010.

Y. Hong, B. Stronach, N. Perrimon, L. Y. Jan, and Y. N. Jan. Drosophila stardust interacts with crumbs to control polarity of epithelia but not neuroblasts. *Nature*, 414(6864):634–638, 2001.

T.-J. Hung and K. J. Kemphues. Par-6 is a conserved pdz domain-containing protein that colocalizes with par-3 in caenorhabditis elegans embryos. *Development*, 126:127–135, 1999.

T. W. Hurd, L. Gao, M. H. Roh, I. G. Macara, and B. Margolis. Direct interaction of two polarity complexes implicated in epthelial tight junction assembly. *Nature Cell Biology*, 5(2):137–142, 2003.

J. B. Hurov, J. L. Watkins, and H. Piwnica-Worms. Atypical pkc phosphorylates par-1 kinases to regulate localization and activity. *Current Biology*, 14:736–741, 2004.

A. Hutterer, J. Betschinger, M. Petronczki, and J. A. Knoblich. Sequential roles of cdc42, par-6, apkc, and lgl in the establishment of epithelial

polarity during drosophila embryogenesis. *Developmental Cell*, 6(6): 845–854, 2004.

J.-R. Huynh and D. St Johnston. The origin of asymmetry : Early polarisation of the drosophila germline cyst and oocyte. *Current Biology*, 14:438–449, 2004.

J.-R. Huynh, M. Petronczki, J. A. Knoblich, and D. St Johnston. Bazooka and par-6 are required with par-1 for the maintenance of oocyte fate in drosophila. *Current Biology*, 11:901–906, 2001a.

J.-R. Huynh, J. M. Shulman, R. Benton, and D. St Johnston. Par-1 is required for the maintenance of oocyte fate in drosophila. *Development*, 128:1201–1209, 2001b.

R. Insolera, S. Chen, and S.-H. Shi. Par proteins and neuronal polarity. *Developmental Neurobiology*, 71:483–494, 2011.

J. Januschke, L. Gervais, S. Dass, J. A. Kaltschmidt, H. Lopez-Schier, D. St. Johnston, A. H. Brand, S. Roth, and A. Guichet. Polar transport in the drosophila oocyte requires dynein and kinesin i cooperation. *Current Biology*, 12:1971–1981, 2002.

J. Januschke, L. Gervais, L. Gillet, G. Keryer, M. Bornens, and A. Guichet. The centrosome-nucleus complex and microtubule organization in the drosophila oocyte. *Development*, 133:129–139, 2006.

G. Joberty, C. Petersen, L. Gao, and I. G. Macara. The cell-polarity protein par6 links par3 and atypical protein kinase c to cdc42. *Nature Cell Biology*, 2:531–539, 2000.

J. Jouette, A. Guichet, and S. B. Claret. Dynein-mediated transport and membrane trafficking control par3 polarised distribution. *eLife*, 8:1–28, 2019.

K. J. Kemphues, J. R. Priess, D. G. Morton, and N. Cheng. Identification of genes required for cytoplasmic localization in c. elegans embryos. *Cell*, 52:311–320, 1988.

P. Khuc Trong, H. Doerflinger, J. Dunkel, D. St Johnston, and R. E. Goldstein. Cortical microtubule nucleation can organise the cytoskeleton of drosophila oocytes to define the anteroposterior axis. *eLife*, 4:1–31, 2015.

S. Kim, I. Gailite, B. Moussian, S. Luschnig, M. Goette, K. Fricke, M. Honemann-Capito, H. Grubmüller, and A. Wodarz. Kinase-activity-independent functions of atypical protein kinase c in drosophila. *Journal of Cell Science*, 122(20):3759–3771, 2009.

J. A. Knoblich. Mechanisms of asymmetric stem cell division. *Cell*, 132: 583–597, 2008.

M. P. Krahn, J. Bückers, L. Kastrup, and A. Wodarz. Formation of a bazooka-stardust complex is essential for plasma membrane polarity in epithelia. *Journal of Cell Biology*, 190:751–760, 2010a.

M. P. Krahn, D. R. Klopfenstein, N. Fischer, and A. Wodarz. Membrane targeting of bazooka/par-3 is mediated by direct binding to phosphoinositide lipids. *Current Biology*, 20:636–642, 2010b.

J. Krauss, S. L. de Quinto, C. Nusslein-Volhard, and A. Ephrussi. Myosin-v regulates oskar mrna localization in the drosophila oocyte. *Current Biology*, 19:1058–1063, 2009.

U. Kuchinke, F. Grawe, and E. Knust. Control of spindle orientation in drosophila by the par-3-related pdz-domain protein bazooka. *Current Biology*, 8:1357–1365, 1998.

K. T. Kumfer, S. J. Cook, J. M. Squirrell, K. W. Eliceiri, N. Peel, K. F. O'Connell, and J. G. White. Cgef-1 and chin-1 regulate cdc-

42 activity during asymmetric division in the caenorhabditis elegans embryo. *Molecular Biology of the Cell*, 21:266–277, 2010.

C. F. Lang and E. Munro. The par proteins : from molecular circuits to dynamic self-stabilizing cell polarity. *Development*, 144:3405–3416, 2017.

P. Laprise and U. Tepass. Novel insights into epithelial polarity proteins in drosophila. *Trends in Cell Biology*, 21:401–408, 2011.

R. Lehmann and C. Nusslein-Volhard. Abdominal segmentation, pole cell formation, and embryonic polarity require the localized activity of oskar, a maternal gene in drosophila. *Cell*, 47:141–152, 1986.

A. Leibfried, S. Müller, and A. Ephrussi. A cdc42-regulated actin cytoskeleton mediates drosophila oocyte polarization. *Development*, 140:362–371, 2013.

D. J. Levitan, L. Boyd, C. C. Mello, K. J. Kemphues, and D. T. Stinchcomb. par-2, a gene required for blastomere asymmetry in caenorhabditis elegans, encodes zinc-finger and atp-binding motifs. *Proceedings of the National Academy of Sciences of the United States of America*, 91: 6108–6112, 1994.

Q. Li, T. Xin, W. Chen, M. Zhu, and M. Li. Lethal(2)giant larvae is required in the follicle cells for formation of the initial ap asymmetry and the oocyte polarity during drosophila oogenesis. *Cell Research*, 18:372–384, 2008.

H. Lin and A. C. Spradling. Fusome asymmetry and oocyte determination in drosophila. *Developmental Genetics*, 16:6–12, 1995.

H. Lin, L. Yue, and A. C. Spradling. The drosophila fusome, a germline-specific organelle, contains membrane skeletal proteins and functions in cyst formation. *Development*, 120:947–956, 1994.

J. M. Lizcano, O. Goransson, R. Toth, M. Deak, N. A. Morrice, J. Boudeau, S. A. Hawley, L. Udd, T. P. Makela, D. G. Hardie, and D. R. Alessi. Lkb1 is a master kinase that activates 13 kinases of the ampk subfamily, including mark/par-1. *The EMBO Journal*, 23:833–843, 2004.

H. López-Schier and D. St Johnston. Delta signaling from the germ line controls the proliferation and differentiation of the somatic follicle cells during drosophila oogenesis. *Genes and Development*, 15(11):1393–1405, 2001.

W. Lu, M. Lakonishok, R. Liu, N. Billington, A. Rich, M. Glotzer, J. R. Sellers, and V. I. Gelfand. Competition between kinesin-1 and myosin-v defines drosophila posterior determination. *eLife*, 9:1–25, 2020.

I. G. Macara and L. McCaffrey. Cell polarity in morphogenesis and metastasis. *Philosophical Transactions of the Royal Society B: Biological Sciences*, 368:1–6, 2013.

J. M. Mach and R. Lehmann. An egalitarian-bicaudald complex is essential for oocyte specification and axis determination in drosophila. *Genes and Development*, 11:423–435, 1997.

S. G. Martin and D. St Johnston. A role for drosophila lkb1 in anterior – posterior axis formation and epithelial polarity. *Science*, 421:379–384, 2003.

S. G. Martin, V. Leclerc, K. Smith-Litiere, and D. St Johnston. The identification of novel genes required for drosophila anteroposterior axis formation in a germline clone screen using gfp-staufen. *Development*, 130:4201–4215, 2003.

F. Martin-Belmonte, A. Gassama, A. Datta, W. Yu, U. Rescher, V. Gerke, and K. Mostov. Pten-mediated apical segregation of phosphoinositides controls epithelial morphogenesis through cdc42. *Cell*, 128(2):383–397, 2007.

M. A. McGill, R. A. McKinley, and T. J. Harris. Independent cadherin-catenin and bazooka clusters interact to assemble adherens junctions. *Journal of Cell Biology*, 185:787–796, 2009.

M. McGrail and T. S. Hays. The microtubule motor cytoplasmic dynein is required for spindle orientation during germline cell divisions and oocyte differentiation in drosophila. *Development*, 124:2409–2419, 1997.

R. F. A. McKinley, C. G. Yu, and T. J. C. Harris. Assembly of bazooka polarity landmarks through a multifaceted membrane-association mechanism. *Journal of Cell Science*, 125:1177–1190, 2012.

J. A. Merkle, J. Wittes, and T. Schüpbach. Signaling between somatic follicle cells and the germline patterns the egg and embryo of drosophila. *Current Topics in Developmental Biology*, 140:55–86, 2020.

E. Morais-de-Sá, V. Mirouse, and D. St Johnston. apkc phosphorylation of bazooka defines the apical/lateral border in drosophila epithelial cells. *Cell*, 141:509–523, 2010.

E. Morais-de-Sá, A. Mukherjee, N. Lowe, and D. St Johnston. Slmb antagonises the apkc / par-6 complex to control oocyte and epithelial polarity. *Development*, 141:2984–2992, 2014.

K. Moravcevic, J. M. Mendrola, K. R. Schmitz, Y.-H. Wang, D. Slochower, P. A. Janmey, and M. A. Lemmon. Kinase associated-1 domains drive mark/par1 kinases to membrane targets by binding acidic phospholipids. *Cell*, 143(6):966–977, 2010.

A. M. Morimoto, K. C. Jordan, K. Tietze, J. S. Britton, E. M. O'Neill, and H. Ruohola-Baker. Pointed, an ets domain transcription factor, negatively regulates the egf receptor pathway in drosophila oogenesis. *Development*, 122(12):3745–3754, 1996.

D. G. Morton, D. C. Shakes, S. Nugent, D. Dichoso, W. Wang, A. Golden, and K. J. Kemphues. The caenorhabditis elegans par-5 gene encodes a 14-3-3 protein required for cellular asymmetry in the early embryo. *Developmental Biology*, 241:47–58, 2002.

F. Motegi, S. Zonies, Y. Hao, A. A. Cuenca, E. Griffin, and G. Seydoux. Microtubules induce self-organization of polarized par domains in caenorhabditis elegans zygotes. *Nature Cell Biology*, 13:1361–1367, 2011.

E. Munro, J. Nance, and J. R. Priess. Cortical flows powered by asymmetrical contraction transport par proteins to establish and maintain anterior-posterior polarity in the early c. elegans embryo. *Developmental Cell*, 7:413–424, 2004.

J. Nance. Par proteins and the establishment of cell polarity during c. elegans development. *BioEssays*, 27:126–135, 2005.

D. Nashchekin, A. Ribeiro Fernandes, and D. St Johnston. Patronin/shot cortical foci assemble the noncentrosomal microtubule array that specifies the drosophila anterior-posterior axis. *Developmental Cell*, 38: 61–72, 2016.

D. Nashchekin, L. Busby, M. Jakobs, I. Squires, and D. St Johnston. Symmetry breaking in the female germline cyst. *Science*, 374:874–879, 2021.

C. Navarro, H. Puthalakath, J. M.Adams, A. Strasser, and R. Lehmann. Egalitarian binds dynein light chain to establish oocyte polarity and maintain oocyte fate. *Nature Cell Biology*, 6(5):427–435, 2004.

F. S. Neuman-Silberberg and T. Schupbach. The drosophila dorsoventral patterning gene gurken produces a dorsally localized rna and encodes a tgfα-like protein. *Cell*, 75(1):165–174, 1993.

R. A. Neumüller and J. A. Knoblich. Dividing cellular asymmetry: Asymmetric cell division and its implications for stem cells and cancer. *Genes and Development*, 23:2675–2699, 2009.

R. Nieuwburg, D. Nashchekin, M. Jakobs, A. P. Carter, P. Khuc Trong, R. E. Goldstein, and D. St Johnston. Localised dynactin protects growing microtubules to deliver oskar mrna to the posterior cortex of the drosophila oocyte. *eLife*, 6:1–25, 2017.

T. Nishimura and K. Kaibuchi. Numb controls integrin endocytosis for directional cell migration with apkc and par-3. *Developmental Cell*, 13 (1):15–28, 2007.

L.-M. Pai, G. Barcelo, and T. Schüpbach. D-cbl, a negative regulator of the egfr pathway, is required for dorsoventral patterning in drosophila oogenesis. *Cell*, 103:51–61, 2000.

R. M. Parton, R. S. Hamilton, G. Ball, L. Yang, C. F. Cullen, W. Lu, H. Ohkura, and I. Davis. A par-1–dependent orientation gradient of dynamic microtubules directs posterior cargo transport in the drosophila oocyte. *The Journal of Cell Biology*, 194(1):121–135, 2011.

P. J. Plant, J. P. Fawcett, D. C. Lin, A. D. Holdorf, K. Binns, S. Kulkarni, and T. Pawson. A polarity complex of mpar-6 and atypical pkc binds, phosphorylates and regulates mammalian lgl. *Nature Cell Biology*, 5(4): 301–308, 2003.

N. Pokrywka and E. C. Stephenson. Microtubules mediate the localization of bicoid rna during drosophila oogenesis. *Development*, 113:55–66, 1991.

F. A. Renschler, S. R. Bruekner, P. L. Salomon, A. Mukherjee, L. Kullmann, M. C. Schütz-Stoffregen, C. Henzler, T. Pawson, M. P. Krahn, and S. Wiesner. Structural basis for the interaction between the cell polarity proteins par3 and par6. *Science Signaling*, 11:1–12, 2018.

V. Riechmann and A. Ephrussi. Axis formation during drosophila oogenesis. *Current Opinion in Genetics and Development*, 11:374–383, 2001.

E. Rodriguez-Boulan and I. G. Macara. Organization and execution of the epithelial polarity programme. *Nature Reviews Molecular Cell Biology*, 15:225–242, 2014.

J. Roignot, X. Peng, and K. Mostov. Polarity in mammalian epithelial morphogenesis. *Cold Spring Harbor Perspectives in Biology*, 5:1–16, 2013.

K. Roper and N. H. Brown. A spectraplakin is enriched on the fusome and organizes microtubules during oocyte specification in drosophila. *Current Biology*, 14:99–110, 2004.

S. Roth and J. A. Lynch. Symmetry breaking during drosophila oogenesis. *Cold Spring Harbor Perspectives in Biology*, 1:a001891, 2009.

S. Roth, F. S. Neuman-Silberberg, G. Barcelo, and T. Schupbach. cornichon and the egf receptor signaling process are necessary for both anterior-posterior and dorsal-ventral pattern formation in drosophila. *Cell*, 81:967–978, 1995.

S. Roth, P. Jordan, and R. Karess. Binuclear drosophila oocytes: Consequences and implications for dorsal-ventral patterning in oogenesis and embryogenesis. *Development*, 126:927–934, 1999.

H. Ruohola, K. Bremmer, D. Baker, J. Swedlow, L. Jan, and Y. Jan. Role of neurogenic genes in establishment of follicle cell fate and oocyte polarity during oogenesis in drosophila. *Cell*, 66:433–449, 1991.

H. Ruohola-Baker, L. Y. Jan, and Y. N. Jan. The role of gene cassettes in axis formation during drosophila oogenesis. *Trends in Genetics*, 10(3): 89–94, 1994.

M. Schelski and F. Bradke. Neuronal polarization: From spatiotemporal signaling to cytoskeletal dynamics. *Molecular and Cellular Neuroscience*, 84:11–28, 2017.

T. Schüpbach. Germ line and soma cooperate during oogenesis to establish the dorsoventral pattern of egg shell and embryo in drosophila melanogaster. *Cell*, 49:699–707, 1987.

L. R. Serbus, B.-J. Cha, W. E. Theurkauf, and W. M. Saxton. Dynein and the actin cytoskeleton control kinesin-driven cytoplasmic streaming in drosophila oocytes. *Development*, 132:3743–3752, 2005.

A. Shewan, D. J. Eastburn, and K. Mostov. Phosphoinositides in cell architecture. *Cold Spring Harbor Perspectives in Biology*, 3(8):1–17, 2011.

K. Shin, S. Straight, and B. Margolis. Patj regulates tight junction formation and polarity in mammalian epithelial cells. *Journal of Cell Biology*, 168 (5):705–711, 2005.

J. M. Shulman, R. Benton, and D. St Johnston. The drosophila homolog of c. elegans par-1 organizes the oocyte cytoskeleton and directs oskar mrna localization to the posterior pole. *Cell*, 101:377–388, 2000.

C. A. Smith, K. M. Lau, Z. Rahmani, S. E. Dho, G. Brothers, Y. M. She, D. M. Berry, E. Bonneil, P. Thibault, F. Schweisguth, R. L. Borgne, and C. J. McGlade. apkc-mediated phosphorylation regulates asymmetric membrane localization of the cell fate determinant numb. *EMBO Journal*, 26(2):468–480, 2007.

A. C. Spradling. Developmental genetics of oogenesis. In *The development of Drosophila melanogaster*. Cold Spring Harbor Lab. Press, 1993.

D. St Johnston and J. Ahringer. Cell polarity in eggs and epithelia: Parallels and diversity. *Cell*, 141:757–774, 2010.

D. St Johnston, D. Beuchle, and C. Nusslein-Volhard. staufen, a gene required to localize maternal rnas in the drosophila egg. *Cell*, 66:51–63, 1991.

N. R. Stevens, A. A. Raposo, R. Basto, D. St Johnston, and J. W. Raff. From stem cell to embryo without centrioles. *Current Biology*, 17(17): 1498–1503, 2007.

Y. Sun, Y. Yan, N. Denef, and T. Schüpbach. Regulation of somatic myosin activity by protein phosphatase 1β controls drosophila oocyte polarization. *Development*, 138:1991–2001, 2011.

B. Sunchu and C. Cabernard. Principles and mechanisms of asymmetric cell division. *Development*, 147:1–13, 2020.

B. Suter and R. Steward. Requirement for phosphorylation and localization of the bicaudal-d protein in drosophila oocyte differentiation. *Cell*, 67: 917–926, 1991.

A. Suzuki and S. Ohno. The par-apkc system: Lessons in polarity. *Journal of Cell Science*, 119:979–987, 2006.

A. Suzuki, M. Hirata, K. Kamimura, R. Maniwa, T. Yamanaka, K. Mizuno, M. Kishikawa, H. Hirose, Y. Amano, N. Izumi, Y. Miwa, and S. Ohno. apkc acts upstream of par-1b in both the establishment and maintenance of mammalian epithelial polarity. *Current Biology*, 14:1425–1435, 2004.

Y. Tabuse, Y. Izumi, F. Piano, K. J. Kemphues, J. Miwa, and S. Ohno. Atypical protein kinase c cooperates with par-3 to establish embryonic polarity in caenorhabditis elegans. *Development*, 125:3607–3614, 1998.

G. Tanentzapf and U. Tepass. Interactions between the crumbs, lethal giant larvae and bazooka pathways in epithelial polarization. *Nature Cell Biology*, 5:46–52, 2003.

W. E. Theurkauf, S. Smiley, M. L. Wong, and B. M. Alberts. Reorganization of the cytoskeleton during drosophila oogenesis: implications for axis specification and intercellular transport. *Development*, 115:923–936, 1992.

W. E. Theurkauf, B. M. Alberts, Y. N. Jan, and T. A. Jongens. A central role for microtubules in the differentiation of drosophila oocytes. *Development*, 118:1169–1180, 1993.

A.-G. Tian and W.-M. Deng. Lgl and its phosphorylation by apkc regulate oocyte polarity formation in drosophila. *Development*, 135:463–471, 2008.

N. Tissot, J.-A. Lepesant, F. Bernard, K. Legent, F. Bosveld, C. Martin, O. Faklaris, Y. Bellaiche, M. Coppey, and A. Guichet. Distinct molecular cues ensure a robust microtubule-dependent nuclear positioning in the drosophila oocyte. *Nature Communications*, 8(15168):1–13, 2017.

P. Tomancak, F. Piano, V. Riechmann, K. C. Gunsalus, K. J. Kemphues, and A. Ephrussi. A drosophila melanogaster homologue of caenorhabditis elegans par-1 acts at an early step in embryonic-axis formation. *Nature Cell Biology*, 2:458–460, 2000.

I. L. Torres, H. Lopez-Schier, and D. St Johnston. A notch/delta-dependent relay mechanism establishes anterior-posterior polarity in drosophila. *Developmental Cell*, 5:547–558, 2003.

V. Trovisco, K. Belaya, D. Nashchekin, U. Irion, G. Sirinakis, R. Butler, J. J. Lee, E. R. Gavis, and D. St Johnston. bicoid mrna localises to the drosophila oocyte anterior by random dynein- mediated transport and anchoring. *eLife*, 5:1–34, 2016.

M. Tworoger, M. Keller Larkin, Z. Bryant, and H. Ruohola-Baker. Mosaic analysis in the drosophila ovary reveals a common hedgehog-inducible

precursor stage for stalk and polar cells. *Genetics*, 151(2):2739–2748, 1999.

T. Vaccari and A. Ephrussi. The fusome and microtubules enrich par-1 in the oocyte, where it effects polarization in conjunction with par-3, bicd, egl, and dynein. *Current Biology*, 12:1524–1528, 2002.

T. Vaccari, C. Rabouille, and A. Ephrussi. The drosophila par-1 spacer domain is required for lateral membrane association and for polarization of follicular epithelial cells. *Current Biology*, 15:255–261, 2005.

M. T. Veeman and J. A. McDonald. Dynamics of cell polarity in tissue morphogenesis: A comparative view from drosophila and ciona. *F1000Research*, 5:1–12, 2016.

Z. G. Venkei and Y. M. Yamashita. Emerging mechanisms of asymmetric stem cell division. *Journal of Cell Biology*, 217:3785–3795, 2018.

R. F. Walther and F. Pichaud. Crumbs/dapkc-dependent apical exclusion of bazooka promotes photoreceptor polarity remodeling. *Current Biology*, 20:1065–1074, 2010.

J. L. Watts, B. Etemad-Moghadam, S. Guo, L. Boyd, B. W. Draper, C. C. Mello, J. R. Priess, and K. J. Kemphues. par-6, a gene involved in the establishment of asymmetry in early c. elegans embryos, mediates the asymmetric localization of par-3. *Development*, 122:3133–3140, 1996.

J. L. Watts, D. G. Morton, J. Bestman, and K. J. Kemphues. The c. elegans par-4 gene encodes a putative serine-threonine kinase required for establishing embryonic asymmetry. *Development*, 127:1467–1475, 2000.

S.-Y. Wei, L. M. Escudero, F. Yu, L.-H. Chang, L.-Y. Chen, Y.-H. Ho, C.-M. Lin, C.-S. Chou, W. Chia, J. Modolell, and J.-C. Hsu. Echinoid is a

component of adherens junctions that cooperates with de-cadherin to mediate cell adhesion. *Developmental Cell*, 8(4):493–504, 2005.

F. Wirtz-Peitz, T. Nishimura, and J. A. Knoblich. Linking cell cycle to asymmetric division: Aurora-a phosphorylates the par complex to regulate numb localization. *Cell*, 135:161–173, 2008.

J. Wittes and T. Schüpbach. A gene expression screen in drosophila melanogaster identifies novel jak/stat and egfr targets during oogenesis. *G3*, 9:47–60, 2019.

H. Wu, W. Feng, J. Chen, L.-N. Chan, S. Huang, and M. Zhang. Pdz domains of par-3 as potential phosphoinositide signaling integrators. *Molecular Cell*, 28(5):886–898, 2007.

X. Wu, P. S. Tanwar, and L. A. Raftery. Drosophila follicle cells: Morphogenesis in an eggshell. *Seminars in Cell and Developmental Biology*, 19:271–282, 2008.

R. Xi, J. R. McGregor, and D. A. Harrison. A gradient of jak pathway activity patterns the anterior-posterior axis of the follicular epithelium. *Developmental Cell*, 4(2):167–177, 2003.

T. Yamanaka, Y. Horikoshi, N. Izumi, A. Suzuki, K. Mizuno, and S. Ohno. Lgl mediates apical domain disassembly by suppressing the par-3–apkc–par-6 complex to orient apical membrane polarity. *Journal of Cell Science*, 119(10):2107–2118, 2006.

T. Zhao, O. S. Graham, A. Raposo, and D. St Johnston. Growing microtubules push the oocyte nucleus to polarize the drosophila dorsal-ventral axis. *Science*, 336:999–1003, 2012.

V. L. Zimyanin, K. Belaya, J. Pecreaux, M. J. Gilchrist, A. Clark, I. Davis, and D. St Johnston. In vivo imaging of oskar mrna transport reveals the mechanism of posterior localization. *Cell*, 134:843–853, 2008.

2. Chapter 2: Establishment of Par polarity following the ligation of the egg chamber

2.1. Author Contributions

The experiments presented in this chapter were designed by myself, my supervisor Ivo Telley, and Jorge de-Carvalho (Instituto Gulbenkian de Ciência). Jorge de-Carvalho and I established and validated fly lines used in this and the following chapters. I performed all experiments presented in this chapter with initial help from Jorge de-Carvalho. Ivo Telley designed and assembled the microscopy and micromanipulation platform. I performed the data analysis presented in this chapter.

2.2. Summary

The *Drosophila melanogaster* oocyte matures inside an egg chamber, surrounded by the germline-derived nurse cells and a layer of somatic follicle cells. The communication between the oocyte and other cells within the egg chamber is necessary for many aspects of oocyte maturation, including the establishment of oocyte polarity. At stage 7 of oogenesis, a group of follicle cells termed posterior follicle cells (PFCs) sends an unidentified signal to the oocyte. This signal leads to asymmetric localization of the partitioning defective (Par) proteins and, ultimately, defines the anterior-posterior body axis. However, apart from this initial role of PFCs, the importance of the constant communication between the oocyte and the surrounding cells for oocyte polarization has not been studied.

We developed an assay that enabled us to cut off the communication between the oocyte and its surrounding by ligating the egg chamber. By segregating the posterior from the anterior of stage 9-10 oocytes, we found that the anterior polarity protein, Par-3/Bazooka, is localizing to the

posterior immediately following the ligation. However, rapid exclusion of the protein followed, thus re-establishing asymmetry in this compartment surrounded only by follicle cells. Interestingly, the center of exclusion also marked the presence of polar cells, a specialized pair of PFCs. The posterior polarity protein, Par-1, was redistributed such that the peak of the signal corresponded to the position of the polar cells. These results suggest that PFCs are capable of sending a polarizing signal at these stages of oogenesis. In unperturbed oocytes, we found that ER membranes of PFCs and the oocyte are connected. This suggests continuous communication between the PFCs and the oocyte via trafficking, even after the putative signal from the PFCs has been sent and polarity has been established. Ligation caused initial disconnection of the PFCs and the oocyte ER membranes, but recovery of the connection soon followed, together with the exclusion of another anterior Par, Par-6. This observation further supports the idea that the re-establishment of the polarity is dependent on the PFCs.

In conclusion, we demonstrate the establishment of Par polarity in the *Drosophila* oocyte when the communication between the oocyte and the nurse cells is interrupted, and we find evidence for a direct role of PFCs in this process.

2.3. Introduction

The establishment of cellular asymmetries is a crucial event in many cellular contexts. The first symmetry-breaking event during development serves to define the body axes of the animal. In this context, the most studied example is the establishment of the anterior-posterior axis in the one-cell stage embryo of the nematode *Caenorhabditis elegans*. The symmetry in the *C. elegans* zygote is broken following fertilization when the cue derived from the sperm causes a local cortical weakening (Motegi and Sugimoto, 2006). This leads to the establishment of the cortical flow

directed away from the position of the sperm entry. The cortical flow moves anterior determinants Par-3, Par-6, and aPKC - that were embedded in the membrane prior to the fertilization - and allows the accumulation of posterior determinants Par-1 and Par-2 (Munro et al., 2004; Goehring et al., 2011). However, the polarity is also established in the absence of the cortical flows, through a pathway that depends on the interaction between Par-2 and centrosome-derived microtubules (Motegi et al., 2011). Interestingly, in the absence of functional centrosomes, Par-2 accumulates in the regions of the embryo with higher curvature, suggesting the role of cell geometry in breaking of Par symmetry (Klinkert et al., 2019). In addition, theoretical work supports the influence of geometry on the polarization of the Par network in the *C. elegans* (Dawes and Iron, 2013; Geßele et al., 2020).

The fruit fly *Drosophila melanogaster* defines both anterior-posterior and dorsal-ventral body axes during oogenesis. The fly oocyte matures inside the egg chamber, a multicellular structure within the ovary. Based on the changes in morphology of the egg chamber, oogenesis can be divided into 14 stages (Spradling, 1993). In addition to the oocyte, the egg chamber contains 15 nurse cells, which are of germline origin, and a layer of somatic epithelial follicle cells. Both of these cell types have an important role in the polarization of the oocyte. Nurse cells produce all components required inside the oocyte for its growth and polarization, while the oocyte remains transcriptionally quiescent during most of the oogenesis. These components are transported into the oocyte through intercellular bridges called ring canals (Mahajan-Miklos and Cooley, 1994). While the exchange of components between the nurse cells and the oocyte happens in bulk, the communication between the oocyte and the follicle cells is tightly regulated in both space and time. At stage 6 of oogenesis, around 200 follicle cells adopt posterior fate as a result of signaling from the oocyte. At stage 7, these posterior follicle cells (PFCs)

send an unknown signal to the oocyte, which is necessary for the establishment of both anterior-posterior and dorsal-ventral polarity (González-Reyes and St Johnston, 1994; González-Reyes et al., 1995; Roth et al., 1995).

As opposed to the *C. elegans* zygote, cortical flows are not involved in symmetry breaking in the *Drosophila* oocyte. Instead, the earliest known sign of oocyte polarity following the signal from PFCs is the di-phosphorylation of non-muscle Myosin II at the posterior of the oocyte (Doerflinger et al., 2022), which causes the posterior localization of Par-1 kinase (Shulman et al., 2000; Tomancak et al., 2000). Following Par-1 localization to the posterior, the anterior group of Par proteins, including aPKC, Par-6, and Par-3/Bazooka, gradually relocalizes from the posterior to the anterolateral cortex (Doerflinger et al., 2010; Jouette et al., 2019).

According to the current understanding, this asymmetry of the Par network is established through phosphorylation events - the posterior kinase Par-1 phosphorylates Bazooka to exclude the aPKC/Par-6/Bazooka complex from the posterior, while the anterior kinase aPKC phosphorylates and excludes Par-1 (Benton and St Johnston, 2003a; Doerflinger et al., 2010). However, the mutual antagonism between anterior and posterior Pars might not be sufficient to explain the observed asymmetric localization since these proteins co-localize at the posterior for several hours from stage 7 to stage 9 of oogenesis (Doerflinger et al., 2010; Jouette et al., 2019).

In light of what is known about the influence of geometry on the polarization of the Par networks in *C. elegans*, the shape of the oocyte emerges as a possible contributor to the establishment or maintenance of polarity. The oocyte is dome-shaped, meaning that the curvature of the posterior membrane is higher compared to the anterior and lateral membrane. This difference in the curvature could serve to strengthen the polarity of the Par network.

In this chapter, I present our attempt to study both the importance of communication between the oocyte and other cells inside the egg chamber, as well as the possible role of geometrical cues on the establishment and maintenance of Par polarity in *Drosophila* oocyte. We accomplish this task by using ligation of egg chambers to divide them into two compartments. Ligation is a method that was originally used $\sim$50 years ago to study embryogenesis in leafhopper and *Drosophila* (Sander, 1971; Schubiger, 1976). The original experiments used the ligation of eggs at different stages of development to determine at which stages communication between the anterior and posterior, or dorsal and ventral sides of the embryo are crucial for further development of different structures of the insect. More recently, the ligation experiments have been combined with live imaging to study the role of Cdk1 waves in regulating the cell cycle in the *Drosophila* syncytial blastoderm (Deneke et al., 2016).

By ligating the egg chamber in different configurations, we were able to cut off the communication between the oocyte and either posterior follicle cells (PFCs) or the nurse cells. We found that Par polarity is rapidly re-established in the compartment that was still in contact with the PFCs. On the contrary, there was no obvious polarity establishment in the compartment that was surrounded by nurse cells at the anterior, and main-body follicle cells at the lateral and the posterior cortex. In addition, we find that Bazooka is excluded from the regions of high curvature that appear after ligation. However, since we sometimes observed some damage to the oocyte cortex in these regions, we were cautious in the interpretation of the observed delocalization of Bazooka at increased curvature.

In conclusion, these results show that the Par polarity in the oocyte does not depend on contact with the nurse cells, and support the proposed role of PFCs in the establishment of Par polarity. More importantly, these results suggest that the PFCs might be necessary to

maintain the Par polarity throughout oogenesis.

2.4. Materials and methods

2.4.1 Fly lines and fly husbandry

Fly stocks were reared according to standard procedures and maintained at 25℃. The list of fly lines used in this chapter is given in Table 2.1.

Table 2.1. Fly lines used in the experiments presented in this chapter

Genotype	**Origin**	**Reference**
w; +; Jupiter::mCherry	Daniel St Johnston	(Lowe et al., 2014)
w; UASp>GFP::Par-1(N1S)/CyO; +	Daniel St Johnston	(Huynh et al., 2001b)
w; UASp>Bazooka::mGFP/CyO; +	Daniel St Johnston	(Benton and St Johnston, 2003b)
w; UASp>Par-6::mCherry/CyO; +	Daniel St Johnston	(Doerflinger et al., 2010)
w; mat-α4>Gal4; +	Bloomington Drosophila Stock Center	BDSC #7062
w; + ; sqh>EYFP::ER	Bloomington Drosophila Stock Center	BDSC #7195 (LaJeunesse et al., 2004)

The Gal4-UASp system was used to express fluorescently labeled polarity proteins specifically in the germline. To express UASp-transgenes, flies were crossed with mat-α4>Gal4 driver in combination with either endogenous-Jupiter::mCherry or endogenous-EYFP::ER. The cross was kept at 25℃ for 3-4 days, after which parents were removed from the vial, and the vial was transferred to 18℃ for the remaining time of the

development. This was done to reduce problems in development caused by high overexpression of polarity proteins. Female offspring of the desired genotype were collected into vials with 3-4 males and fresh yeast. The flies were kept at 18℃ for 3-4 days before dissection.

Detailed genotypes of flies used in the experiments presented in this chapter are given in Table 2.2.

Table 2.2. Genotypes of flies used in the experiments presented in this chapter.

Genotype	**Figures**
w; mata-α4>Gal4/UASp>Bazooka::mGFP; Jupiter:mCherry/Jupiter::mCherry	2.1, 2.2, 2.3
w; mata-α4>Gal4/UASp>GFP::Par-1(N1S); Jupiter:mCherry/Jupiter::mCherry	2.4
w; mata-α4>Gal4/UASp>Par-6::mCherry; sqh>EYFP::ER/sqh>eYFP::ER	2.5

2.4.2 Cleaning of coverslips and preparation of ligation needle

22x22 mm no. 1.5 coverslip (Marienfeld) were placed into a ceramic rack which was immersed in NaOH (3M) and sonicated for 10 min. The rack was dipped-and-drained in a beaker with MilliQ water, transferred to clean MilliQ water, and sonicated for 10 min. Finally, the rack was transferred into a new beaker with clean MilliQ water and sonicated for 10 more minutes. Coverslips were spin-dried and stored in a clean rack until use. To prepare the ligation needle, a glass rod was pulled on a vertical pipette puller (Narishige PC-10), using a one-step pulling protocol and 70% heating power. The needle was forged on a glass microforge (Narishige MF-900).

2.4.3 Sample preparation, ligation and imaging

Ovaries were dissected in a drop of halocarbon oil (Voltalef 10S, Arkema) and placed on a clear coverslip using tweezers to separate individual germaria. Imaging was performed on a Nikon Eclipse Ti-E microscope equipped with a Yokogawa CSU-W Spinning Disk confocal scanner and a piezoelectric stage (737.2SL, Physik Instrumente), using a 40x water immersion objective and 488 nm laser line for excitation of GFP or YFP, and 561 nm laser line for excitation of mCherry. Images were acquired at 73 focal planes with 0.5 μm z-spacing. x-y pixel size was 162 nm. Andor iXon3 888 EMCCD camera was used for time-lapse acquisitions; images were acquired every 30 s for at least 60 minutes. Unperturbed egg chambers were imaged for 4-5 frames before ligation, after which the ligation needle was lowered using the Sutter MPC-200 micromanipulator. The ligation needle was lowered slowly to minimize damage to the egg chamber. In a typical experiment, it would take around 2-3 minutes to ligate the egg chamber completely.

2.4.4 Image processing

Image deconvolution was done in Huygens (Scientific Volume Imaging) using a theoretical point spread function (PSF), 40 iterations, a signal-to-noise ratio of 8, and the automatic brick layout. The background was estimated by measuring the signal in areas where there was no egg chamber. Deconvolution was done separately for each channel. Images shown in the figures were made by calculating the sum of 11 z-slices in Fiji/ImageJ (National Institutes of Health; Schindelin et al. (2012)). The final figures were assembled in Illustrator (Adobe).

2.4.5 Image and data analysis

All measurements were performed in Fiji/ImageJ on a sum of 11 z-slices. Membrane intensity of the polarity proteins in the posterior compartment was measured by drawing a 10-pixel wide segmented line around the membrane. The position of polar cells was tracked using the Low light tracking tool (Krull et al., 2014). Data analysis and plotting were performed in R (R Core Team, 2021). Values of intensities in each of the oocytes were binned into 100 bins and intensities were normalized for each frame using min-max normalization. For each frame, the mean of the normalized intensities across all experiments was calculated and this mean value was normalized again using min-max normalization. The final plots were made by projecting the normalized means on a circle where position 0° represents the position of the polar cells.

2.5. Results

2.5.1 The assay for ligation of the egg chambers

In this chapter, I describe the assay for ligating the egg chambers. We used a micrometer sized glass needle, which we lowered at the egg chamber using the micromanipulation device (Figure 2.1A), and we coupled this with live imaging to monitor the localization of polarity factors inside the oocyte (Figure 2.1B). This assay could serve two purposes. First, it allows us to divide the egg chamber into two compartments. In the anterior compartment, the oocyte is surrounded by the nurse cells and the main-body follicle cells. In the posterior compartment, the oocyte is surrounded only by the follicle cells. However, the follicle cells that surround the oocyte in this compartment are either main-body follicle cells or the posterior follicle cells (Figure 2.1A). Therefore, we can study if cutting off the communication between the oocyte and any of these subtypes of cells - nurse cells, main-body follicle cells, or posterior follicle

cells - influences the polarity of the oocyte.

The second use of the ligation assay is to study the influence of geometry and scaling on the polarity of the oocyte. The ligation of the egg chamber changes the curvature of the membrane in some parts of the oocyte. This local change in curvature could cause the removal or the accumulation of polarity factors. In addition, by changing the position of the ligation needle with respect to the position of the nurse cells, we could control the size of the sub-compartments and use this to study the influences of the scaling on the polarity.

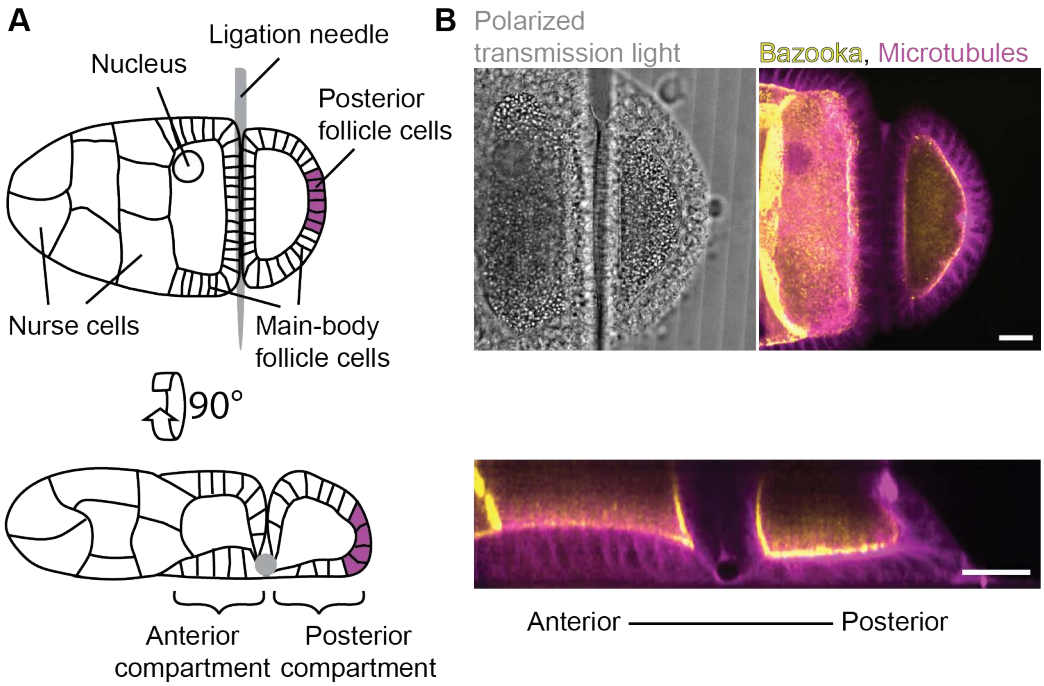

Figure 2.1. **The experimental assay for ligation of the egg chamber. (A)** Scheme of the top and side view of the ligation assay. The ligation needle is lowered on the egg chamber, separating the egg chamber into two compartments. In the anterior compartment, the oocyte is cut off from the posterior follicle cells. In the posterior compartment, the oocyte is cut off from the nurse cells. **(B)** Top and side view of ligated egg chamber expressing Bazooka::GFP (yellow) and the microtubule reporter Jupiter::mCherry (magenta). Transmission light (left) and fluorescence (right) micrograph. The scale bars represent 20 μm.

2.5.2 Bazooka asymmetry is rapidly re-established in the compartment surrounded only by the follicle cells

First, we tested how the ligation of the egg chamber influences the localization of the anterior Par protein Par-3/Bazooka. We used the Gal4-UASp system to drive the expression of GFP-tagged Bazooka (Bazooka::GFP) only in the germline. This approach provides a good signal of Bazooka in the oocyte, which facilitates live imaging. In addition,

expressing the protein only in the germline prevents masking of the signal inside the oocyte by the signal from Bazooka localized at the apical side of the follicle cells (Jouette et al., 2019). We also used mCherry tagged Jupiter (Jupiter::mCherry) as a label for microtubules in both germline and soma (Lowe et al., 2014).

We performed ligation in stages 9 and 10A of oogenesis when Bazooka is excluded from the posterior oocyte membrane (Figure 2.2A-B, -5 min). Following ligation, we could observe the accumulation of Bazooka at the posterior cortex (Figure 2.2A-B, 0 min). This is presumably caused by flow induced by the pressing of the egg chamber. However, Bazooka is rapidly excluded again from the posterior (Figure 2.2B, 60 min, arrowheads). On the other hand, we could observe the increase of the Bazooka signal at the anterior membrane of this compartment (Figure 2.2B, 60 min, arrow). Therefore, we can recapitulate the original localization pattern of Bazooka in the compartment that is surrounded only by the follicle cells - Bazooka localizes to the anterolateral cortex and is removed from the posterior. In contrast, we did not observe the reproducible establishment of Bazooka polarity in the anterior compartment, which is surrounded by the nurse cells and the main-body follicle cells.

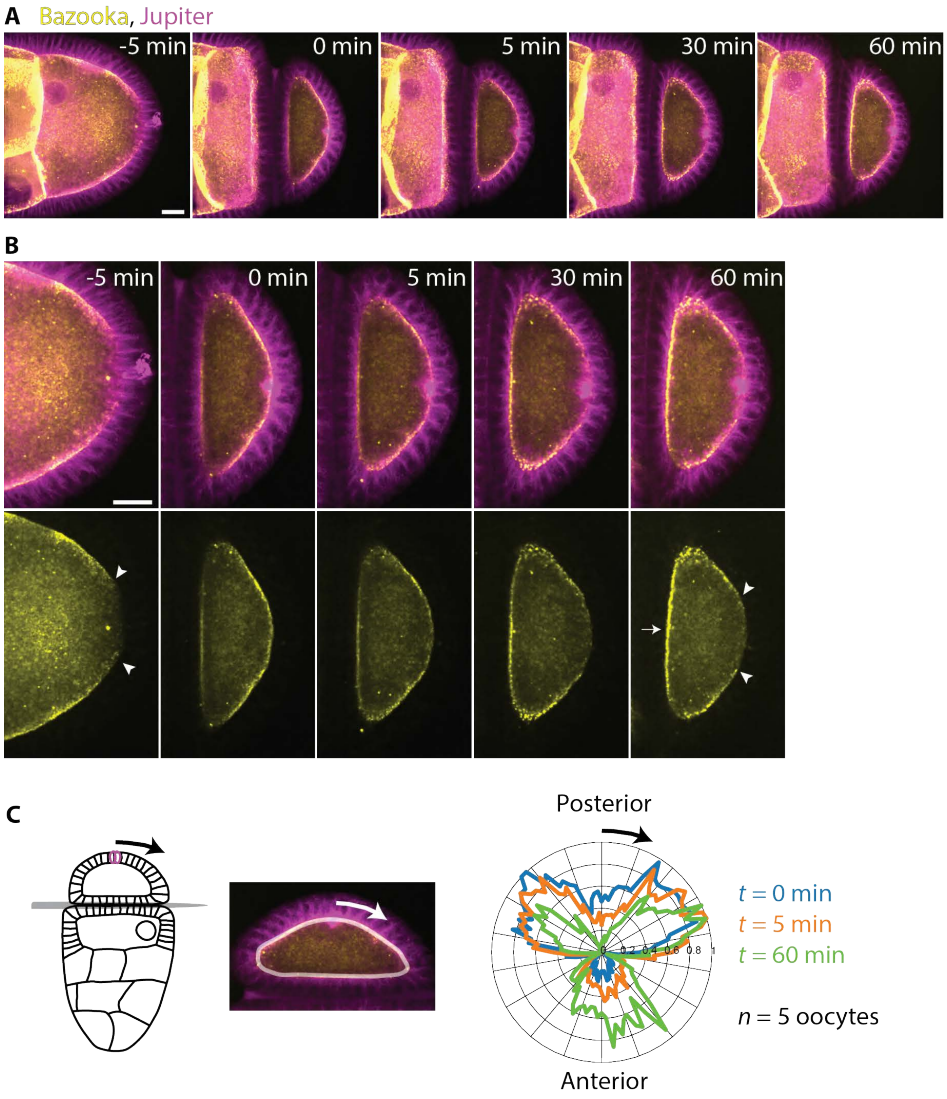

Figure 2.2. **Bazooka is excluded from the posterior membrane in the posterior compartment. (A)** Time-lapse images of an egg chamber expressing Bazooka::GFP (yellow) and the microtubule reporter Jupiter::mCherry (magenta) before (-5 min) and after the ligation of the egg chamber. **(B)** Zoom-in of the posterior compartment of the egg chamber shown in panel A. Top: merged channels, bottom: Bazooka::GFP. Before ligation, Bazooka is excluded from the posterior (a region highlighted by the arrowheads in the first image of the bottom panel).

continues on next page

Figure 2.2. *continued from previous page*

Immediately after ligation (0 min), Bazooka accumulates at the posterior. After 60 min, Bazooka is again excluded from the posterior (arrowheads in the last image) and accumulates at the anterior of the compartment (arrow in the last image). **(C)** The average intensity profile of Bazooka::GFP signal measured along the oocyte cortex as represented by the white line in the micrograph. The position 0° represents the position of the polar cells (the pair of follicle cells with a higher level of Jupiter::mCherry expression). Scale bars represent 20 μm.

To quantify the changes in the Bazooka localization following ligation, we measured the intensity of the Bazooka::GFP signal along the circumference of the posterior compartment (Figure 2.2C). This quantification confirmed that the intensity of the Bazooka::GFP signal decreases over time at the posterior and increases at the anterior of the compartment.

In ligation experiments, we could observe the partial exclusion of Bazooka in the regions of the high curvature close to the ligation needle (Figure 2.2B, 60 min and 2.2C). However, in these regions, we could also sometimes observe the damage that resulted in the leaking of the oocyte cytoplasm into the follicle cells, making these results difficult to interpret. To try to avoid this caveat, we ligated the egg chamber diagonally to change the geometry of the posterior compartment (Figure 2.3A). Nevertheless, Bazooka continued to be excluded from the region where the polar cells - a pair of follicle cells with the highest expression of Jupiter::mCherry - were located (Figure 2.3A, B). Polar cells are important for differentiation of the posterior follicle cells (PFCs) and mark the center of the layer of the posterior follicle cells. Therefore, the observation that Bazooka is always excluded from the region around the polar cells suggested that the PFCs might be involved in the exclusion of Bazooka following the ligation of the egg chamber.

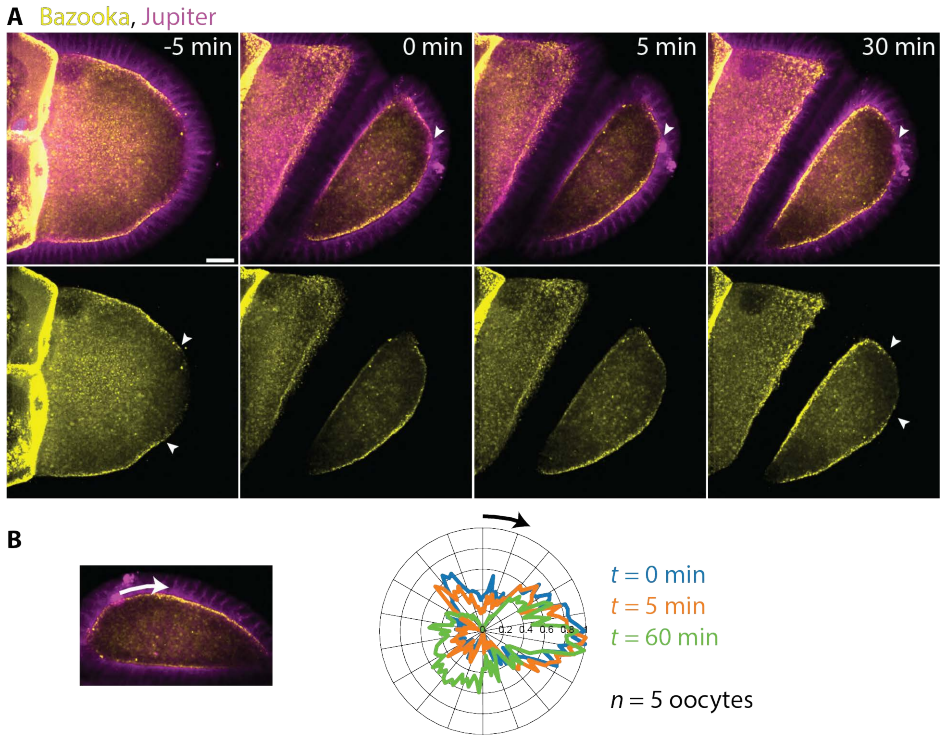

Figure 2.3. **Bazooka is excluded from the region marked by the polar cells. (A)** Time-lapse images of an egg chamber expressing Bazooka::GFP (yellow) and the microtubule reporter Jupiter::mCherry (magenta) before (-5 min) and after the ligation of the egg chamber. Top: merged channels, bottom: Bazooka::GFP. Before ligation, Bazooka is excluded from the posterior (a region highlighted by the arrowheads in the first image of the bottom panel). Immediately after ligation (0 min), Bazooka accumulates at the posterior. After 30 min, Bazooka is excluded from the region marked by the presence of the polar cells (the pair of follicle cells with a higher level of Jupiter::mCherry expression highlighted by the arrowhead in the upper panel). **(B)** The average intensity profile of Bazooka::GFP signal measured along the oocyte cortex as shown in Figure 2.2C. The position 0° represents the position of the polar cells. The scale bar represents 20 μm.

2.5.3 Par-1 signal is re-centered around the polar cells following ligation

Next, we tested how the ligation of the egg chamber influences the localization of Par-1, which normally localizes to the posterior of the oocyte (Figure 2.4A-B, -5 min). We again used the Gal4-UASp system to drive the expression of GFP tagged Par-1 (GFP::Par-1) in the germline and performed ligation in stage 9 and 10A egg chambers. Immediately after ligation, we could observe a slight but reproducible asymmetry of the GFP::Par-1 signal with respect to the polar follicle cells (Figure 2.4B, 0 min and Figure 2.4C). The center of GFP::Par-1 signal was always moved towards the tip of the ligation needle and might be due to transient geometric asymmetry during ligation (note: the needle is pressing on the egg chamber in an oblique way until it touches the glass bottom, causing ligation at the needle tip first and then further towards the shaft of the needle - that could cause asymmetric cytoplasmic flow). However, the symmetry was soon re-established, and at the end of the experiment, the signal was centered around the polar cells (Figure 2.4B, 60 min and Figure 2.4C). This again suggested that the PFCs are involved in the re-localization of the Par proteins following the ligation.

Interestingly, we could sometimes observe accumulation of Par-1 at the anterior membrane of the posterior compartment (arrow in Figure 2.4B, 60 min), although this was not as robust as the appearance of Bazooka in this region (Figure 2.4C). The observation that both Bazooka and Par-1 accumulate at this membrane following ligation suggested that their interaction might not be sufficient for their mutual exclusion.

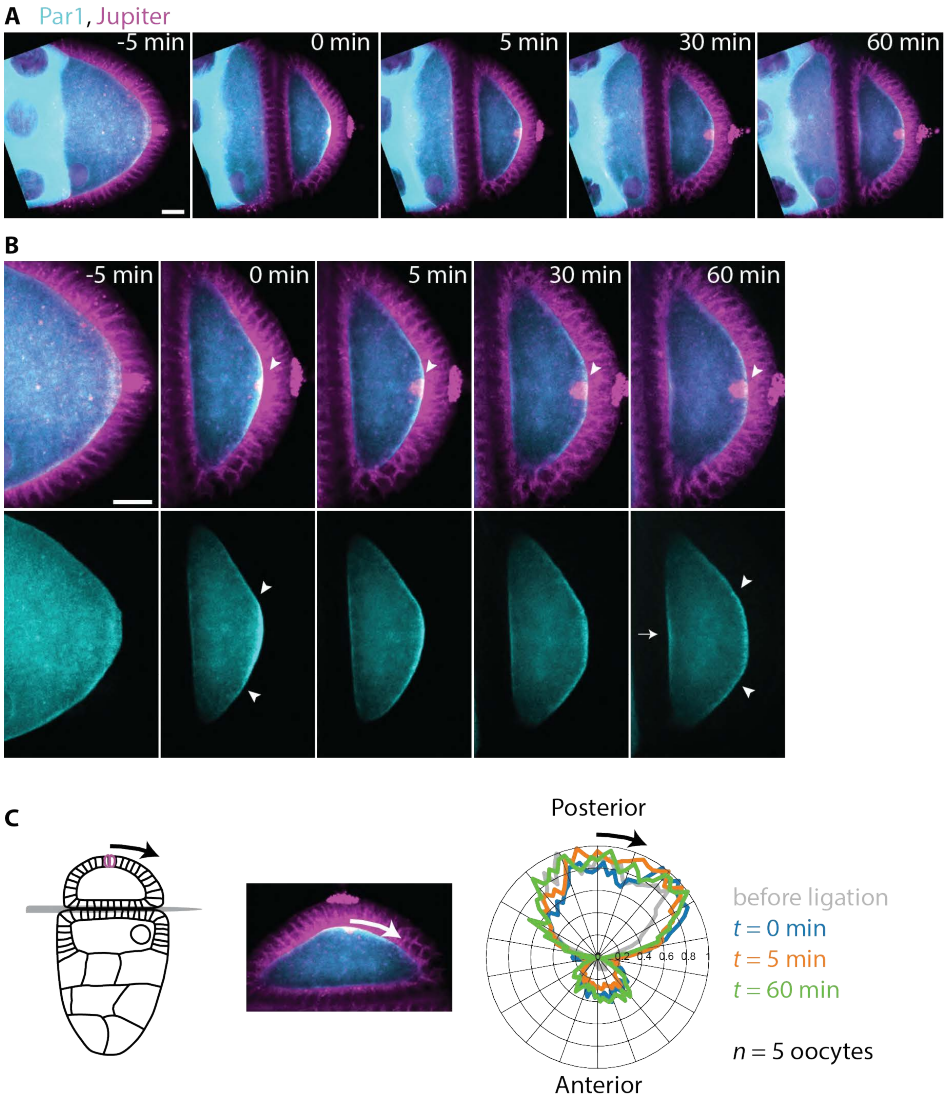

Figure 2.4. **Ligation of an egg chamber expressing Par1::GFP. (A)** Time-lapse images of an egg chamber expressing GFP::Par-1 (cyan) and the microtubule reporter Jupiter::mCherry (magenta) before (-5 min) and after the ligation of the egg chamber. **(B)** Zoom-in of the posterior compartment of the egg chamber shown in panel A. Top: merged channels, bottom: GFP::Par-1. Immediately after ligation (0 min), the GFP::Par-1 signal is asymmetric with respect to the polar cells (a region highlighted by the arrowheads in the second image of the bottom panel).

continues on next page

Figure 2.4. *continued from previous page*

After 60 min, the GFP::Par-1 signal is centered around the polar cells (arrowheads in the last image of the bottom panel) and accumulates at the new anterior (arrow in the last image of the bottom panel). The position of the polar cells is highlighted by the arrow in the upper panel. **(C)** The average intensity profile of the GFP::Par-1 signal measured along the oocyte cortex, as shown in the scheme on the left. The position 0° represents the position of the polar cells. Note that the center of the signal is shifted slightly to the right immediately after ligation (t = 0 min), but slowly reverts to zero degrees after 60 min. Scale bars represent 20 μm.

2.5.4 Morphological changes in the oocyte-PFC interface after ligation

PFCs are known to play a crucial role in triggering the Par polarity inside the oocyte by sending a yet unidentified signal at stage 7 (González-Reyes and St Johnston, 1994; González-Reyes et al., 1995; Roth et al., 1995). However, their role in the following stages of oogenesis has not been investigated. Our observation that the PFCs mark the final location of both Bazooka exclusion and Par-1 accumulation in the ligation experiments suggests that they might be able to send the polarizing signal throughout oogenesis. To test whether there is a connection between the PFCs and the oocyte at stage 9, we used flies expressing EYFP::ER to visualize the endoplasmatic reticulum (ER). We hypothesized that the ER plays a central role in establishing a connection for trafficking between the oocyte and the PFCs, which would deliver the polarizing signal. In addition to EYFP::ER, we used the Gal4-UASp system to drive the germline expression of mCherry tagged Par-6 (Par-6::mCherry). Par-6 is the anterior Par protein which is excluded from the posterior of the oocyte from stage 9 (Doerflinger et al., 2010). Interestingly, we could observe a continuous ER structure between the oocyte and the PFCs at stage 9 of oogenesis (Figure 2.5A-B, -5 min). The region of connection between the

PFCs and the oocyte coincided with the exclusion zone of Par-6::mCherry. Next, we tested if the connection between the oocyte and the PFCs is preserved following the ligation. We ligated the egg chambers expressing EYFP::ER and Par-6::mCherry and observed the loss of connection and posterior accumulation of Par-6 immediately after ligation (Figure 2.5B, 0 min). However, both the connection and the exclusion of Par-6 at the posterior were restored by the end of the experiment (Figure 2.5B, 60 min). These results further support the hypothesis that the restoration of Par polarity in the posterior compartment following the ligation is caused by the signal from PFCs. In addition, the observation of the continuous ER membrane between the PFCs and the oocyte at stage 9 egg chambers suggests that the PFCs might be necessary to maintain Par polarity inside the oocyte throughout the oogenesis. The experiments in which we further tested this hypothesis will be presented in the following chapters.

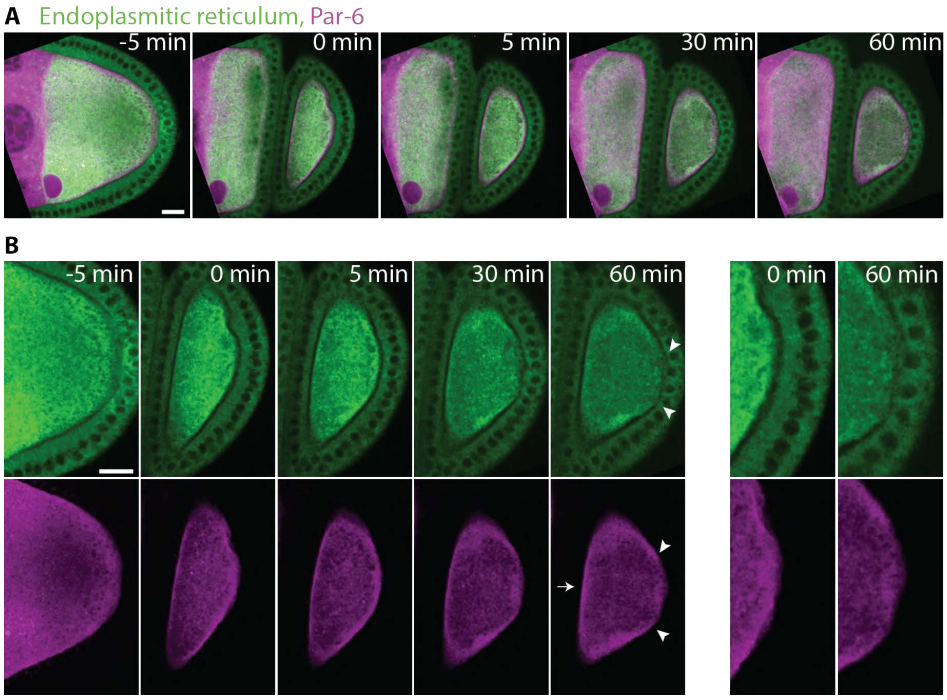

Figure 2.5. **Ligation in egg chambers expressing EYFP::ER and Par-6::mCherry. (A)** Time-lapse images of an egg chamber expressing EYFP::ER (green) and Par-6::mCherry (magenta) before (-5 min) and after the ligation of the egg chamber. **(B)** Zoom-in of the posterior compartment of the egg chamber shown in panel A. Top: EYFP::ER, bottom: Par-6::mCherry. Before ligation (-5 min), ER membranes of the oocyte and the PFCs are connected, while Par-6 is excluded from the posterior. Immediately after ligation (0 min), the connection between the oocyte and the PFCs is lost, while Par-6 accumulates at the posterior. After 60 min, the connection is re-established (arrowheads in the upper panel), while Par-6 is excluded from the posterior (arrowheads in the bottom panel) and accumulates at the anterior of the compartment (arrow in the bottom panel). The rightmost images are zoom-ins of the oocyte-PFCs interface at 0 and 60 min. Scale bar represents 20 μm

2.6. Discussion

The polarity of the *Drosophila* oocyte has been studied since the 1980s when large-scale genetic screens showed that both anterior-posterior and

dorsal-ventral axes of the future embryo are determined by the mother fly (Schüpbach and Wieschaus, 1986; Schüpbach, 1987). Since then, the genetic screens and the follow-up characterization of mutants have remained the cornerstone of the research in the field. There is no doubt that these approaches have provided, and keep providing, crucial insights into the process of oogenesis. However, they do come with some drawbacks. When it comes to studying the polarity of the oocyte in mid-oogenesis, the main problems arise because many genes, including all of the *par* genes, are necessary during the earlier stages of oogenesis (Huynh et al., 2001b; Cox et al., 2001a; Vaccari and Ephrussi, 2002; Huynh et al., 2001a; Cox et al., 2001b; Benton et al., 2002; Martin and St Johnston, 2003). Similarly, communication between the soma and the germline is needed from the earliest phases of oogenesis onwards (Merkle et al., 2020).

Here, we developed a way to acutely perturb the communication between the oocyte and its surroundings and study how this affects the Par polarity in the oocyte. Of course, this approach has its caveats, the main being that the invasive nature of the approach might cause experimental artifacts. To minimize the possible misinterpretations of our experiments, we focused on asking which aspects of the polarity are still functional in the minimized system. After perturbing any system, it is easy to find the aspects that no longer function correctly. However, by following the process of recovery, we can find the components that are sufficient for the establishment of the functional system.

Ligation of the egg chambers in mid-oogenesis perturbs the localization of both anterior and posterior Par proteins. However, the polarity is reproducibly re-established in the posterior compartment, where the communication between the nurse cells and the oocyte is cut off. Therefore, the system in which the oocyte is surrounded by the two types of follicle cells - the PFCs and the main-body follicle cells - is sufficient to

establish the Par polarity in the oocyte. These experiments did not conclusively show whether the process is cell-autonomous - that is, if the oocyte can establish the polarity on its own - or if the follicle cells play an active role. However, the observation that Bazooka is always excluded from the membrane that is in contact with the PFCs suggests a role of PFCs in this process.

The experiments in which we follow the localization of ER membranes further support this idea. We found that ER membranes of the oocyte and the PFCs seem connected in mid-oogenesis. This connection is perturbed following ligation, resulting in the posterior localization of Par-6. However, the recovery of the connection seems to follow, accompanied by the exclusion of Par-6.

Taken together, these observations prompted us to formulate the hypothesis that PFCs play an active role in the maintenance of the Par polarity in the oocyte. To test this, we designed new experiments, which are presented in the following two chapters.

Our approach did not prove to be an efficient way to manipulate the geometry of the egg chamber. However, the influence of geometry on the polarity of the oocyte remains an open possibility. The shape of the oocyte may serve only as a reinforcement of the polarity, while the PFCs act as the main regulator. Therefore, it might be interesting to study geometrical cues in the mutants in which the PFCs do not differentiate correctly. Indeed, in *C. elgans* zygote, the influence of geometry became obvious only when using mutants in which the canonical ways of polarity establishment are impaired (Geßele et al., 2020).

2.7. Acknowledgements

I thank Ivo Telley for supervision, Jorge de-Carvalho for the initial help with experiments, and all members of the Telley lab for fruitful discussions. I also thank the staff of the Fly Facility, the Advanced Imaging Facility (AIF),

and the Technical Support Service at the Instituto Gulbenkian de Ciência (IGC). Finally, I thank Daniel St. Johnston (The Gurdon Institute) for fly line donations and The Bloomington Drosophila Stock Center for their services.

2.8. Bibliography

R. Benton and D. St Johnston. Drosophila par-1 and 14-3-3 inhibit bazooka/par-3 to establish complementary cortical domains in polarized cells. *Cell*, 115:691–704, 2003a.

R. Benton and D. St Johnston. A conserved oligomerization domain in drosophila bazooka/par-3 is important for apical localization and epithelial polarity. *Current Biology*, 13:1330–1334, 2003b.

R. Benton, I. M. Palacios, and D. St Johnston. Drosophila 14-3-3 / par-5 is an essential mediator of par-1 function in axis formation. *Developmental Cell*, 3:659–671, 2002.

D. N. Cox, B. Lu, T.-Q. Sun, L. T. Williams, and Y. N. Jan. Drosophila par-1 is required for oocyte differentiation and microtubule organization. *Current Biology*, 11:75–87, 2001a.

D. N. Cox, S. A. Seyfried, L. Y. Jan, and Y. N. Jan. Bazooka and atypical protein kinase c are required to regulate oocyte differentiation in the drosophila ovary. *PNAS*, 98(25):14475–14480, 2001b.

A. T. Dawes and D. Iron. Cortical geometry may influence placement of interface between par protein domains in early caenorhabditis elegans embryos. *Journal of Theoretical Biology*, 333:27–37, 2013.

V. E. Deneke, A. Melbinger, M. Vergassola, and S. D. Talia. Waves of cdk1 activity in s phase synchronize the cell cycle in drosophila embryos article waves of cdk1 activity in s phase synchronize the cell cycle in drosophila embryos. *Developmental Cell*, 38:399–412, 2016.

H. Doerflinger, N. Vogt, I. L. Torres, V. Mirouse, I. Koch, C. Nüsslein-Volhard, and D. St Johnston. Bazooka is required for polarisation of the drosophila anterior-posterior axis. *Development*, 137:1765–1773, 2010.

H. Doerflinger, V. Zimyanin, and D. St Johnston. The drosophila anterior-posterior axis is polarized by asymmetric myosin activation. *Current Biology*, 32:374–385, 2022.

R. Geßele, J. Halatek, L. Würthner, and E. Frey. Geometric cues stabilise long-axis polarisation of par protein patterns in c. elegans. *Nature Communications*, 11:1–12, 2020.

N. W. Goehring, P. Khuc Trong, J. S. Bois, D. Chowdhury, E. M. Nicola, A. A. Hyman, and S. W. Grill. Polarization of par proteins by advective triggering of a pattern-forming system. *Science*, 334:1137–1141, 2011.

A. González-Reyes and D. St Johnston. Role of oocyte position in establishment of anterior-posterior polarity in drosophila. *Science*, 266: 639–642, 1994.

A. González-Reyes, H. Elliott, and D. St Johnston. Polarization of both major body axes in drosophila by gurken-torpedo signalling. *Nature*, 375: 645–658, 1995.

J.-R. Huynh, M. Petronczki, J. A. Knoblich, and D. St Johnston. Bazooka and par-6 are required with par-1 for the maintenance of oocyte fate in drosophila. *Current Biology*, 11:901–906, 2001a.

J.-R. Huynh, J. M. Shulman, R. Benton, and D. St Johnston. Par-1 is required for the maintenance of oocyte fate in drosophila. *Development*, 128:1201–1209, 2001b.

J. Jouette, A. Guichet, and S. B. Claret. Dynein-mediated transport and membrane trafficking control par3 polarised distribution. *eLife*, 8:1–28, 2019.

K. Klinkert, N. Levernier, P. Gross, C. Gentili, L. von Tobel, M. Pierron, C. Busso, S. Herrman, S. W. Grill, K. Kruse, and P. Gönczy. Aurora a depletion reveals centrosome- independent polarization mechanism in caenorhabditis elegans. *eLife*, 8:1–31, 2019.

A. Krull, A. Steinborn, V. Ananthanarayanan, D. Ramunno-Johnson, U. Petersohn, and I. M. Tolic-Nørrelykke. Fiji: an open-source platform for biological-image analysis. *Optics Express*, 22:210–228, 2014.

D. R. LaJeunesse, S. M. Buckner, J. Lake, C. Na, A. Pirt, and K. Fromson. Three new drosophila markers of intracellular membranes. *BioTechniques*, 36:784–790, 2004.

N. Lowe, J. S. Rees, J. Roote, E. Ryder, I. M. Armean, G. Johnson, E. Drummond, H. Spriggs, J. Drummond, J. P. Magbanua, H. Naylor, B. Sanson, R. Bastock, S. Huelsmann, V. Trovisco, M. Landgraf, S. Knowles-Barley, J. D. Armstrong, H. White-Cooper, C. Hansen, R. G. Phillips, The UK Drosophila Protein Trap Screening Consortium, K. S. Lilley, S. Russell, and D. St Johnston. Analysis of the expression patterns, subcellular localisations and interaction partners of drosophila proteins using a pigp protein trap library. *Development*, 141:3994–4005, 2014.

S. Mahajan-Miklos and L. Cooley. Intercellular cytoplasm transport during drosophila oogenesis. *Developmental Biology*, 165:336–351, 1994.

S. G. Martin and D. St Johnston. A role for drosophila lkb1 in anterior – posterior axis formation and epithelial polarity. *Science*, 421:379–384, 2003.

J. A. Merkle, J. Wittes, and T. Schüpbach. Signaling between somatic follicle cells and the germline patterns the egg and embryo of drosophila. *Current Topics in Developmental Biology*, 140:55–86, 2020.

F. Motegi and A. Sugimoto. Sequential functioning of the ect-2 rhogef, rho-1 and cdc-42 establishes cell polarity in caenorhabditis elegans embryos. *Nature Cell Biology*, 8:978–985, 2006.

F. Motegi, S. Zonies, Y. Hao, A. A. Cuenca, E. Griffin, and G. Seydoux. Microtubules induce self-organization of polarized par domains in caenorhabditis elegans zygotes. *Nature Cell Biology*, 13:1361–1367, 2011.

E. Munro, J. Nance, and J. R. Priess. Cortical flows powered by asymmetrical contraction transport par proteins to establish and maintain anterior-posterior polarity in the early c. elegans embryo. *Developmental Cell*, 7:413–424, 2004.

R Core Team. *R: A Language and Environment for Statistical Computing*. R Foundation for Statistical Computing, Vienna, Austria, 2021. URL `https://www.R-project.org/`.

S. Roth, F. S. Neuman-Silberberg, G. Barcelo, and T. Schupbach. cornichon and the egf receptor signaling process are necessary for both anterior-posterior and dorsal-ventral pattern formation in drosophila. *Cell*, 81:967–978, 1995.

K. Sander. Pattern formation in longitudinal halves of leaf hopper eggs (homoptera) and some remarks on the definition of ”embryonic regulation”. *Wilhelm Roux Archiv für Entwicklungsmechanik der Organismen*, 167:336–352, 1971.

J. Schindelin, I. Arganda-Carreras, E. Frise, V. Kaynig, M. Longair, T. Pietzsch, S. Preibisch, C. Rueden, S. Saalfeld, B. Schmid, J.-Y. Tinevez, D. J. White, V. Hartenstein, K. Eliceiri, P. Tomancak, and A. Cardona. Fiji: an open-source platform for biological-image analysis. *Nature Methods*, 9:676–682, 2012.

T. Schüpbach. Germ line and soma cooperate during oogenesis to establish the dorsoventral pattern of egg shell and embryo in drosophila melanogaster. *Cell*, 49:699–707, 1987.

T. Schüpbach and E. Wieschaus. Maternal-effect mutations altering the anterior-posterior pattern of the drosophila embryo. *Roux's Archives of Developmental Biology*, 195:302–317, 1986.

G. Schubiger. Adult differentiation from partial drosophila embryos after egg ligation during stages of nuclear multiplication and cellular blastoderm. *Developmental Biology*, 50:476–488, 1976.

J. M. Shulman, R. Benton, and D. St Johnston. The drosophila homolog of c. elegans par-1 organizes the oocyte cytoskeleton and directs oskar mrna localization to the posterior pole. *Cell*, 101:377–388, 2000.

A. C. Spradling. Developmental genetics of oogenesis. In *The development of Drosophila melanogaster*. Cold Spring Harbor Lab. Press, 1993.

P. Tomancak, F. Piano, V. Riechmann, K. C. Gunsalus, K. J. Kemphues, and A. Ephrussi. A drosophila melanogaster homologue of caenorhabditis elegans par-1 acts at an early step in embryonic-axis formation. *Nature Cell Biology*, 2:458–460, 2000.

T. Vaccari and A. Ephrussi. The fusome and microtubules enrich par-1 in the oocyte, where it effects polarization in conjunction with par-3, bicd, egl, and dynein. *Current Biology*, 12:1524–1528, 2002.

3. Chapter 3: Contact between PFCs and the oocyte maintains Par polarity in the oocyte

Parts of this chapter are adapted from:

A. Milas, J. de-Carvalho, I. A. Telley. Follicle cell contact maintains main body axis polarity in the *Drosophila melanogaster* oocyte. *bioRxiv*, 2022, DOI: https://doi.org/10.1101/2022.03.03.482911

3.1. Author Contributions

The experiments presented in this chapter were designed by myself and my supervisor Ivo Telley. I performed all experiments and the data analysis presented in this chapter, supervised by Ivo Telley and with initial help from Jorge de-Carvalho (Instituto Gulbenkian de Ciência). Ivo Telley designed and assembled the microscopy and micromanipulation platform. The article on which this chapter is based was written by me and Ivo Telley.

3.2. Summary

The formation of the anterior-posterior body axis in *Drosophila melanogaster* requires signaling from the posterior follicle cells (PFCs) to the stage 7 oocyte, leading to asymmetric localization of the partitioning defective (Par) proteins. This causes polarization of the microtubule network, which directs kinesin-dependent transport of *oskar* mRNA to the posterior of the oocyte during stages 9 and 10A. However, although several studies have concluded the necessity of signaling using genetic approaches, neither the nature of the signal nor the possible role of the PFCs in the following stages of oogenesis are known.

In this chapter, I present experiments that highlight contact between the oocyte and the PFCs until late stage 10B of oogenesis. In contrast, a visible intercellular gap exists between the oocyte and the follicle cells surrounding it on the lateral side. Starting at late stage 10B, the posterior contact is lost, followed by accumulation of the anterior Par protein Par-3/Bazooka at the posterior of the oocyte. After accumulation, Bazooka co-localizes with the posterior Par protein Par-1 for some time, but soon after Par-1 dissociates from the posterior. Mechanical detachment of PFCs at stages 9 and 10A causes premature posterior accumulation of Bazooka. Furthermore, inhibition of posterior fate determination causes the gap to spread all around the oocyte cortex, disrupting the Par polarity of the oocyte.

In conclusion, we provide the first evidence that mechanical contact of posterior follicle cells (PFCs) with the oocyte cortex maintains the Par polarity throughout oogenesis.

3.3. Introduction

A large majority of animals form two embryonic body axes (Niehrs, 2010). In many animals, these body axes are formed after fertilization, during early embryonic growth and segmentation. In *Drosophila melanogaster*, the anterior-posterior axis is maternally established, gradually during 14 stages of oogenesis, with the final goal of delivering *oskar* mRNA to the posterior end and *bicoid* mRNA to the anterior end of the oocyte (Riechmann and Ephrussi, 2001). The first sign of anterior-posterior polarity is the positioning of the oocyte to the posterior of the egg chamber at stage 1, which is achieved through differential adhesion between the oocyte and the somatic cells at the posterior of the egg chamber (Godt and Tepass, 1998; González-Reyes and St Johnston, 1998a).

At stage 6, the posteriorly positioned oocyte secrets the EGF-like ligand, Gurken, which will cause the subset of follicle cells at the posterior

to adopt posterior fate. In the following stage, these posterior follicle cells (PFCs) will signal back to the oocyte to determine its posterior pole (González-Reyes and St Johnston, 1994; González-Reyes et al., 1995; Roth et al., 1995). However, the molecular nature of the signal coming back from the PFCs remains elusive. Additionally, it is unclear if this signal acts solely as a trigger that breaks the symmetry or if PFCs play a role in the maintenance of oocyte polarity.

The earliest known signature of mid-stage oocyte polarisation following the signal from PFCs is the di-phosphorylation of non-muscle Myosin II at the posterior of the oocyte (Doerflinger et al., 2022). This is necessary for the posterior localization of Par-1 kinase, a component of a highly conserved network of Partitioning defective (Par) proteins (Shulman et al., 2000; Tomancak et al., 2000). Following Par-1 localization to the posterior, the anterior group of Par proteins, including aPKC, Par-6, and Par-3/Bazooka, relocalizes from the posterior to the anterolateral cortex (Doerflinger et al., 2010; Jouette et al., 2019). Posteriorly localized Par-1 inhibits microtubule nucleation, causing plus ends of microtubules to preferentially accumulate at the posterior (Nashchekin et al., 2016; Parton et al., 2011). Polarization of the microtubule network is necessary to direct kinesin-dependent transport of *oskar* mRNA to the posterior during stages 9 and 10A (Lu et al., 2018, 2020; Zimyanin et al., 2008). Therefore, the polarity of the Par network must be maintained during these stages.

The asymmetry of the Par network is thought to be self-maintaining through mutual antagonism between anterior and posterior Par proteins (Hoege and Hyman, 2013; Lang and Munro, 2017; Motegi and Seydoux, 2013). Par-1 phosphorylates Bazooka to exclude the complex of aPKC/Par-6/Bazooka from the posterior, while aPKC phosphorylates Par-1 leading to the removal of Par-1 from the anterolateral membrane (Benton and St Johnston, 2003a; Doerflinger et al., 2010). Interestingly, anterior and posterior Par proteins colocalize at the posterior of the oocyte

from stage 7 to stage 9, suggesting that mutual antagonism might not be sufficient to maintain Par polarity (Doerflinger et al., 2010; Jouette et al., 2019).

Here, we show that at late stage 10B of oogenesis the cell-cell interface of the oocyte and PFCs visibly enlarges, suggesting contact loss. This is first followed by the accumulation of Bazooka to the posterior of the oocyte, where it co-localizes with Par-1 for some time, after which Par-1 is removed from the posterior. Mechanical detachment of PFCs from the oocyte at stages 9 and 10A by micromanipulation causes loss of contact and premature accumulation of Bazooka. When PFCs do not differentiate correctly and maintain the main-body fate, the contact is not established, resulting in the loss of Bazooka exclusion at the posterior of the oocyte. We conclude that the PFCs maintain the exclusion of Bazooka until late stage 10B of oogenesis through a contact-dependent mechanism.

3.4. Materials and methods

3.4.1 Fly lines and fly husbandry

Fly stocks were reared according to standard procedures and maintained at 25℃. The list of fly lines used in this chapter is given in Table 3.1.

Table 3.1. Fly lines used in the experiments presented in this chapter

Genotype	Origin	Reference
w; +; Jupiter::mCherry	Daniel St Johnston	(Lowe et al., 2014)
w; UASp>GFP::Par-1(N1S)/CyO; +	Daniel St Johnston	(Huynh et al., 2001)
w; UASp>Bazooka::mGFP/CyO; +	Daniel St Johnston	(Benton and St Johnston, 2003b)
w; UASp>Bazooka::mCherry/CyO; +	Bloomington Drosophila Stock Center	BDSC #65844
w; mat-α4>Gal4; +	Bloomington Drosophila Stock Center	BDSC #7062
w; +; mat-α4>Gal4	Bloomington Drosophila Stock Center	BDSC #7063
w; +; UAS>hop-dsRNAi/TM3,Sb	Bloomington Drosophila Stock Center	BDSC #32966
w; +; GR1>Gal4	Bloomington Drosophila Stock Center	BDSC #36287

To express fluorescently labeled polarity proteins specifically in the germline, the flies carrying UASp-transgenes were crossed with mat-α4>Gal4 driver using the protocol described in section 2.4.1. To induce main-body fate in all follicle cells, JAK/hopscotch kinase was knocked down by driving expression of UAS>hop-dsRNAi using GR1>Gal4 driver (Alégot et al., 2018; Wittes and Schüpbach, 2019). These crosses were carried out at 25℃ to increase the efficiency of RNA interference. Detailed genotypes of flies used in the experiments

presented in this chapter are given in Table 3.2.

Table 3.2. Genotypes of flies used in the experiments presented in this chapter.

Genotype	Figures
w; mata-α4>Gal4/UASp>Bazooka::mGFP; Jupiter:mCherry/Jupiter::mCherry	3.1, 3.2, 3.5
w; UASp>GFP::Par-1(N1S)/UASp>Bazooka::mCherry; mata-α4>Gal4/+	3.3
w; mata-α4>Gal4/UASp>Bazooka::mGFP; GR1>GAL4, Jupiter::mCherry/UAS>hop-RNAi	3.7
w; mata-α4>Gal4/UASp>GFP::Par-1(N1S); GR1>GAL4, Jupiter::mCherry/UAS>hop-RNAi	3.8

3.4.2 Microscopy

Samples were prepared for imaging as described in section 2.4.3. Imaging was performed on a Nikon Eclipse Ti-E microscope equipped with a Yokogawa CSU-W Spinning Disk confocal scanner and a piezoelectric stage (737.2SL, Physik Instrumente), using 40x water immersion objective and 488 nm and 561 nm laser lines for excitation of GFP and mCherry, respectively. Images were acquired at 73 focal planes with 0.5 μm z-spacing. x-y pixel size was 162 nm. An Andor Zyla 4.2 sCMOS camera, was used for snapshot images of whole egg chambers for analyses shown in Figures 3.1, 3.2, 3.3, 3.7 and 3.8. An Andor iXon3 888 EMCCD camera was used for time-lapse acquisitions in the detachment experiment. Images were acquired every 30 s for 60 minutes.

3.4.3 Image analysis

Images were deconvolved as described in section 2.4.4. Images shown in the figures were made by calculating the sum of 6 z-slices in Fiji/ImageJ

(National Institutes of Health; Schindelin et al. (2012)). All measurements were performed in Fiji/ImageJ on a sum of 6 z-slices. The intensity profiles shown in Figures 3.1, 3.2, 3.5C and 3.7 were measured by drawing a 10-pixel wide line from the oocyte to the follicle cells and measuring the mean intensity across the line in all three channels (Bazooka::GFP, Jupiter::mCherry, and polarized transmission light). These measurements were performed on deconvolved images. Profiles of signal intensities at the posterior membrane of the oocytes (Figure 3.5B) were calculated by drawing a 10 px wide segmented line across the oocyte posterior cortex. Values of intensities for each frame were normalized using min-max normalization. The zero position on the x-axis represents the polar cells. These measurements were performed on raw images. All calculations and plotting were done using Python.

3.5. Results

3.5.1 Posterior re-localization of Bazooka following contact loss with PFCs in stage 10B oocytes

The localization patterns of Bazooka have been well described up until early stage 10 of oogenesis. At stages 7 and 8, Bazooka localizes to the posterior of the oocyte, where it overlaps with the Par-1 domain, until stage 9 when it is excluded from the posterior (Doerflinger et al., 2010; Jouette et al., 2019). However, the dynamics of Bazooka localization in the following stages is not known. To assess this, we performed live cell imaging of stage 10 and 11 egg chambers expressing Bazooka tagged with GFP (Bazooka::GFP) and Jupiter tagged with mCherry (Jupiter::mCherry) as a reporter for microtubules. We used the Gal4/UASp system to express Bazooka only in the germline since Bazooka localizes to the apical side of follicle cells, thus masking the localization of Bazooka at the oocyte membrane (Jouette et al., 2019). In agreement with previous

results, all but one oocyte show exclusion of Bazooka at stage 10A (n=13). More interestingly, the oocyte is tightly connected to the PFCs at this stage, i.e., a clear cellular boundary between the oocyte and the PFCs is not detected in fluorescence confocal images of microtubules and in polarized transmission light microscopy images (Figure 3.1A, arrowheads). On the other hand, there is a visible gap between the lateral follicle cells and the oocyte. This differential contact correlated with the accumulation of Bazooka; Bazooka localizes at the membrane where the oocyte is not in contact with the follicle cells but is excluded where the contact is established (Figure 3.1A). At stage 11, the cell-cell contact between the oocyte and the PFCs is lost, and a clear boundary is visible, while the exclusion of Bazooka is lost as well (Figure 3.1B).

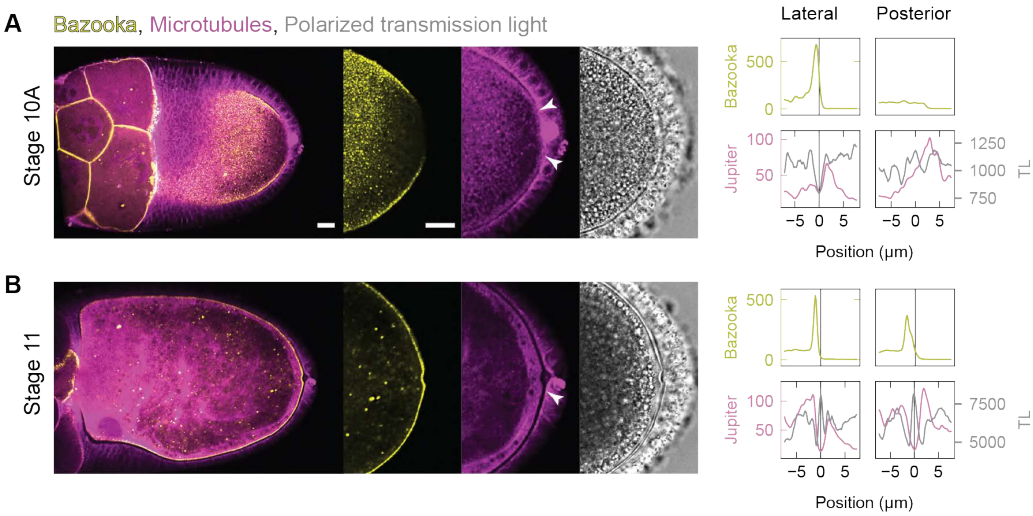

Figure 3.1. **Localization of Bazooka during stages 10 and 11 of oogenesis.** On the left are still images of stage 10A **(A)** and 11 **(B)** egg chambers expressing Bazooka::GFP (yellow) and the microtubule reporter Jupiter::mCherry (magenta) next to a transmission light micrograph (grey). The right graphs are intensity profiles of Bazooka::GFP (yellow), Jupiter::mCherry (magenta), and transmission light (grey) signal along a straight line crossing cell boundaries from the oocyte to either lateral or posterior follicle cells. The x-axis origin and the vertical line represent the local minimum of the Jupiter::mCherry (magenta) signal, which we interpret as extended intercellular space (gap) between the oocyte and the follicle cells. If the intercellular space is not clearly discernible, position 0 μm represents the midpoint of the line. **(A)** At stage 10A, the gap is visible between the oocyte and the lateral follicle cells but not between the oocyte and the posterior follicle cells. The accumulation of Bazooka correlates with the existence of the gap. **(B)** At stage 11, both the gap and Bazooka accumulation are visible at the posterior. The scale bars represent 20 μm.

To understand if the formation of an intercellular space (gap) between PFCs and the oocytes precedes or follows the accumulation of Bazooka at the posterior, we analyzed stage 10B egg chambers in which this transition likely occurs (Figure 3.2). The posterior gap is visible in 83% (30 out of 36) stage 10B egg chambers (Figure 3.2B-D). However, Bazooka

was still excluded from the posterior in 12 of these oocytes (Figure 3.2B, D). Importantly, we did not observe egg chambers where Bazooka accumulated to the posterior before the gap formed. We conclude that the loss of contact between the oocyte and PFCs precedes the accumulation of Bazooka (Figure 3.2E).

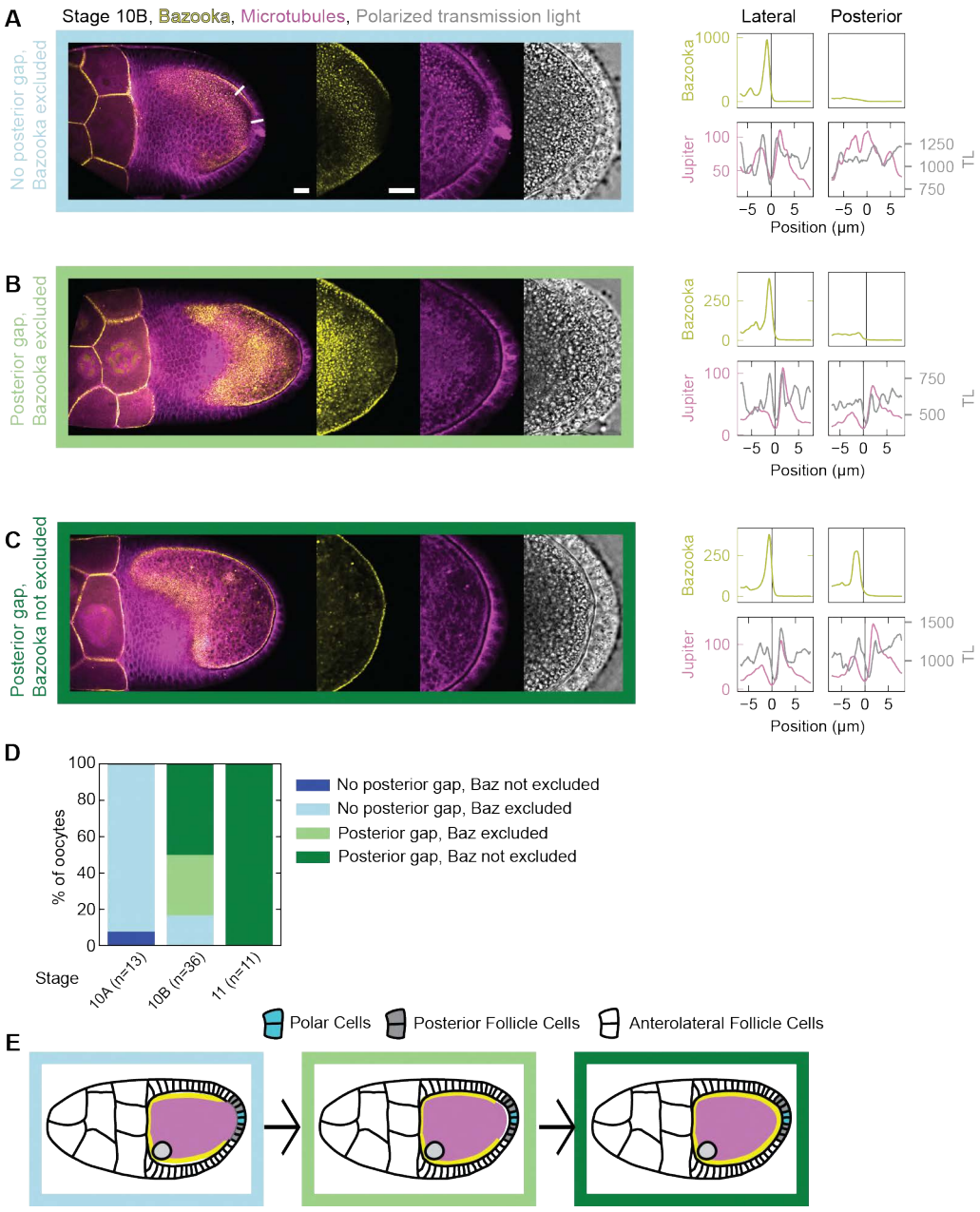

Figure 3.2. **Bazooka accumulates at the posterior following the loss of contact between the oocyte and PFCs at stage 10B of oogenesis. (A–C)** On the left are still images of stage 10B egg chambers expressing Bazooka::GFP (yellow) and the microtubule reporter Jupiter::mCherry (magenta) next to a transmission light micrograph (grey).

continues on next page

Figure 3.2. *continued from previous page*

The right graphs are intensity profiles of Bazooka::GFP (yellow), Jupiter::mCherry (magenta), and transmission light (grey) signal along a straight line crossing cell boundaries from the oocyte to either lateral or posterior follicle cells (see the first image of the panel A). The x-axis origin and vertical line represent the local minimum of the Jupiter::mCherry (magenta) signal, which we interpret as extended intercellular space (gap) between the oocyte and the follicle cells. Whenever this intercellular space is not clearly discernible, position 0 μm represents the midpoint of the line. **(A)** At the beginning of stage 10B, a gap is detected between the oocyte and the lateral follicle cells but not the posterior follicle cells. Accumulation of Bazooka at the oocyte membrane correlates with the existence of the gap. **(B)** Later in stage 10B, a gap is formed at the posterior, but Bazooka does not yet accumulate at the respective oocyte membrane. **(C)** Eventually, Bazooka accumulates to the posterior after the formation of the gap. The scale bars represent 20 μm for panels A–C. **(D)** Distribution of egg chambers showing one of the four possible phenotypes at stages 10A, 10B, and 11. The colors in the plot correspond to the color of the frame surrounding the images in panels A–C. *n* is the number of egg chambers quantified. **(E)** Scheme showing the timeline of events during stage 10B. Loss of contact between the oocyte and PFCs precedes the accumulation of Bazooka to the posterior.

3.5.2 Bazooka accumulates to the posterior before Par-1 clearance at late stage 10B of oogenesis

In *par-1* mutant oocytes, Bazooka localizes all around the cortex, suggesting that Par-1 phosphorylates Bazooka to exclude it from the posterior (Benton and St Johnston, 2003a). To assess if Par-1 needs to be removed from the posterior before Bazooka accumulates, we imaged oocytes expressing fluorescently tagged Par-1 and Bazooka. At stage 10A, we found Bazooka exclusion and Par-1 enrichment in all analyzed oocytes (n=12) (Figure 3.3A, D). On the other hand, at stage 11, both the exclusion of Bazooka and the accumulation of Par-1 at the posterior were lost (n=10) (Figure 3.3C, D).

At stage 10B, Bazooka exclusion was lost in 25 out of 40 oocytes. However, Par-1 was still present at the posterior in 12 of these oocytes (Figure 3.3B, D). Importantly, we never found Par-1 disappearing from the posterior before the accumulation of Bazooka. Therefore, Bazooka first accumulates to the posterior, which eventually leads to the removal of Par-1 from this region. This result suggests that Bazooka accumulation is not the consequence of Par-1 removal and that Par-1 is not sufficient to exclude Bazooka from the posterior.

Taken together, these observations suggest that the loss of contact between PFCs and the oocyte is followed first by recruitment of Bazooka to the posterior, and only thereafter, Par-1 delocalizes from the posterior. We hypothesize that cell-cell contact between PFCs and the oocyte is required to exclude Bazooka from the posterior oocyte membrane.

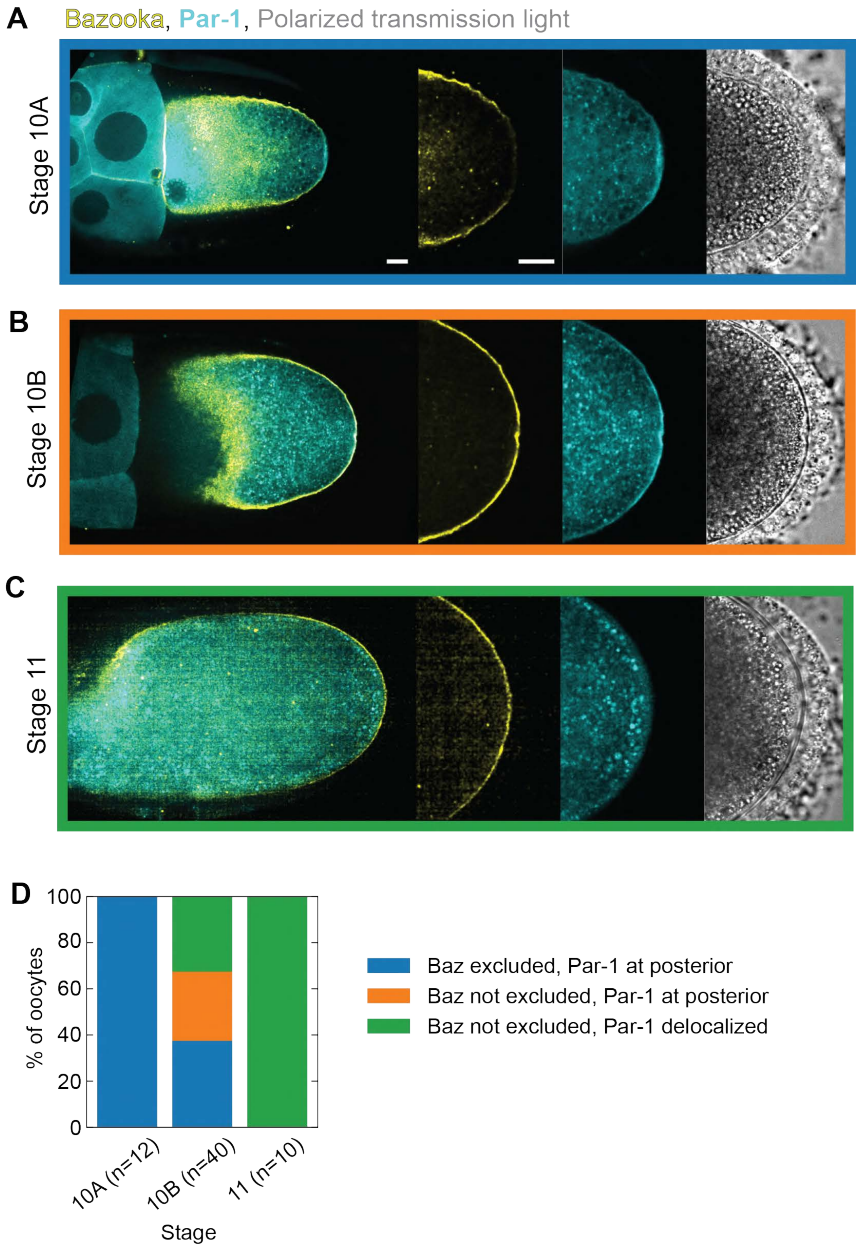

Figure 3.3. **Localization of Par-1 and Bazooka during stages 10 and 11 of oogenesis.** **(A–C)** Stage 10A, 10B and 11 egg chambers expressing Bazooka::mCherry (yellow) and Par-1::GFP (cyan) in the germline. **(A)** At stage 10A, the mutual exclusion zone between Bazooka and Par-1 exists at the posterior.

continues on next page

Figure 3.3. *continued from previous page*

(B) During stage 10B, Bazooka accumulates to the posterior before delocalization of Par-1. **(C)** At stage 11, both the exclusion of Bazooka and the accumulation of Par-1 at the posterior are lost. **(D)** Distribution of egg chambers showing different posterior Par protein localization patterns. The colors in the plot correspond to the color of the frame surrounding the images in panels A–C. Note that Par-1 delocalization never precedes the accumulation of Bazooka. Scale bars represent 20 μm, *n* is the number of egg chambers quantified.

3.5.3 Mechanical detachment of PFCs from the oocyte causes posterior accumulation of Bazooka

To directly test if the contact interaction between the oocyte and the PFCs leads to the exclusion of Bazooka, we designed an experiment by which PFCs were mechanically detached from the oocyte. We used a blunt glass micropipette mounted on a micromanipulator to aspirate and pull on the PFCs, aiming for detachment from the oocyte but keeping them intact (Figure 3.4).

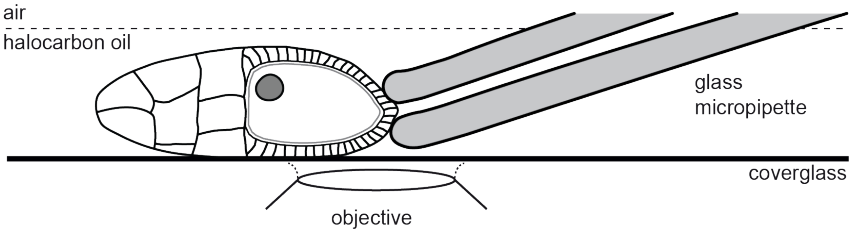

Figure 3.4. **Schematic showing experimental assay to mechanically detach PFCs from the oocyte.** A holding micropipette is used to aspirate and pull on the PFCs.

We combined this assay with live imaging of egg chambers expressing Bazooka::GFP in the germline and Jupiter::mCherry in all tissues to observe any changes in polarity in the oocyte (Figure 3.5A). Indeed, we could observe the accumulation of Bazooka to the posterior of the oocyte

following detachment of the PFCs (Figure 3.5A, B). Importantly, this accumulation was accompanied by the appearance of the intercellular space between oocyte and PFC boundaries (Figure 3.5C). We conclude that mechanical pulling on PFCs causes premature intercellular gap formation, which results in the accumulation of Bazooka to the posterior of the oocyte. This suggests that a firm cell-cell interaction between PFCs and the oocyte is important for maintaining Bazooka exclusion at the posterior end of the oocyte.

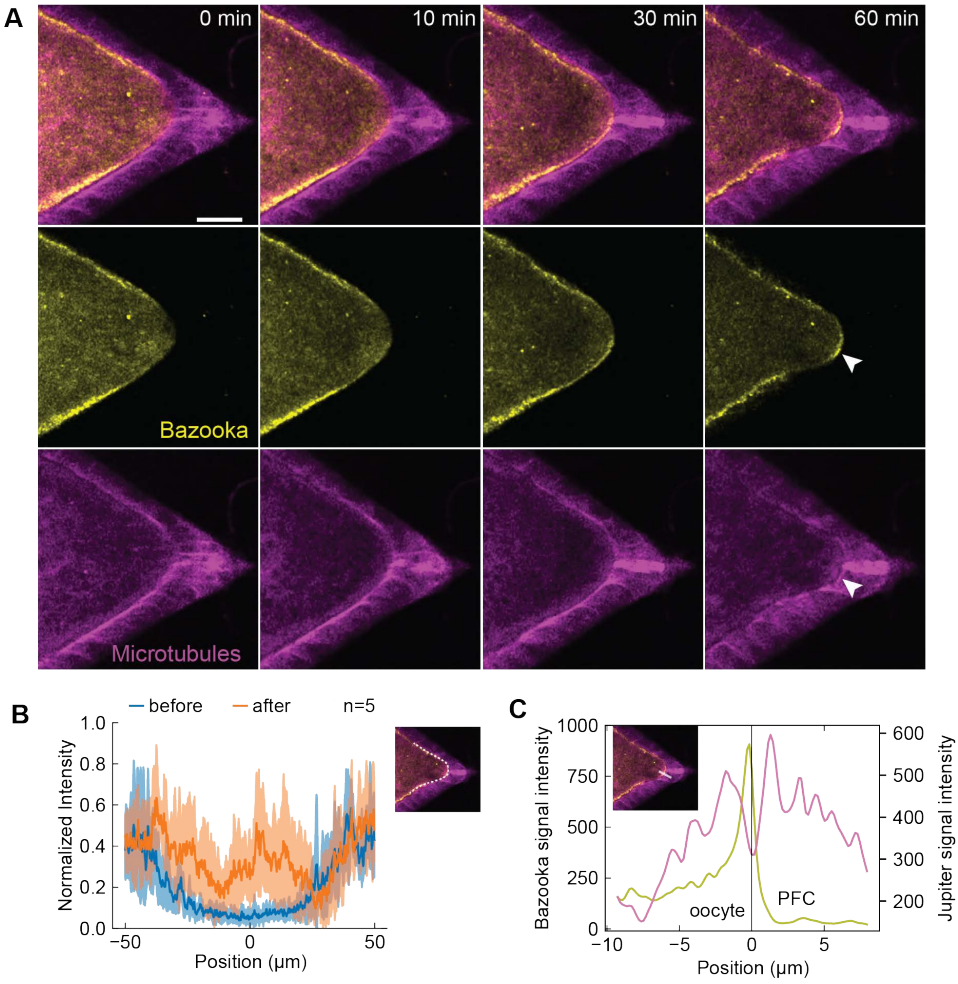

Figure 3.5. **Mechanical detachment of PFCs from the oocyte causes posterior accumulation of Bazooka. (A)** Time-lapse images of an egg chamber expressing Bazooka::GFP (yellow) and the microtubule reporter Jupiter::mCherry (magenta) following detachment of PFCs from the oocyte. Top: merged channels, middle: Bazooka::GFP, bottom: Jupiter::mCherry. Formation of the intercellular space and accumulation of Bazooka are detected at the posterior (arrowheads). Scale bar, 20 μm.

continues on next page

Figure 3.5. *continued from previous page*

(B) The average intensity profile of Bazooka::GFP signal at the posterior of the oocyte, measured along the oocyte cortex as represented by the white line in the inset image. The blue curve is the intensity measured before the PFCs were pulled, and the orange curve is the intensity after 60 min of continuous pulling. The shaded region designates the standard deviation. The x-axis origin represents the position of the polar cells. *n* is the number of experiments. **(C)** Intensity profile of Bazooka::GFP (yellow) and Jupiter::mCherry (magenta) along the line crossing cell boundaries from the oocyte to posterior follicle cells, as shown in the inset. The x-axis origin and vertical line represent the local minimum of the Jupiter::mCherry signal, which we interpret as intercellular space between the oocyte and the follicle cells.

3.5.4 Inhibition of posterior fate determination causes premature gap formation at the posterior and loss of Par polarity in the oocyte

To complement the mechanical manipulation approach, we decided to use genetic approaches to test whether the follicle cells need to adopt the posterior fate to be able to establish contact with the oocyte. For the cells at the posterior of the egg chamber to differentiate correctly, three signaling pathways need to be activated during stages 6 and 7 of oogenesis (Figure 3.6A). First, the germline secretes Delta to activate Notch in the surrounding layer of follicle cells (López-Schier and St Johnston, 2001). Next, the polar cells at the anterior and the posterior of the egg chamber secrete Unpaired to activate the JAK-STAT pathway in the adjacent follicle cells causing them to adopt the terminal fate (Xi et al., 2003). In the absence of further signaling, the terminal follicle cells will adopt the anterior fate (Xi et al., 2003). However, at the posterior of the egg chamber, the oocyte secretes Gurken to activate the EGF pathway in the adjacent layer of terminal follicle cells, which adopt the posterior fate (González-Reyes et al., 1995; Roth et al., 1995; González-Reyes and St

Johnston, 1998b). The inhibition of the JAK-STAT pathway was shown to be sufficient to inhibit the differentiation of main-body cells, resulting in the germline that is surrounded by the uniform layer of main-body follicle cells (Figure 3.6B) (Alégot et al., 2018; Wittes and Schüpbach, 2019). Therefore, we knocked-down *hopscotch (hop)* which is the *Drosophila* homolog of the *jak* gene. We predicted that if the posterior follicle cells do not differentiate correctly and keep the main-body fate instead, the gap between the oocyte and the follicle cells should spread all around the oocyte cortex already at stages 9 and 10A of oogenesis.

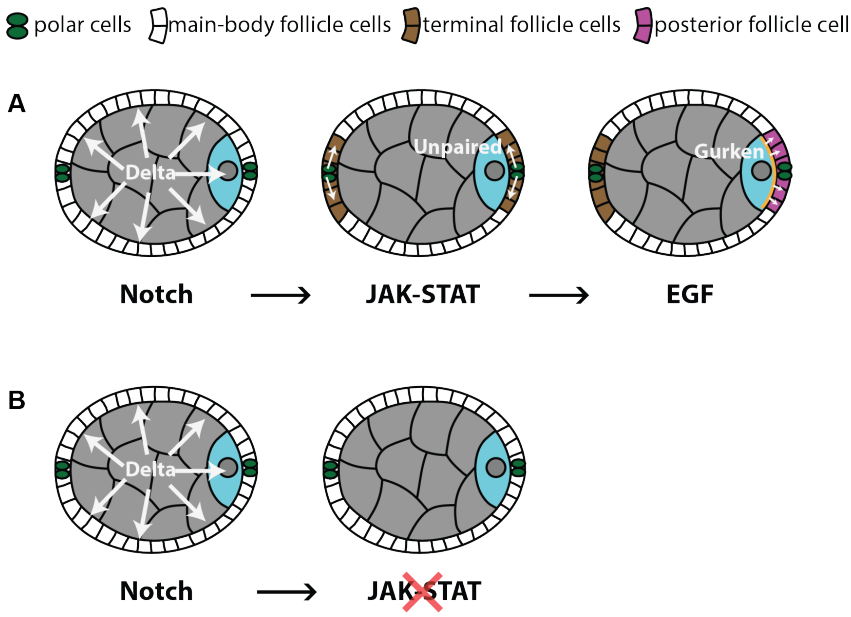

Figure 3.6. **Signaling pathways involved in the follicle cell patterning. (A)** At stage 6 of oogenesis, the germline signals to the follicle cells to activate the Notch pathway. This is needed for the follicle cells to be able to respond to the Unpaired that is secreted by the anterior and posterior pair of polar cells and adopt the terminal fate. At stage 7, the oocyte secretes Gurken to activate the EGF pathway in the adjacent terminal follicle cells inducing posterior follicle cell fate. The anterior terminal follicle cells, which do not receive Gurken signaling, will differentiate into three types of anterior follicle cells (not shown in the scheme). **(B)** Inhibition of the JAK-STAT pathway inhibits any further differentiation, and all follicle cells maintain the main-body fate.

To knock down *hop* in follicle cells, we expressed UAS>hop-dsRNAi using GR1>Gal4 driver, which drives the expression in all follicle cells. The knock-down of *hop* resulted in egg chambers that are rounder than the wild-type, which is in agreement with previous reports on the effects of inhibition of the JAK-STAT pathway (Figure 3.7A) (Alégot et al., 2018; Wittes and Schüpbach, 2019). As we predicted, in these egg chambers, the gap between the oocyte and the follicle cells was detectable all around the oocyte cortex (Figure 3.7).

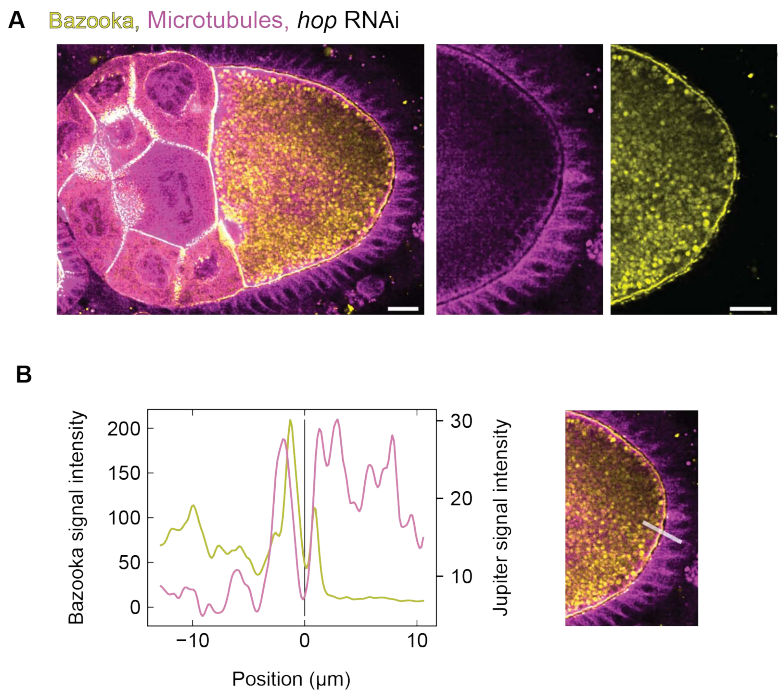

Figure 3.7. **Disruption of JAK-STAT signaling in follicle cells disrupts contact between the oocyte and the follicle cells and Bazooka localization in the oocyte. (A)** Still image of an egg chamber expressing Bazooka::GFP (yellow) and the microtubule reporter Jupiter::mCherry (magenta) in which *hop* was knocked down in follicle cells. The gap is visible between the oocyte and the follicle cells at the posterior, and Bazooka::GFP is not excluded from the oocyte posterior. **(B)** Intensity profile of Bazooka::GFP (yellow) and Jupiter::mCherry (magenta) along the line crossing cell boundaries from the oocyte to the follicle cells, as shown in the micrograph on the right. The x-axis origin and vertical line represent the local minimum of the Jupiter::mCherry signal, which we interpret as intercellular space between the oocyte and the follicle cells. Note that there are two peaks of the Bazooka signal, coming from the oocyte and the follicle cell cortex. Scale bars, 20 μm.

To test if the polarity of the Par network is disrupted in these oocytes, we used UASp>Bazooka::GFP or UASp>GFP::Par-1 in combination with mat-α4>Gal4 driver to express the fluorescently labeled proteins in the

germline. We observed that Bazooka is not excluded from the oocyte posterior when the oocyte and the PFCs do not establish contact (Figure 3.7A, B). In contrast, Par-1 was either completely absent from the oocyte membrane (Figure 3.8A) or polarized in a seemingly random fashion, away from the oocyte posterior (Figure 3.8B).

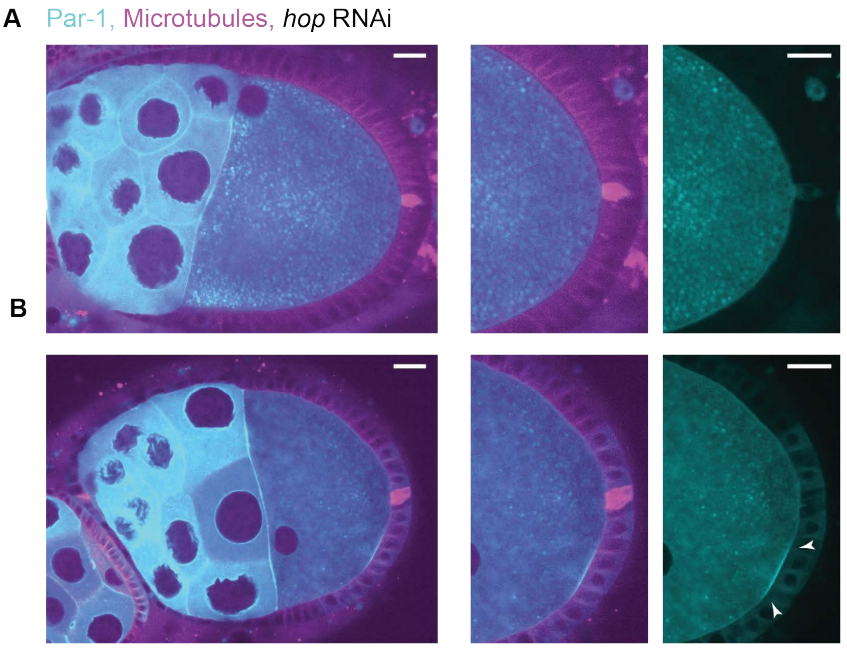

Figure 3.8. **Disruption of JAK-STAT signaling in follicle cells disrupts Par-1 localization in the oocyte. (A-B)** Still images of egg chambers expressing GFP::Par-1 (cyan) and the microtubule reporter Jupiter::mCherry (magenta) in which *hop* was knocked down in follicle cells. Par-1 is either completely absent from the oocyte membrane **(A)** or mislocalized away from the oocyte posterior **(B)**. Scale bars, 20 μm.

3.6. Discussion

In *Drosophila*, the canonical events of oocyte polarization ultimately lead to the delivery of mRNAs to specific regions of the oocyte, which causes a symmetry break of gene expression that defines the head and tail of the future embryo (St Johnston and Nusslein-Volhard, 1992). The main

posterior determinant is *oskar* mRNA, which is delivered to the posterior by two distinct processes – directed transport and cytoplasmic streaming (Lu et al., 2018). Delivery through kinesin-dependent directed transport occurs during the mid-stages of oogenesis. At this time, the microtubule cytoskeleton needs to be polarized so that plus ends preferentially accumulate at the posterior. This is achieved through Par-1 dependent inhibition of microtubule nucleation at the posterior (Nashchekin et al., 2016; Parton et al., 2011). Our results show that cell contact with PFCs inhibits Bazooka accumulation and retains Par-1 localization at the posterior of the oocyte. Therefore, PFCs have a crucial role in maintaining the polarization of the microtubule cytoskeleton during stages when *oskar* mRNA is delivered to the posterior by microtubule-mediated directed transport. At stage 10B, the mechanism of directed transport is substituted by cytoplasmic streaming, which delivers mRNA particles in bulk to the posterior where *oskar* is anchored by myosin V (Lu et al., 2018).

Interestingly, this is the stage at which we observe the loss of contact between the PFCs and the oocyte, as well as the loss of Par polarity. However, since polarization of the microtubule network is not necessary for cytoplasmic streaming, this does not compromise *oskar* localization during late oogenesis. Instead of maintaining tight contact between PFCs and the oocyte, molecular components building the eggshell can now be deposited into the intercellular space by the follicle cells to prepare for egg maturation (Cavaliere et al., 2008).

What distinguishes the cell-cell contact to PFCs from that of lateral follicle cells? Recent screening found that components of extracellular matrix (ECM) and ECM-associated proteins are upregulated in PFCs (Wittes and Schüpbach, 2019). A growing body of evidence suggests that there is a crosstalk between cell-ECM and cell-cell adhesion (Mui1 et al., 2016). For example, integrins have been reported to increase the strength

of cadherin adhesions (Martinez-Rico et al., 2010). Therefore, PFCs-ECM interaction may affect the adhesion between the PFCs and the oocyte. Alternatively, differential expression of eggshell genes occurs in the different subtypes of follicle cells. The eggshell is composed of five distinct layers, for which the molecular components are secreted by the follicle cells. The first layer is the vitelline membrane, which starts to be deposited at stage 9, at the time when Bazooka is excluded from the posterior (Cavaliere et al., 2008). There are four vitelline membrane genes, one of which, *VM32E*, is expressed in the main-body follicle cells but not in the PFCs (Gargiulo et al., 1991). At stage 10, VM32E protein is found at the interface between main-body follicle cells and the oocyte, but not at the posterior (Andrenacci et al., 2001). Interestingly, the protein spreads to the posterior by stage 11, which is the time when the connection between the PFCs and the oocyte is lost. Therefore, VM32E may be involved in separating follicle cells from the oocyte. Alternatively, the loss of contact between the PFCs and the oocyte could result from the deposition of the second layer of eggshell, a vax layer, which starts at late stage 10 (Cavaliere et al., 2008).

Whatever the mechanism of keeping the oocyte and PFCs in close contact is, it seems to be important to maintain Bazooka exclusion. Interestingly, the first anterior-posterior polarization event - positioning of the oocyte to the posterior of the germline cyst at stage 1 – is facilitated by cadherin-mediated adhesion between follicle cells and the oocyte (Godt and Tepass, 1998; González-Reyes and St Johnston, 1998a). In addition, the Par network becomes transiently polarized around this stage, with Par-1 at the posterior and Bazooka at the anterior of the oocyte (Vaccari and Ephrussi, 2002). Based on this, it has been suggested that follicle cells are also involved in this first polarization of the oocyte (Roth and Lynch, 2009).

A change in adhesion between PFCs and the oocyte has been

proposed as a mechanism by which the polarizing signal could be transferred from the PFCs to the oocyte at stage 7 (Poulton and Deng, 2007). How could the adhesion between follicle cells and the oocyte translate into oocyte polarization? Signals derived from cell-cell contact are regulators of polarization in many cells and contexts (Ebnet et al., 2018). The most obvious downstream target of adhesion between the PFCs and the oocyte is the actin cytoskeleton. Cell adhesion modulates actin organization and dynamics (Bachir et al., 2017). On the other hand, an intact actin cytoskeleton is required both for posterior enrichment of Par-1 and exclusion of Bazooka (Doerflinger et al., 2006; Jouette et al., 2019). Recently, myosin II activation at the posterior of the oocyte has been identified as the first known signal of oocyte polarity following the signal from PFCs. It has been proposed that activated myosin II increases tension at the oocyte posterior, which might be necessary to recruit Par-1 (Doerflinger et al., 2022). E-cadherin has been reported to promote the recruitment and activation of myosin II in epithelia (Shewan et al., 2005). Therefore, it is possible that adhesion between the oocyte and PFCs causes specific activation of myosin II at the posterior. Alternatively, the polarizing cue could be transferred from PFCs to the oocyte through a trafficking dependent process. Endocytosis is elevated at the posterior of the oocyte, and this has been linked to posterior localization of *oskar* (Tanaka and Nakamura, 2008; Vanzo et al., 2007). Additionally, Bazooka is not excluded from the posterior following either knockdown of Rab-5 or expression of a dominant negative form of Rab-5 in the oocyte. On the contrary, overexpression of the PIP5Kinase Skittles (SKTL), which produces phosphoinositide PI(4,5)P2, bypasses the need for Par-1 to have Bazooka excluded from the posterior. PI(4,5)P2 plays a role in the first steps of endocytosis, suggesting that SKTL overexpression rescues Bazooka exclusion in *par-1* mutants by increasing endocytosis (Jouette et al., 2019). The trafficking could work either through direct delivery of a

polarizing signal or by a passive process, for example by remodeling the posterior membrane or through membrane flows (Gerganova et al., 2021).

3.7. Acknowledgements

I thank Ivo Telley for supervision, Jorge de-Carvalho for the initial help with experiments, and all members of the Telley lab for fruitful discussions. I also thank the staff of the Fly Facility, the Advanced Imaging Facility (AIF), and the Technical Support Service at the Instituto Gulbenkian de Ciência (IGC). Finally, I thank Daniel St. Johnston (The Gurdon Institute) for fly line donations and The Bloomington Drosophila Stock Center for their services.

3.8. Bibliography

H. Alégot, P. Pouchin, O. Bardot, and V. Mirouse. Jak-stat pathway induces drosophila follicle elongation by a gradient of apical contractility. *eLife*, 7: 1–21, 2018.

D. Andrenacci, F. M. Cernilogar, C. Taddei, D. Rotoli, V. Cavaliere, F. Graziani, and G. Gargiulo. Specific domains drive vm32e protein distribution and integration in drosophila eggshell layers. *Journal of Cell Science*, 14:2819–2829, 2001.

A. I. Bachir, A. R. Horwitz, W. J. Nelson, and J. M. Bianchini. Actin-based adhesion modules mediate cell interactions with the extracellular matrix and neighboring cells. *Cold Spring Harbor Perspectives in Biology*, 9: 1–19, 2017.

R. Benton and D. St Johnston. Drosophila par-1 and 14-3-3 inhibit bazooka/par-3 to establish complementary cortical domains in polarized cells. *Cell*, 115:691–704, 2003a.

R. Benton and D. St Johnston. A conserved oligomerization domain

in drosophila bazooka/par-3 is important for apical localization and epithelial polarity. *Current Biology*, 13:1330–1334, 2003b.

V. Cavaliere, F. Bernardi, P. Romani, S. Duchi, and G. Gargiulo. Building up the drosophila eggshell: First of all the eggshell genes must be transcribed. *Developmental Dynamics*, 237:2061–2072, 2008.

H. Doerflinger, R. Benton, I. L. Torres, M. F. Zwart, and D. St Johnston. Drosophila anterior-posterior polarity requires actin-dependent par-1 recruitment to the oocyte posterior. *Current Biology*, 16:1090–1095, 2006.

H. Doerflinger, N. Vogt, I. L. Torres, V. Mirouse, I. Koch, C. Nüsslein-Volhard, and D. St Johnston. Bazooka is required for polarisation of the drosophila anterior-posterior axis. *Development*, 137:1765–1773, 2010.

H. Doerflinger, V. Zimyanin, and D. St Johnston. The drosophila anterior-posterior axis is polarized by asymmetric myosin activation. *Current Biology*, 32:374–385, 2022.

K. Ebnet, D. Kummer, T. Steinbachera, A. Singh, M. Nakayama, and M. Matis. Regulation of cell polarity by cell adhesion receptors. *Seminars in Cell and Developmental Biology*, 81:2–12, 2018.

G. Gargiulo, S. Gigliotti, C. Malva, and F. Graziani. Cellular specificity of expression and regulation of drosophila vitelline membrane protein 32e gene in the follicular epithelium: identification of cis-acting elements. *Mechanisms of Development*, 35:193–203, 1991.

V. Gerganova, I. Lamas, D. M. Rutkowski, A. Vještica, D. Gallo Castro, V. Vincenzetti, D. Vavylonis, and S. G. Martin. Cell patterning by secretion-induced plasma membrane flows. *Science Advances*, 7:1–19, 2021.

D. Godt and U. Tepass. Drosophila oocyte localization is mediated by differential cadherin-based adhesion. *Nature*, 395(6700):387–391, 1998.

A. González-Reyes and D. St Johnston. Role of oocyte position in establishment of anterior-posterior polarity in drosophila. *Science*, 266: 639–642, 1994.

A. González-Reyes and D. St Johnston. The drosophila ap axis is polarised by the cadherin-mediated positioning of the oocyte. *Development*, 125 (18):3635–3644, 1998a.

A. González-Reyes and D. St Johnston. Patterning of the follicle cell epithelium along the anterior-posterior axis during drosophila oogenesis. *Development*, 125(15):2837–2846, 1998b.

A. González-Reyes, H. Elliott, and D. St Johnston. Polarization of both major body axes in drosophila by gurken-torpedo signalling. *Nature*, 375: 645–658, 1995.

C. Hoege and A. A. Hyman. Principles of par polarity in caenorhabditis elegans embryos. *Nature Reviews Molecular Cell Biology*, 14:315–322, 2013.

J.-R. Huynh, J. M. Shulman, R. Benton, and D. St Johnston. Par-1 is required for the maintenance of oocyte fate in drosophila. *Development*, 128:1201–1209, 2001.

J. Jouette, A. Guichet, and S. B. Claret. Dynein-mediated transport and membrane trafficking control par3 polarised distribution. *eLife*, 8:1–28, 2019.

C. F. Lang and E. Munro. The par proteins : from molecular circuits to dynamic self-stabilizing cell polarity. *Development*, 144:3405–3416, 2017.

H. López-Schier and D. St Johnston. Delta signaling from the germ line controls the proliferation and differentiation of the somatic follicle cells during drosophila oogenesis. *Genes and Development*, 15(11):1393–1405, 2001.

N. Lowe, J. S. Rees, J. Roote, E. Ryder, I. M. Armean, G. Johnson, E. Drummond, H. Spriggs, J. Drummond, J. P. Magbanua, H. Naylor, B. Sanson, R. Bastock, S. Huelsmann, V. Trovisco, M. Landgraf, S. Knowles-Barley, J. D. Armstrong, H. White-Cooper, C. Hansen, R. G. Phillips, The UK Drosophila Protein Trap Screening Consortium, K. S. Lilley, S. Russell, and D. St Johnston. Analysis of the expression patterns, subcellular localisations and interaction partners of drosophila proteins using a pigp protein trap library. *Development*, 141:3994–4005, 2014.

W. Lu, M. Lakonishok, A. S. Serpinskaya, D. Kirchenbüechler, S. Ling, and V. I. Gelfand. Ooplasmic flow cooperates with transport and anchorage in drosophila oocyte posterior determination. *Journal of Cell Biology*, 217:3497–3511, 2018.

W. Lu, M. Lakonishok, R. Liu, N. Billington, A. Rich, M. Glotzer, J. R. Sellers, and V. I. Gelfand. Competition between kinesin-1 and myosin-v defines drosophila posterior determination. *eLife*, 9:1–25, 2020.

C. Martinez-Rico, F. Pincet, J.-P. Thiery, and S. Dufour. Integrins stimulate e-cadherin-mediated intercellular adhesion by regulating src-kinase activation and actomyosin contractility. *Journal of Cell Science*, 123:712–722, 2010.

F. Motegi and G. Seydoux. The par network: Redundancy and robustness in a symmetry-breaking system. *Philosophical Transactions of the Royal Society B: Biological Sciences*, 368:1–11, 2013.

K. L. Mui1, C. S. Chen, and R. K. Assoian. The mechanical regulation of integrin-cadherin crosstalk organizes cells, signaling and forces. *Journal of Cell Science*, 129:1093–1100, 2016.

D. Nashchekin, A. Ribeiro Fernandes, and D. St Johnston. Patronin/shot cortical foci assemble the noncentrosomal microtubule array that specifies the drosophila anterior-posterior axis. *Developmental Cell*, 38: 61–72, 2016.

C. Niehrs. On growth and form: a cartesian coordinate system of wnt and bmp signaling specifies bilaterian body axes. *Development*, 137:845–857, 2010.

R. M. Parton, R. S. Hamilton, G. Ball, L. Yang, C. F. Cullen, W. Lu, H. Ohkura, and I. Davis. A par-1–dependent orientation gradient of dynamic microtubules directs posterior cargo transport in the drosophila oocyte. *The Journal of Cell Biology*, 194(1):121–135, 2011.

J. S. Poulton and W.-M. Deng. Cell-cell communication and axis specification in the drosophila oocyte. *Developmental Biology*, 311:1–10, 2007.

V. Riechmann and A. Ephrussi. Axis formation during drosophila oogenesis. *Current Opinion in Genetics and Development*, 11:374–383, 2001.

S. Roth and J. A. Lynch. Symmetry breaking during drosophila oogenesis. *Cold Spring Harbor Perspectives in Biology*, 1:a001891, 2009.

S. Roth, F. S. Neuman-Silberberg, G. Barcelo, and T. Schupbach. cornichon and the egf receptor signaling process are necessary for both anterior-posterior and dorsal-ventral pattern formation in drosophila. *Cell*, 81:967–978, 1995.

J. Schindelin, I. Arganda-Carreras, E. Frise, V. Kaynig, M. Longair, T. Pietzsch, S. Preibisch, C. Rueden, S. Saalfeld, B. Schmid, J.-Y. Tinevez, D. J. White, V. Hartenstein, K. Eliceiri, P. Tomancak, and A. Cardona. Fiji: an open-source platform for biological-image analysis. *Nature Methods*, 9:676–682, 2012.

A. M. Shewan, M. Maddugoda, A. Kraemer, S. J. Stehbens, S. Verma, E. M. Kovacs, and A. S. Yap. Myosin 2 is a key rho kinase target necessary for the local concentration of e-cadherin at cell-cell contacts. *Molecular Biology of the Cell*, 16:4531–4542, 2005.

J. M. Shulman, R. Benton, and D. St Johnston. The drosophila homolog of c. elegans par-1 organizes the oocyte cytoskeleton and directs oskar mrna localization to the posterior pole. *Cell*, 101:377–388, 2000.

D. St Johnston and C. Nusslein-Volhard. The origin of pattern and polarity in the drosophila embryo. *Cell*, 68:201–219, 1992.

T. Tanaka and A. Nakamura. The endocytic pathway acts downstream of oskar in drosophila germ plasm assembly. *Development*, 135:1107–1117, 2008.

P. Tomancak, F. Piano, V. Riechmann, K. C. Gunsalus, K. J. Kemphues, and A. Ephrussi. A drosophila melanogaster homologue of caenorhabditis elegans par-1 acts at an early step in embryonic-axis formation. *Nature Cell Biology*, 2:458–460, 2000.

T. Vaccari and A. Ephrussi. The fusome and microtubules enrich par-1 in the oocyte, where it effects polarization in conjunction with par-3, bicd, egl, and dynein. *Current Biology*, 12:1524–1528, 2002.

N. Vanzo, A. Oprins, D. Xanthakis, A. Ephrussi, and C. Rabouille. Stimulation of endocytosis and actin dynamics by oskar polarizes the drosophila oocyte. *Developmental Cell*, 12:543–555, 2007.

J. Wittes and T. Schüpbach. A gene expression screen in drosophila melanogaster identifies novel jak/stat and egfr targets during oogenesis. *G3*, 9:47–60, 2019.

R. Xi, J. R. McGregor, and D. A. Harrison. A gradient of jak pathway activity patterns the anterior-posterior axis of the follicular epithelium. *Developmental Cell*, 4(2):167–177, 2003.

V. L. Zimyanin, K. Belaya, J. Pecreaux, M. J. Gilchrist, A. Clark, I. Davis, and D. St Johnston. In vivo imaging of oskar mrna transport reveals the mechanism of posterior localization. *Cell*, 134:843–853, 2008.

4. Chapter 4: Posterior follicle cells maintain main body axis polarity in the oocyte

Parts of this chapter are adapted from:

A. Milas, J. de-Carvalho, I. A. Telley. Follicle cell contact maintains main body axis polarity in the *Drosophila melanogaster* oocyte. *bioRxiv*, 2022, DOI: https://doi.org/10.1101/2022.03.03.482911

4.1. Author Contributions

The experiments presented in this chapter were designed by myself and my supervisor Ivo Telley. I performed all experiments with initial help from Jorge de-Carvalho (Instituto Gulbenkian de Ciência). I performed all the data analysis presented in this chapter, except for the analysis shown in Figure 4.9C, which was done by Ivo Telley. Ivo Telley designed and assembled the microscopy and laser ablation platform. The article on which this chapter is based was written by me and Ivo Telley.

4.2. Summary

In *Drosophila melanogaster*, the anterior-posterior body axis is maternally established and governed by differential localization of partitioning defective (Par) proteins within the oocyte. At mid-oogenesis, Par-1 accumulates at the posterior end of the oocyte, while Par-3/Bazooka is excluded there but maintains its localization along the remaining oocyte cortex. This mutual exclusion leads to a polarised microtubule network and accumulation of posterior determinant *oskar* later in oogenesis. Reciprocal biochemical interactions between Par proteins provided explanation for cortical exclusion and domain formation at mid-oogenesis. However, both past studies and our observations show that Par-1 and

Bazooka can colocalize during early and late oogenesis. In addition, our results presented in the previous two chapters showed that the posterior follicle cells (PFCs) maintain the exclusion of Bazooka from the posterior of the oocyte until late oogenesis.

In this chapter, we used laser ablation to further probe the maintenance role of PFCs and test the current understanding of the interactions between Par proteins in mid-oogenesis. As expected, laser ablation of stage 9 or 10A egg chambers resulted in localization of Bazooka to the posterior membrane. However, accumulation of Bazooka was limited to the membrane in contact with the ablated follicle cells, meaning that the intact PFCs maintained the ability to exclude Bazooka. This occurs before Par-1 is removed, suggesting that the phosphorylation of Bazooka by Par-1 is insufficient to maintain Bazooka exclusion in the absence of PFC contact. Par-1 did get excluded from the posterior after accumulation of Bazooka, followed by exclusion of *oskar* mRNA and local accumulation of microtubules.

In conclusion, we show that the mutual antagonism between Par proteins is not sufficient to maintain the polarity of the Par network and the microtubule cytoskeleton in the oocyte during mid-oogenesis. Instead, PFCs maintain both Bazooka exclusion and Par-1 enrichment at the posterior of the oocyte with a cell-size precision. This enables the anchoring of *oskar* mRNA to the posterior of the oocyte and the polarization of the microtubule network.

4.3. Introduction

Asymmetric localization of Par proteins is the hallmark of the cellular polarities across the metazoa (Goldstein and Macara, 2007). In *C. elegans* zygote, Par proteins form two mutually exclusive domains to define the anterior-posterior axis. The Par-3/Par-6/aPKC complex localizes to the anterior, while Par-1, Par-2, and Lgl localize to the

posterior. The main mechanism by which Pars regulate each other is through phosphorylation. Par-1 phosphorylates Par-3, while aPKC phosphorylates Par-1. The phosphorylation changes the protein's net charge and decreases its affinity for membrane binding (Hoege and Hyman, 2013; Lang and Munro, 2017; Motegi and Seydoux, 2013).

In stage 9 *Drosophila* oocyte, Par proteins form an anterolateral domain - enriched in Par3/Bazooka, Par6, and aPKC - and a posterior domain defined by the localization of Par-1 and Lgl (Doerflinger et al., 2010; Morais-de-Sá et al., 2014; Shulman et al., 2000; Doerflinger et al., 2006; Tian and Deng, 2008). The phosphorylation events that occur in *C. elegans* seem to be conserved in this system. When the phosphorylation sites of either Bazooka or Par-1 are mutated, they localize all around the oocyte cortex (Benton and St Johnston, 2003a; Doerflinger et al., 2010). Furthermore, Bazooka localization is impaired in *par-1* mutants and vice versa (Benton and St Johnston, 2003a; Doerflinger et al., 2010; Becalska and Gravis, 2010).

However, although the antagonism between anterior and posterior Pars is undoubtedly necessary to maintain the polarization, growing evidence indicates that it might not be sufficient. The asymmetric localization of Pars described above is evident only starting at stage 9 of oogenesis, while Par-1, Bazooka, and Par-6 all colocalize at the posterior of the oocyte at stages 7 and 8 (Doerflinger et al., 2010; Jouette et al., 2019). Our results presented in the previous chapter further support this idea. We showed that Bazooka accumulates at the posterior of the oocyte at late stage 10B, where it colocalizes with Par-1. Therefore, the two Par domains are clearly distinguishable for only about 12 hours it takes for the oocyte to develop from the late stage 9 to the late stage 10B of oogenesis (Jia et al., 2016).

During this time, *oskar* and *bicoid* mRNAs are delivered to the posterior and the anterior of the oocyte, respectively. This ultimately defines the anterior-posterior axis of the future embryo (Riechmann and

Ephrussi, 2001). *oskar* mRNA is removed from the cortex at which the microtubules nucleate by the kinesin-dependent transport (Lu et al., 2018, 2020; Zimyanin et al., 2008). Therefore, the microtubule nucleation has to be inhibited at the posterior of the oocyte. This is accomplished by posteriorly localized Par-1, which inhibits the cortical recruitment of the microtubule-assembling Shot/Patronin complex (Nashchekin et al., 2016; Parton et al., 2011). Therefore, although the period at which Par polarity is maintained is short compared to the ten days of oogenesis, this transient Par asymmetry is crucial for egg development.

Our observations from the previous chapter showed that the contact between the oocyte and the posterior follicle cells (PFCs) is necessary to maintain the posterior exclusion of Bazooka up until late stage 10B of oogenesis. In this chapter, I present our effort to further dissect the role of PFCs during mid-oogenesis. Instead of physical manipulations, we use laser ablation to destroy a subset of PFCs. We show that exclusion of Bazooka from the posterior is lost following laser ablation of the PFCs. Bazooka accumulates to the posterior before Par-1 is removed, indicating that Par-1 phosphorylation of Bazooka is insufficient to maintain its exclusion in the absence of PFCs. Par-1 is eventually removed from the posterior, followed by the removal of *oskar* mRNA and posterior nucleation of microtubules. Therefore, the PFCs enable both Bazooka exclusion and Par-1 enrichment at the posterior to maintain the proper localization of mRNAs and polarization of the microtubule cytoskeleton.

4.4. Materials and methods

4.4.1 Fly lines and fly husbandry

Fly stocks were reared according to standard procedures and maintained at 25℃. The list of fly lines used in this chapter is given in Table 4.1.

Table 4.1. Fly lines used in the experiments presented in this chapter. BDSC = Bloomington Drosophila Stock Center

Genotype	**Origin**	**Reference**
w; +; Jupiter::mCherry	Daniel St Johnston	(Lowe et al., 2014)
w; +; Jupiter::GFP	BDSC	BDSC #6836
w; UASp>GFP::Par-1(N1S)/CyO; +	Daniel St Johnston	(Huynh et al., 2001)
w; UASp>Bazooka::mGFP/CyO; +	Daniel St Johnston	(Benton and St Johnston, 2003b)
w; UASp>Bazooka::mCherry/CyO; +	BDSC	BDSC #65844
w; GFP::aPKC; +	Eurico Morais-de-Sá	(Chen et al., 2018)
w; +; osk>osk::MS2(10x)/TM3, Sb	Anne Ephrussi	(Zimyanin et al., 2008)
w; hsp83>MCP::mCherry/CyO; +	Anne Ephrussi	(Gáspár et al., 2017; Weil et al., 2006)
w; mat-α4>Gal4; +	BDSC	BDSC #7062
w; +; mat-α4>Gal4	BDSC	BDSC #7063

The UASp>GFP::Par-1(N1S) isoform rescues the *par-1* mutant (Doerflinger et al., 2006). The rescuing activity of the UASp>Bazooka::mGFP transgene was demonstrated by Benton and St Johnston, 2003b. To express fluorescently labeled polarity proteins specifically in the germline, the flies carrying UASp-transgenes were crossed with mat-α4>Gal4 driver using the protocol described in section 2.4.1. Detailed genotypes of flies used in the experiments presented in this chapter are given in Table 3.2.

Table 4.2. Genotypes of flies used in the experiments presented in this chapter.

Genotype	Figures
w; mata-α4>Gal4/UASp>Bazooka::mGFP; Jupiter:mCherry/Jupiter::mCherry	4.1, 4.2, 4.4
w; mata-α4>Gal4/UASp>GFP::Par-1(N1S); Jupiter:mCherry/Jupiter::mCherry	4.5
w; UASp>GFP::Par-1(N1S)/UASp>Bazooka::mCherry; mata-α4>Gal4/+	4.6, 4.7
w; UASp>GFP::Par-1(N1S)/hsp83>MCP::mCherry; mata-α4>Gal4/osk>osk::MS2(10x)	4.9
w; +/hsp83>MCP::mCherry; Jupiter::GFP/osk>osk::MS2(10x)	4.10
w; GFP::aPKC/UASp>Bazooka::mCherry; +/mata-α4>Gal4	4.11

4.4.2 Sample preparation

For experiments shown in Figures 4.2-4.6, ovaries were dissected in a drop of halocarbon oil (Voltalef 10S, Arkema) placed on a clean coverslip, using tweezers to separate individual germaria. For experiments shown in Figures 4.7-4.11, ovaries were dissected in a drop of Schneider's medium supplemented with 10% FBS and 200 μg/mL insulin. Dissected ovaries were incubated 2x30s in 20 μL of supplemented Schneider's medium. Finally, ovaries were transferred to a drop of supplemented Schneider's medium on a clean coverslip next to a drop of halocarbon oil, and individual germaria were pulled into the oil. This latter protocol improved the sample lifetime and allowed for longer time-lapse imaging.

4.4.3 Microscopy

Imaging was performed on a Nikon Eclipse Ti-E microscope equipped with a Yokogawa CSU-W Spinning Disk confocal scanner and a piezoelectric stage (737.2SL, Physik Instrumente), using 40x water

immersion objective and 488 nm and 561 nm laser lines for excitation of GFP and mCherry, respectively. Images were acquired at 73 focal planes with 0.5 μm z-spacing. x-y pixel size was 162 nm. An Andor iXon3 888 EMCCD camera was used for time-lapse acquisitions. Images were acquired every 30 s (in experiments shown in Figures 4.1, 4.2, 4.4, 4.5) or every 60 s (in experiments shown in Figures 4.6 and 4.7) for 60–90 minutes. To assess Par protein dynamics at longer timescales (Figures 4.9, 4.10, 4.11), images were acquired every 5 min for at least 150 minutes.

4.4.4 Laser ablation

The laser ablation system used is described elsewhere (de Carvalho et al., 2022). Follicle cells were ablated using circular ablation (60 px diameter, 5 px step size). Ablation was performed several times while moving manually in the z-direction to UV-expose the entire depth of the cells. In samples that were not dissected in Schneider's medium, ablation was performed 25 times using 50% laser power. When the sample was dissected in Schneider's medium laser ablation became more effective, presumably because the egg chambers are surrounded by a thin layer of the aqueous solution. Therefore, ablation in these samples was performed five times using 20% laser power. To control for unspecific effects of laser ablation, the ooplasm was ablated using identical power settings

4.4.5 Fluorescence recovery after photobleaching (FRAP)

Par1::GFP at the oocyte membrane was bleached along a $\sim$100 px long line using the laser used for the ablation (2% laser power, 1 px step size). Bleaching was performed in 10 z-planes with 0.5 μm spacing between planes. Images were acquired every 15 s for 15 min. At least two images before photobleaching were acquired.

4.4.6 Image analysis

Images were deconvolved as described in section 2.4.4. Images shown in the figures were made by calculating the sum of 6 z-slices in Fiji/ImageJ (National Institutes of Health; Schindelin et al. (2012)). All measurements were performed in Fiji/ImageJ on 6 z-slices. All measurements were performed on raw images.

Profiles of signal intensities at the posterior membrane of the oocytes were calculated by drawing a 10 px wide segmented line across the oocyte posterior cortex. Values of intensities for each frame were normalized using min-max normalization. The zero position on the x-axis represents the reference point, i.e., the polar cells or the ablation spot.

To calculate the posterior to lateral intensity ratio, a 10 px wide and $\sim$50 μm long line was drawn at the posterior and lateral membrane cortex of the oocyte. Mean intensity across this line was calculated, and the mean value of the background signal was subtracted from this value. The background signal was measured by drawing a 10 px wide and $\sim$50 μm long line in an area of the image where there was no egg chamber.

To measure the change in intensity over time, a 10 px wide segmented line was drawn, covering only the membrane that was previously in contact with ablated follicle cells. The line was manually moved if necessary due to the x-y drift of the sample. The mean value of intensity across this line was measured in all time frames. Background signal was measured in the ooplasm next to the posterior membrane of the oocyte, using a 10 px wide and $\sim$50μm long line. The intensity shown in the graphs was calculated by subtracting the mean value of the background signal from the mean intensity at the membrane. To produce the heatmaps, the profile of intensity across the line was obtained, and the mean background signal was subtracted. Since the length of the ablation region was different in different experiments, the values of pixel intensities were binned into 30 bins. The final heatmaps show the intensity in 30 bins

averaged over several experiments.

Mean fluorescence intensities of the photobleached region were measured by drawing a 10 px wide line over the region. To correct for photobleaching, the mean intensity of the reference signal was measured inside the ooplasm. The background signal, measured outside of the egg chamber, was subtracted from the signal measured in both bleached and reference regions. The normalized intensity was calculated as: $I = \frac{I_{ROI}}{I_{ROI,0}} \cdot \frac{I_{REF,0}}{I_{REF}}$.

Where I_{ROI} and I_{REF} are background-subtracted intensity at the bleached region and reference region, respectively. $I_{ROI,0}$ and $I_{REF,0}$ are intensities before bleaching.

The normalized intensity was fitted to single exponential equations of the form: $I = 1 - e^{-kt}$.

Finally, the half-time of recovery was calculated as: $t_{\frac{1}{2}} = \frac{ln2}{k}$.

Statistical analysis, curve fitting, and plotting were done using Python. Information on sample size, statistical tests, and p-values are shown in figures or mentioned in figure captions.

4.5. Results

4.5.1 Posterior follicle cells maintain the posterior exclusion of Bazooka with cell size-precision

Since cell differentiation of follicle cells into PFCs is necessary to establish the polarity of the oocyte in the first place, mutants that disrupt their differentiation do not allow testing of their role in polarity maintenance throughout oogenesis. Therefore, we sought a more acute and spatially targeted perturbation method for disrupting PFCs. We used pulsed UV laser ablation to destroy a small number of PFCs and monitor the resulting changes in Par protein localization in the oocyte, comparing locations where PFCs were removed versus where they are intact. First, we

performed ablation in stage 9 or 10A egg chambers that express Bazooka::GFP in the germline and Jupiter::mCherry in all tissues. In every experiment, Bazooka was excluded from the posterior prior to the ablation (Figure 4.1A, t = –1 min). The ablation of a few PFCs resulted in the accumulation of Bazooka exclusively to the membrane region facing the ablated cells (Figure 4.1B-C). Bazooka did not localize at neighboring regions where PFCs were intact (Figure 4.1B, arrowheads). A quantification of Bazooka::GFP intensity along the posterior cortex of the oocyte showed a signal peak confined to the location of ablated PFCs (Figure 4.1C, vertical lines).

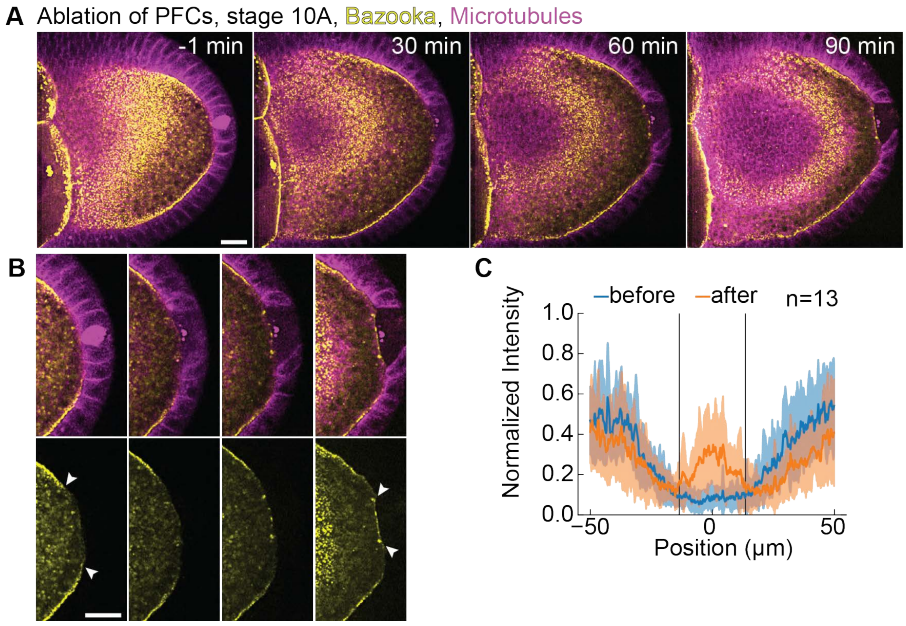

Figure 4.1. **Bazooka localizes to the posterior following ablation of PFCs. (A)** Two-colour time-lapse images of an egg chamber expressing Bazooka::GFP in the germline (yellow) and the microtubule reporter Jupiter::mCherry (magenta) before (-1 min) and after ablation of PFCs. **(B)** Zoom-in of the posterior end of the egg chamber shown in panel A. Top: merged channels, bottom: Bazooka::GFP. Before ablation, Bazooka is excluded from the posterior, a region highlighted by the arrowheads in the first image of the bottom panel. After 90 min, accumulation of Bazooka is visible at the oocyte membrane facing the ablated cells (arrowheads in the last image). **(C)** Average intensity profile of Bazooka::GFP signal at the posterior of the oocyte before (blue) and after (orange) ablation. The shaded region designates the standard deviation. The x-axis origin represents the position of the ablated region. Vertical lines denote the average width of the ablated region. Note that the increase of the signal is visible only inside the ablated region. The scale bars represent 20 μm, *n* is the number of experiments.

Next, we tested if the polar cells need to be ablated for Bazooka to accumulate at the posterior. Polar cells are a specialized pair of posterior follicle cells that mark the center of the layer of around 200 PFCs. These cells are easily distinguishable among the PFCs layer due to the high

expression of Jupiter::mCherry (Figure 4.2A). When ablated posterior follicle cells did not include the pair of polar cells, we could again observe the accumulation of Bazooka to the membrane that was in contact with the ablated cells (Figure 4.2A-C).

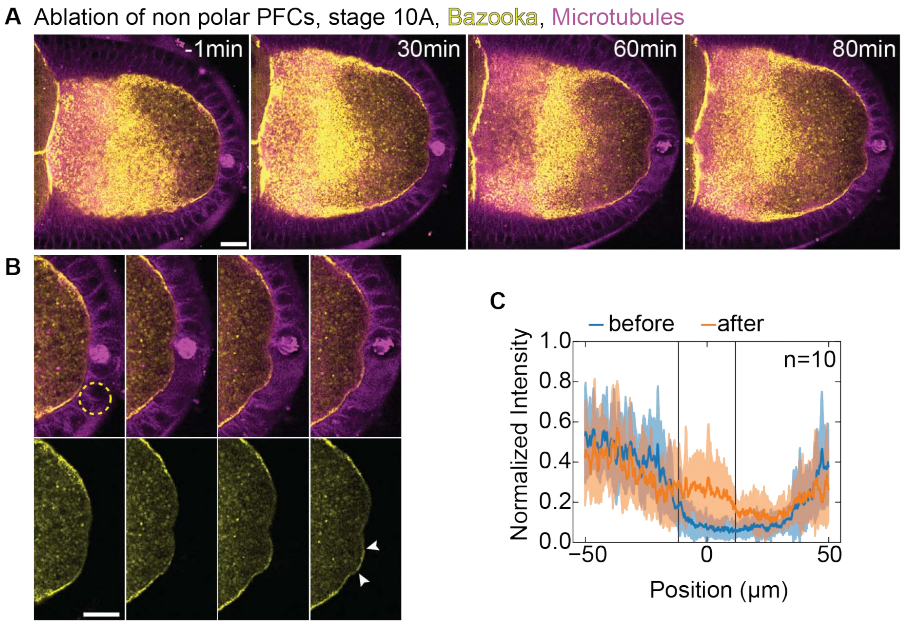

Figure 4.2. **Bazooka localizes to the posterior following ablation of PFCs when polar cells are intact.** **(A)** Two-colour time-lapse images of an egg chamber expressing Bazooka::GFP in the germline (yellow) and the microtubule marker Jupiter::mCherry (magenta) before (-1 min) and after ablation of PFCs. **(B)** Zoom-in of the posterior of the egg chamber shown in panel A. Top: merged channels, bottom: Bazooka::GFP. The dashed circle in the first image of the top panel represents the ablation spot. Note that polar cells (pair of cells with a high Jupiter signal) are not ablated. After 80 min, the accumulation of Bazooka::GFP is visible at the oocyte membrane facing the ablated cells (arrowheads in the last image).

continues on next page

Figure 4.2. *continued from previous page*

(C) Average intensity profile of Bazooka::GFP signal at the posterior of the oocyte before (blue) and after (orange) ablation. The shaded region represents the standard deviation. The x-axis origin represents the position of the ablated region. Vertical lines denote the average width of the ablated region. Note that the signal increases markedly only within the ablated region. The scale bars represent 20 μm, *n* is the number of experiments.

To account for possible turnover kinetics and photobleaching, we compared Bazooka::GFP intensity at cortices either facing posterior or facing lateral follicle cells (Figure 4.3A, inset), confirming a significant increase and in some experiments a full recovery of Bazooka::GFP localization at the posterior. A temporal analysis of Bazooka::GFP intensity after PFC ablation revealed a fast increase ($<$5 min delay) (Figure 4.3B). The accumulation seemed faster and achieved steady-state earlier if polar cells were left intact. We generated a spatiotemporal map of average Bazooka::GFP intensity along the oocyte cortex facing ablated PFCs (Figure 4.3C, D). Whenever the ablated region contained the pair of polar cells, Bazooka accumulated in random patches, presumably by being recruited from the cytoplasmic pool (Figure 4.3C). In contrast, when the ablated region was flanked by still intact polar cells on one side, and main-body follicle cells on the other side, we noticed a signal flow from the anterolateral cortex facing the main-body follicle cells (Figure 4.3D). We concluded that Bazooka predominantly diffused along the membrane from the cortical pool of the anterolateral side towards the posterior end.

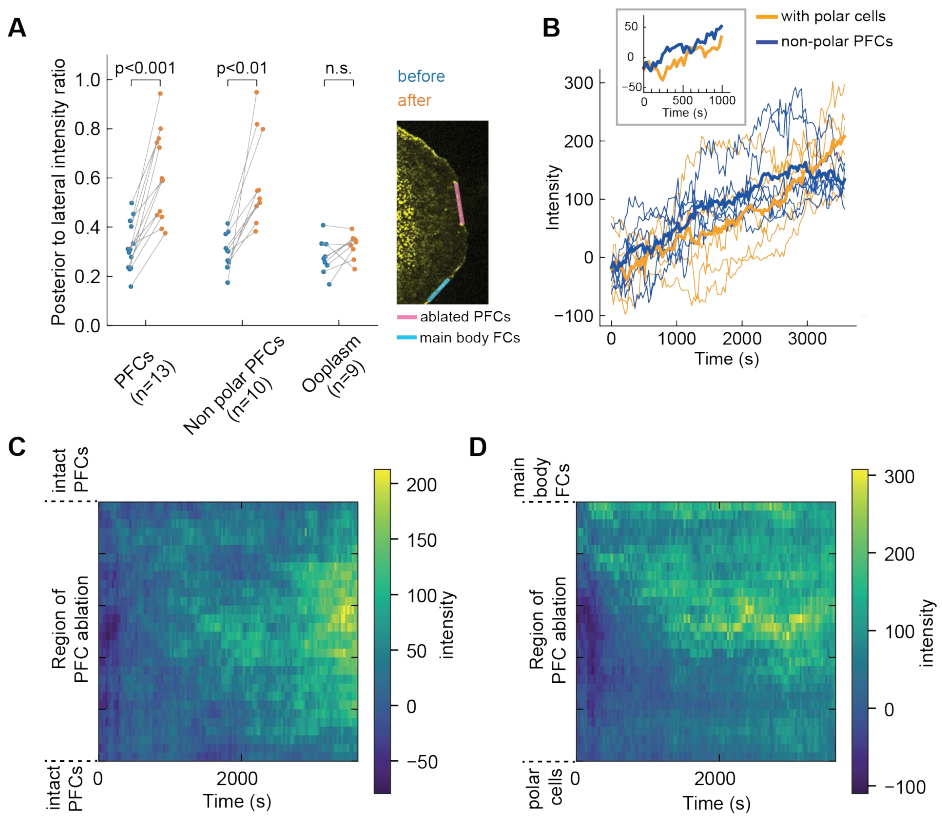

Figure 4.3. **Dynamics of Bazooka localization to the posterior following ablation of PFCs. (A)** Ratio between average Bazooka::GFP intensities along the oocyte membrane facing ablated PFCs and lateral main-body follicle cells, as shown in the inset image, before (blue) and after (orange) ablation for three types of ablation. PFCs: ablation of PFCs, including ablation of polar cells (as in Figure 4.1). Non polar PFCs: ablation of PFCs that do not include polar cells (as in Figure 4.2). Ooplasm: ablation inside the ooplasm (as in Figure 4.4). A ratio equal to 1 means complete loss of Bazooka exclusion. Wilcoxon signed-rank test was performed to assess significance (n.s.=not significant).

continues on next page

Figure 4.3. *continued from previous page*

(B) Intensity of Bazooka::GFP signal at the oocyte membrane facing the ablated follicle cells as a function of time, grouped in experiments where polar cells were ablated (orange, n=5) or left intact (blue, n=6). The thick lines represent the average of each group, thin colored lines are individual oocytes. The intensity of the ooplasm was subtracted from the Bazooka::GFP intensity, so that zero intensity (on average) means the exclusion of Bazooka. Inset: Average curves in the first 15 min. **(C)** Time series of Bazooka::GFP intensity along the oocyte membrane facing ablated PFCs (y-axis) after PFC ablation, represented as a heat map. The ablated follicle cells included the polar cells, and the ablated region is flanked by still intact PFCs. **(D)** As in panel C, but for ablations that excluded polar cells, so that the ablated region was flanked by intact polar cells on one side (bottom of the y-axis) and main-body follicle cells on the other side (top of the y-axis). Note the signal inflow from the top of the graph. For all panels $t = 0$ is the first frame after ablation, n is the number of experiments.

To assure that accumulation of Bazooka is not caused by nonspecific effects of pulsed laser ablation, we performed ablation inside the ooplasm, close to the posterior membrane of the oocyte (Figure 4.4). We did not observe any accumulation of Bazooka at the oocyte membrane, or around the region that was ablated (Figure 4.4B, C).

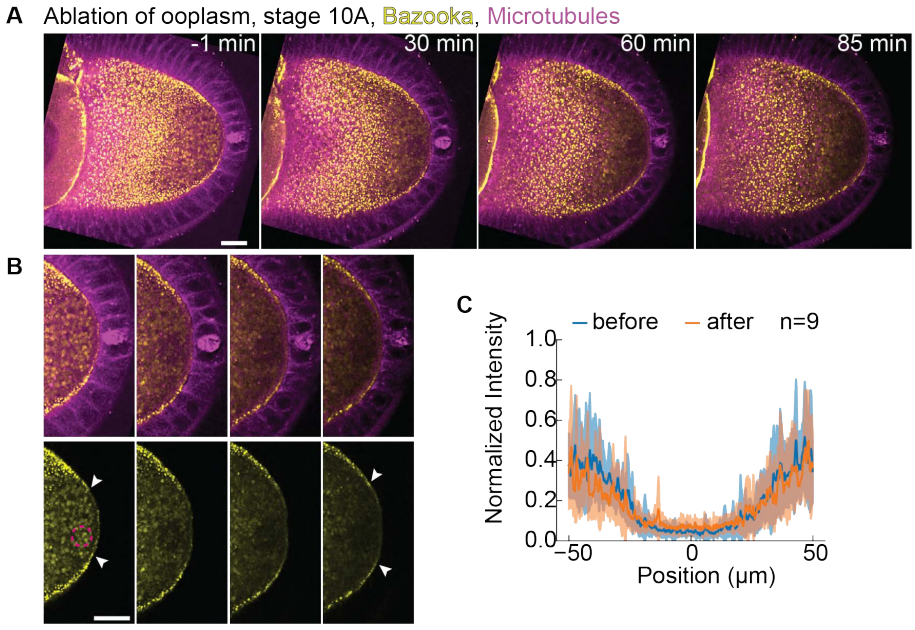

Figure 4.4. **Bazooka does not localize to the posterior following ablation of the ooplasm. (A)** Two-colour time-lapse images of an egg chamber expressing Bazooka::GFP in the germline (yellow) and microtubule marker Jupiter::mCherry (magenta) before (-1 min) and after ablation within the ooplasm. **(B)** Zoom-in of the posterior of the egg chamber shown in panel A. Top: merged channels, bottom: Bazooka::GFP. The dashed circle in the first image of the bottom panel shows the position of the ablation spot. Bazooka remains excluded from the posterior after ablation (arrowheads). **(C)** Average intensity profile of Bazooka::GFP signal at the posterior of the oocyte before (blue) and after (orange) ablation within the ooplasm. The shaded region designates the standard deviation. The x-axis origin represents the position of polar cells. The scale bars represent 20 μm, *n* is the number of experiments.

We also addressed if ablation of follicle cells may cause nonspecific accumulation of any protein to the membrane. Thus, as an additional control experiment, we UV targeted main-body follicle cells in egg chambers expressing Par-1::GFP in the germline and Jupiter::mCherry. At this stage, Par-1 is restricted to the posterior of the oocyte and there is no Par-1 signal at the oocyte membrane in contact with main-body follicle

cells (Figure 4.5A). Importantly, we did not observe any increase in GFP signal following ablation (Figure 4.5B, C). From all these experiments, we conclude that individual PFCs are required to locally maintain the posterior exclusion of Bazooka throughout mid-oogenesis.

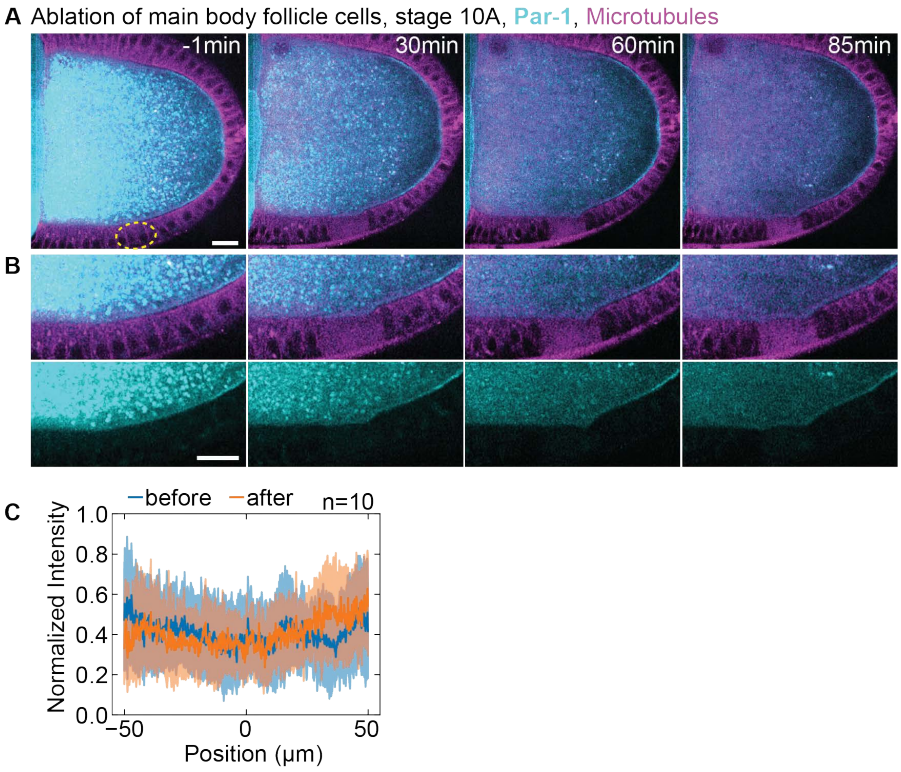

Figure 4.5. **Par-1 does not localize to the oocyte membrane following ablation of the main-body follicle cells. (A)** Two-colour time-lapse images of an egg chamber expressing Par-1::GFP in the germline (cyan) and microtubule marker Jupiter::mCherry (magenta) before (-1 min) and after ablation of main-body follicle cells. The dashed circle in the first image represents the ablation spot. **(B)** Zoom-in of the lateral side of the egg chamber shown in panel A. Top: merged channels, bottom: Par-1::GFP. **(C)** Average intensity profile of Par-1::GFP signal around the ablated region before (blue) and after (orange) ablation of the main-body follicle cells. The shaded region designates the standard deviation. The x-axis origin represents the center of the ablated region. The scale bars represent 20 μm, *n* is the number of experiments.

4.5.2 Stage dependent maintenance of Par-1 localization by PFCs.

Next, we wanted to test if Par-1 needs to be excluded from the posterior before Bazooka can accumulate, upon ablation of PFCs. According to the mutual exclusion hypothesis of the Par protein network, Par-1 presence is responsible for the exclusion of the anterior Par protein complex, including Bazooka, through kinase activity (Benton and St Johnston, 2003a). Therefore, we performed the ablation experiments in egg chambers expressing Par-1::GFP and Bazooka::mCherry in the germline. With this combination of polarity protein reporters, we again observed the accumulation of Bazooka to the posterior following the ablation of PFCs (Figures 4.6 and 4.7).

A first analysis suggested that Par-1 does not decrease as rapidly as expected. Ectopic localization of Bazooka was preceded by a rather slow disappearance of Par-1 (Figure 4.6). However, we realized that the developmental stage marks a difference in Par-1 kinetics upon PFC ablation. In stage 10A oocytes, Par-1 signal marginally decreases within a one-hour time frame (Figure 4.6). In contrast, stage 9 oocytes exhibited a noticeable and significant decrease in the region that had been in contact with ablated PFCs (Figure 4.7).

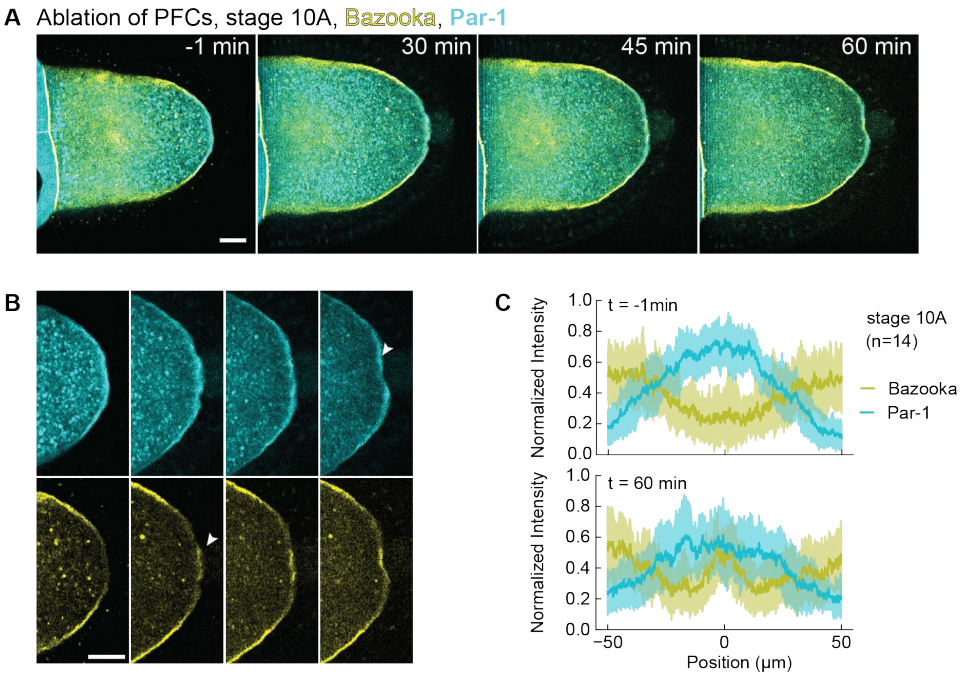

Figure 4.6. **Par-1 loss from the posterior following PFC ablation is slow in stage 10A oocytes (A)** Two-colour time-lapse images of a stage 10A egg chamber expressing Par1::GFP in the germline (cyan) and Bazooka::mCherry (yellow) before (-1 min) and after ablation of PFCs. **(B)** Zoom-in of the posterior of the egg chamber shown in panel A. Top: Par1::GFP, bottom: Bazooka::mCherry. Following ablation, Bazooka accumulates to the posterior, while Par-1 marginally delocalizes (arrowheads). **(C)** Average intensity profile of Par-1::GFP (cyan) and Bazooka::mCherry (yellow) signal at the posterior of stage 10A oocytes before (top graph) and after ablation of PFCs (bottom graph). The shaded region designates the standard deviation. The x-axis origin represents the position of the polar cells (top) or the center of the ablation spot (bottom). Note that the Par-1 signal does not decrease much. The scale bars represent 20 μm, *n* is the number of experiments.

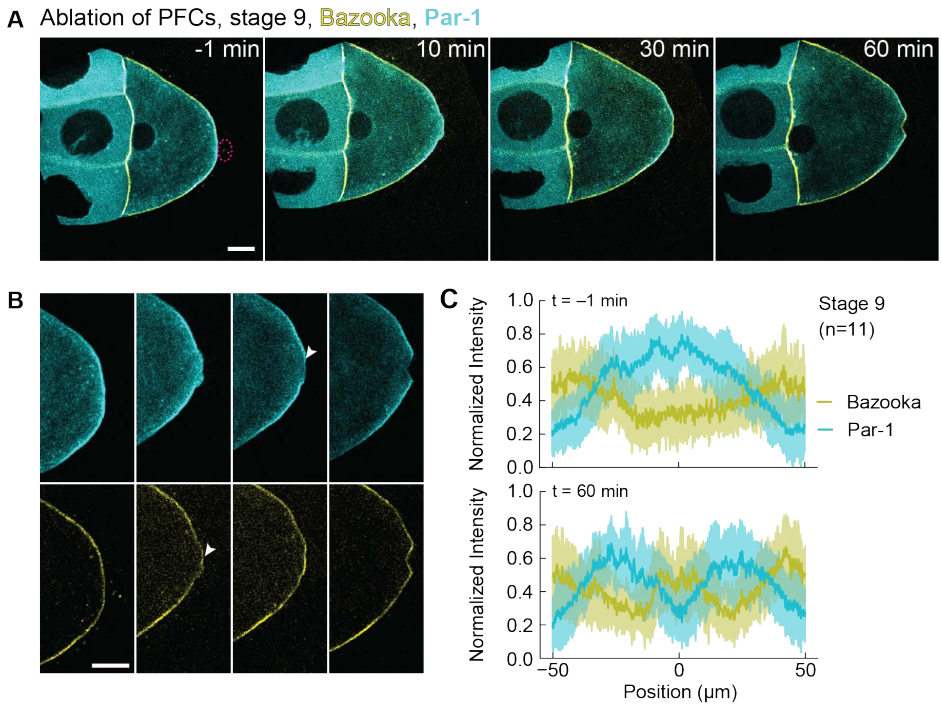

Figure 4.7. **Par-1 delocalizes from the posterior following PFC ablation at stage 9 (A)** Two-colour time-lapse images of a stage 9 egg chamber expressing Par1::GFP in the germline (cyan) and Bazooka::mCherry (yellow) before (-1 min) and after ablation of PFCs. **(B)** Zoom-in of the posterior of the egg chamber shown in panel A. Top: Par1::GFP, bottom: Bazooka::mCherry. Following ablation, Bazooka accumulates to the posterior, while Par-1 is still present but slowly delocalizing (arrowheads). **(C)** Average intensity profile of Par-1::GFP (cyan) and Bazooka::mCherry (yellow) signal at the posterior of stage 9 oocytes (top graph) and one hour after ablation of PFCs (bottom graph). The shaded region designates the standard deviation. The x-axis origin represents the position of the polar cells (top) or the center of the ablation spot (bottom). Note that Bazooka is excluded from the region where Par-1 is present before ablation (top), but it accumulates there after ablation of PFCs (bottom). In contrast, Par-1 delocalizes from the posterior after ablation (bottom, blue). The scale bars represent 20 μm, *n* is the number of experiments.

Slow signal changes can be either a consequence of a late response to the perturbation or due to photobleaching. Thus, we performed a

comparative analysis within each oocyte. Ectopic accumulation of Bazooka at the posterior was significant when compared to the lateral cortex (Figure 4.8A), while Par-1 signal decrease was not significant in stage 10A (Figure 4.8B). We conclude that Par-1 is not sufficient to keep Bazooka excluded from the posterior after PFC ablation. Moreover, Par-1 localization is controlled by PFCs in a stage-dependent manner.

We noticed that Par-1 loss seemed to start in the center of the cortex region which lost contact with PFCs (Figure 4.6B, arrowhead), and extended towards the cortical boundaries facing intact PFCs. To obtain better insight, we generated a spatiotemporal map of Par-1::GFP intensity along the oocyte cortex facing the ablated PFCs (Figure 4.8C). This analysis confirmed a progressive signal loss that occurs symmetrically around the ablation center. In an effort to decompose cortical mobility and turnover kinetics of Par-1::GFP at the posterior cortex, we performed FRAP analysis in the absence of perturbation. Typical Par-1::GFP recovery time was $<$1 min (Figure 4.8D), which contrasts the slow Par-1 delocalization after perturbation, occurring typically within one hour (Figure 4.8C). This suggests that the signal coming from PFCs does not affect Par-1 directly, but regulates its posterior accumulation through regulation of Par-1 molecular binding sites.

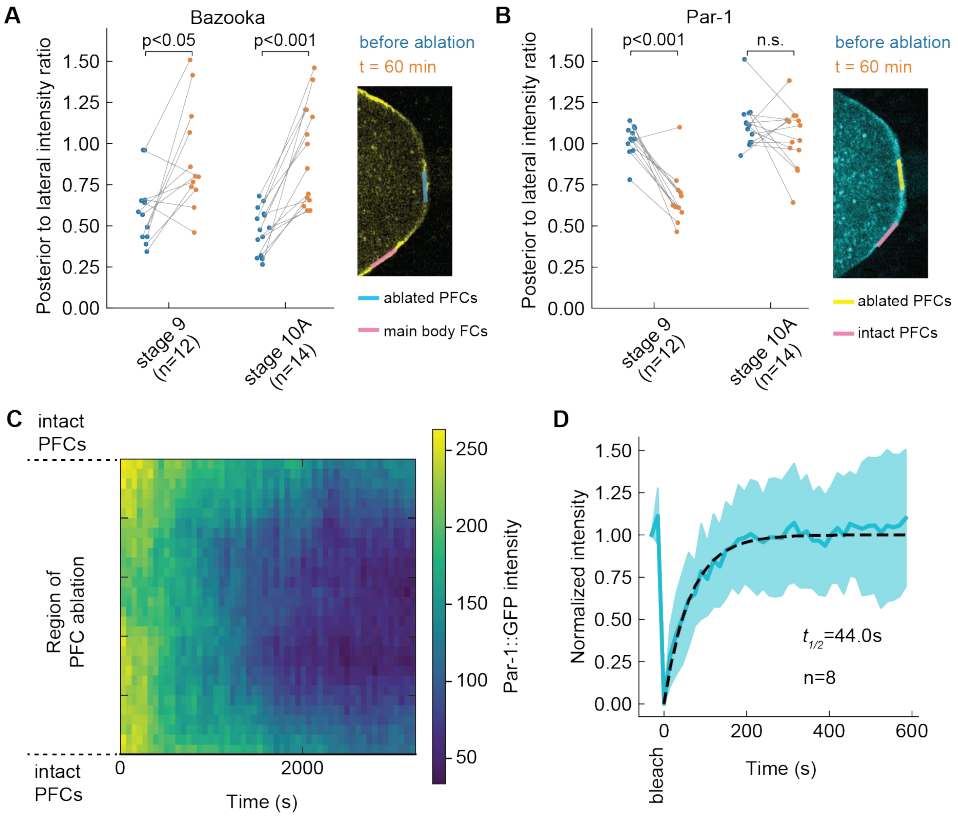

Figure 4.8. **Quantification of Bazooka and Par-1 posterior localization following ablation of PFCs. (A)** Ratio between Bazooka::mCherry intensities at the posterior and lateral membrane of the oocyte (facing main body follicle cells), as depicted in the inset image, before (blue) and one hour after (orange) ablation. The ratio 0 signifies complete posterior exclusion, and 1 and beyond denote localization. There is a significant increase in the ratio for both stages 9 and 10A, showing the accumulation of Bazooka to the posterior. **(B)** Ratio between Par-1::GFP intensities at the membrane of the oocyte facing posterior ablated PFCs and intact PFCs sightly lateral, as depicted in the inset image, before (blue) and one hour after (orange) ablation. There is no significant reduction of the ratio in stage 10A which would indicate delocalization of Par-1. Wilcoxon signed-rank test was performed to assess significance (n.s. = not significant).

continues on next page

Figure 4.8. *continued from previous page*

(C) Time series of Par-1::GFP intensity along the oocyte membrane facing ablated PFCs (y-axis) after PFC ablation, represented as a heat map. **(D)** Normalized signal recovery after fluorescence photobleaching for Par1::GFP signal at the oocyte membrane. The thick blue line is the mean, the shaded region designates the standard deviation, and the dashed line is the fitted curve obtained by fitting a single exponential function. For all panels, *n* is the number of experiments.

4.5.3 Posterior *oskar* mRNA is lost upon PFC ablation

A downstream process of Par polarity in the oocyte is *oskar* mRNA accumulation at the posterior, which ultimately defines the tail of the future organism (Riechmann and Ephrussi, 2001). This is achieved by directed transport on a slightly polarized microtubule network and anchoring at the posterior cortex (Lu et al., 2018, 2020; Zimyanin et al., 2008). We wanted to understand if the response of Par proteins to PFC ablation would also affect *oskar* localization. To this end, we performed live cell imaging of stage 8–10A egg chambers expressing Par-1::GFP and *osk*MS2 under its native driver together with MCP::mCherry (Figure 4.9A). Upon PFC ablation, Par-1 delocalizes slowly, as shown previously (Figure 4.9B, top). More strikingly, *oskar* also delocalizes, first in the region previously in contact with ablated PFCs, and gradually also at the flanking regions (Figure 4.9B, bottom). Qualitatively, *oskar* loss showed a delay, and kinetics seemed slower for later stages. This impression prompted us to analyze the kinetics of signal decrease for both Par-1 and *oskar* by fitting single exponential decay functions with delay (Figure 4.9C) Indeed, *oskar* delocalization occurred with a statistically significant delay relative to Par-1 (which occurs immediately within temporal resolution). In stage 8 oocytes the overall kinetics appeared extremely fast while in stage 10A *oskar* localization shows more stability. We conclude that PFCs are required to maintain body axis definition in the oocyte until stage 10 by

defining *oskar* mRNA localization.

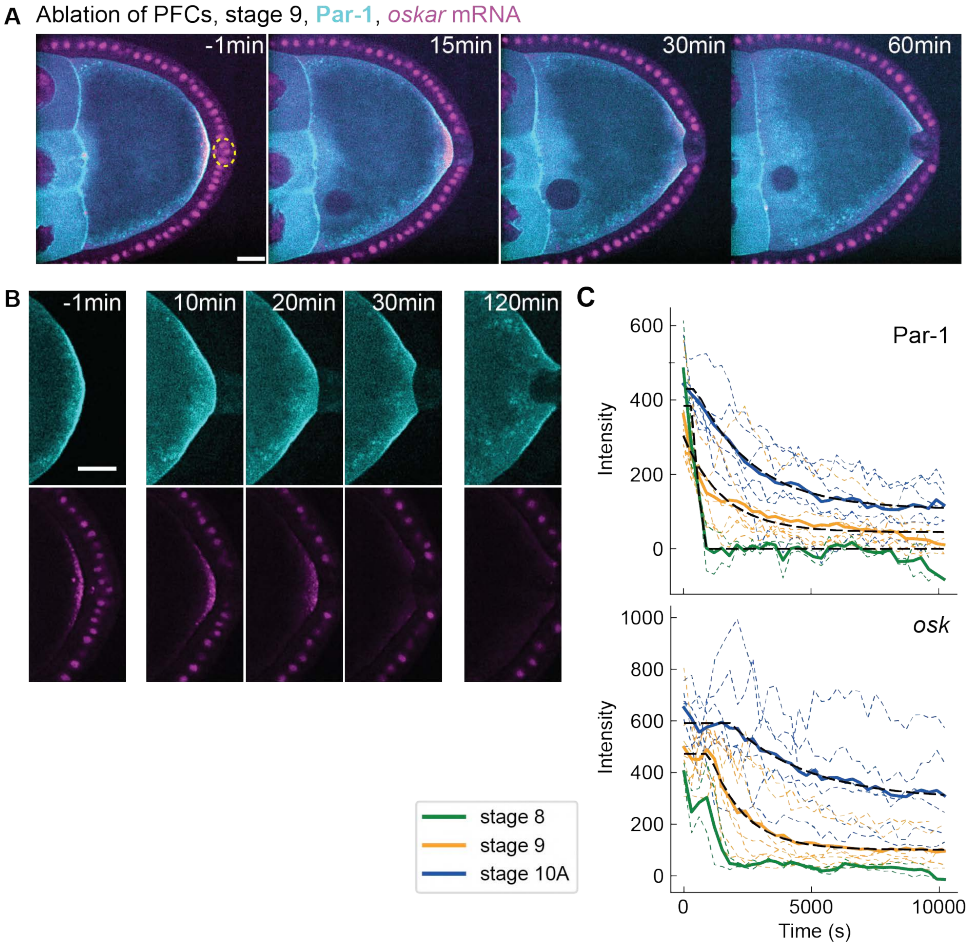

Figure 4.9. **Posterior *oskar* mRNA is lost shortly after Par-1 (A)** Two-colour time-lapse images of an egg chamber expressing Par1::GFP in the germline (cyan) and *oskMS2*-MCP::mCherry (magenta) before (-1 min) and after ablation of PFCs (yellow dashed circle). **(B)** Zoom-in of the posterior of the egg chamber shown in panel A. Top: Par-1::GFP, bottom: *oskMS2*-MCP::mCherry. Both Par-1 and *osk* delocalize from the cortex facing ablated PFCs.

continues on next page

Figure 4.9. *continued from previous page*

(C) Intensity of Par-1 (top) and *osk* mRNA (bottom) at the posterior of the oocyte facing ablated PFCs, for stages 8 (n=2), 9 (n=7) and 10A (n=6). Thin dashed lines are individual experiments, the solid lines are the averages for each stage, and the black dashed line represents a fit to a single exponential decay with time delay. While Par-1 signal loss is immediate, *osk* mRNA decreases with increasing delay; the estimated 95% CI (min) are for stage 8: [13.3, 16.5], for stage 9: [15.5, 18.9], for stage 10A: [24.4, 36.0]. The x-axis origin represents the center of the ablated region. The scale bars represent 20 μm.

Finally, motivated by earlier reports of Par-1 being a microtubule nucleation inhibitor (Doerflinger et al., 2010; Nashchekin et al., 2016; Parton et al., 2011), we predicted that the delocalization of Par-1 upon PFC ablation should enable microtubule growth in that region. The growth of microtubules from the posterior towards the cytoplasm could explain the loss of *oskar* due to directed transport away from the cortex. Indeed, in some oocytes, we observed a local signal increase of the microtubule reporter Jupiter::GFP where *oskar* signal decreased (Figure 4.10A). However, growth sometimes initiated considerably later than *oskar* delocalization, so that in some oocytes we did not observe any growth within the time of observation (Figure 4.10B). Thus, this result shows that the maintenance of Par polarity by PFCs is functionally important for robust microtubule cytoskeleton polarization. However, loss of *oskar* upon PFC ablation is likely not caused by microtubule reorganization but rather by loss of cortical anchoring.

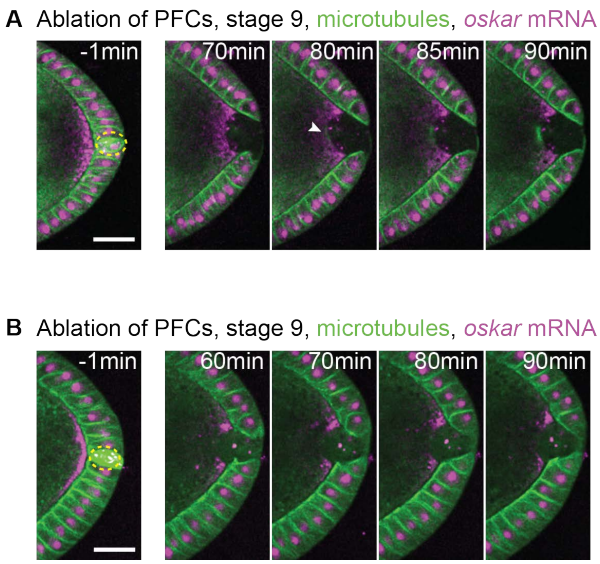

Figure 4.10. **Microtubules nucleate at the oocyte membrane facing the ablated cells. (A)** Two-colour time-lapse images of an egg chamber expressing Jupiter::GFP (green) and *oskMS2*-mCherry (magenta) before (-1 min) and after ablation of PFCs. This example shows microtubule growth at the posterior 80–90 min following ablation. **(B)** As in panel A, showing an example of an oocyte that did not yet exhibit microtubule growth 90 min after PFC ablation. The scale bars represent 20 μm.

4.5.4 aPKC kinetics after PFC ablation does not explain Par-1 removal from the posterior

According to the current model of Par network polarization in the *Drosophila* oocyte, Par-1 is excluded from the anterolateral membrane through phosphorylation by the kinase aPKC, which is recruited to the membrane through interaction with Bazooka (Doerflinger et al., 2010). Conceivably, accumulation of Bazooka at the posterior after PFC ablation may recruit aPKC, eventually leading to Par-1 delocalization at the posterior. To obtain insight into the sequence of events, we performed live imaging of egg chambers from flies that endogenously express aPKC::GFP (Chen et al., 2018) and Bazooka::mCherry in the germline

(Figure 4.11). Since both follicle cells and germline express aPKC, the initial posterior exclusion of aPKC in the oocyte is masked by the apical signal in follicle cells. However, once PFCs are ablated their aPKC::GFP signal disappears and any fluorescence detected can be attributed to aPKC in the oocyte (Figure 4.11B, bottom row). Therefore, our assay allows us to unambiguously detect possible accumulation of aPKC following ablation of PFCs. Although the signal of endogenously driven protein expression is significantly lower when compared to using GAL4/UASp expression system, we were able to observe the accumulation of aPKC in most of the oocytes (Figure 4.11B, arrowheads).

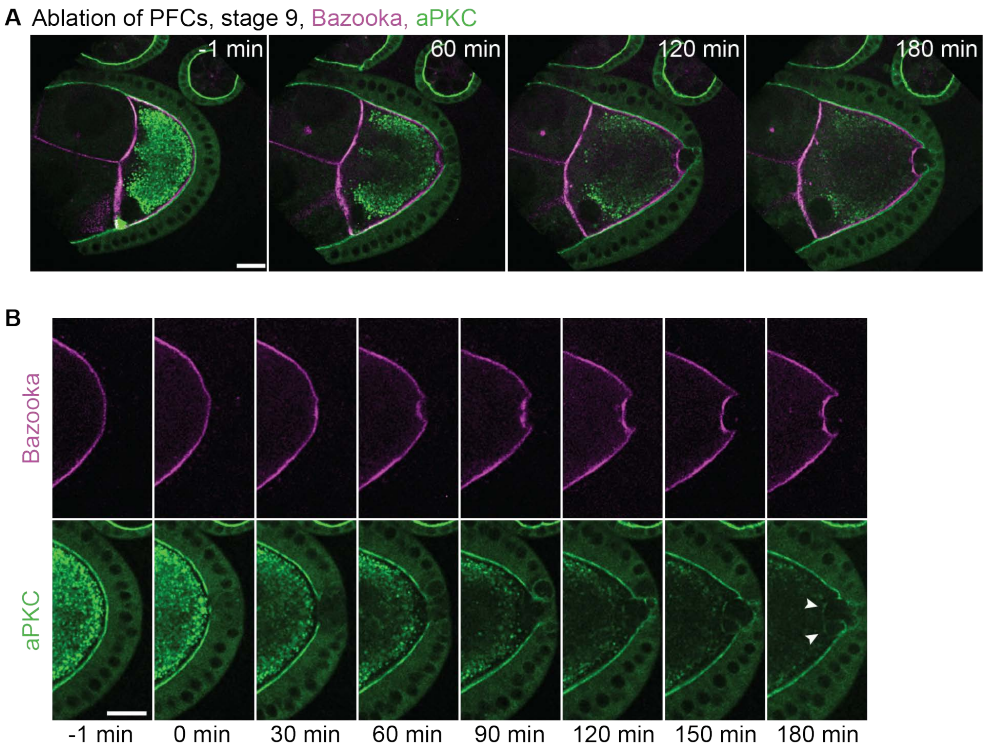

Figure 4.11. **aPKC accumulates to the posterior following accumulation of Bazooka.** **(A)** Two-colour time-lapse images of an egg chamber expressing Bazooka::mCherry (magenta) in the germline and aPKC::GFP (green) endogenously before (-1 min) and after ablation of PFCs. **(B)** Zoom-in of the posterior of the egg chamber shown in panel A. Top: aPKC::GFP, bottom: Bazooka::mCherry. Both aPKC::GFP and Bazooka::mCherry accumulate at the posterior of the oocyte at the end of the experiment (arrowheads). The scale bars represent 20 μm.

Intensity analysis of aPKC::GFP showed that stage 9 oocytes had significant accumulation. More importantly, aPKC localization lagged upon perturbation and was always preceded by the accumulation of Bazooka (Figure 4.12A, B). Interestingly, we did not detect a significant increase in aPKC at stage 10A (Figure 4.12B) which could be explained by the signal detection limit in our imaging. More assuringly, the loss of Par-1 was faster than the kinetics of aPKC ectopic localization after perturbation (Figure

4.12C), suggesting that Par-1 loss occurred before aPKC localized. We conclude that aPKC accumulation is insufficient for Par-1 displacement, and the maintenance of Par-1 localization at the posterior requires the oocyte to be in contact with PFCs.

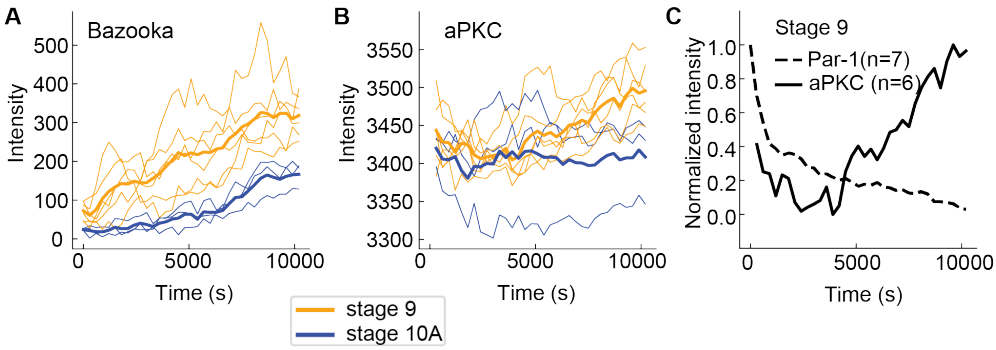

Figure 4.12. **Dynamics of the Par proteins re-localization following the ablation of PFCs. (A)** Bazooka::mCherry intensity at the oocyte cortex facing the ablated PFCs, as a function of time for oocytes at stage 9 (orange, n=6) and 10A (blue, n=3). Thin lines are individual experiments, thick lines are stage averages. **(B)** As in panel A but for aPKC::GFP. Note the delayed increase in stage 9, and the lack of signal increase in stage 10A. **(C)** Normalized average intensities of Par1::GFP (dashed line) and aPKC::GFP (solid line) at stage 9 as a function of time following the ablation of PFCs. Note the delay of aPKC signal increase. For all panels, time zero marks the first frame after ablation.

4.6. Discussion

In this chapter, I presented work that aimed to dissect the role of PFCs in the maintenance of anterior-posterior polarization of the oocyte using laser ablation of PFCs. This approach not only confirmed the importance of PFCs in maintaining the posterior exclusion of Bazooka but also provided much better spatiotemporal control compared to mechanical perturbations used in previous chapters. This allowed us to gain novel insights into possible mechanisms by which PFCs regulate the localization of Par proteins in the oocyte.

Both accumulation of Bazooka and delocalization of Par-1 following ablation of PFCs are restricted to the membrane that was in direct contact with ablated follicle cells. We conclude that the remaining PFCs continue transducing the signal that excludes Bazooka and retains Par-1. This agrees with previously reported work studying mosaic mutants in components of signaling pathways that are necessary for the differentiation of PFCs (Frydman and Howard, 2001; Poulton and Deng, 2006; Xi et al., 2003). In sum, these studies showed that *oskar* mRNA and Staufen protein correctly localize to the membrane facing WT follicle cells, while their localization is lost at the membrane facing neighboring cells that did not adopt posterior fate. This observation argues against the idea that the polarizing signal is a diffusible molecule within the extracellular space.

Another interesting observation is that Bazooka localizes to the posterior faster when the ablation region is flanked by main-body follicle cells (see Figure 4.3B). This could be explained by lateral diffusion of Bazooka from the cortex next to the ablation region (Figure 4.3D). Contrary, when the ablation region is flanked by the intact PFCs on both sides, Bazooka is recruited to the membrane only from the cortical pool (Figure 4.3C).

In this chapter, we also directly show that PFCs are necessary to maintain the posterior enrichment of Par-1. Interestingly, the process of Par-1 delocalization upon ablation of PFCs depends on the stage of oogenesis, with a transition from a relatively fast removal at stage 9, to very slow or no removal at stage 10A. This transition could be because there is more posteriorly localized Oskar protein at stage 10A, which recruits Par-1 through a positive feedback loop (Zimyanin et al., 2007). However, localization of Bazooka does not show stage dependence and occurs even when Par-1 remains at the posterior. This further confirms that Par-1 is not sufficient to exclude Bazooka.

Interestingly, Par-1 loss starts in the center of the cortex region, which lost contact with PFCs, and extends towards the cortical boundaries facing intact PFCs (Figure 4.8C). This could be explained by the later diffusion of Par-1 from the regions facing the intact PFCs. However, Par-1 turnover, as measured by FRAP, is much faster than the speed of its delocalization. Therefore, the signal from PFCs does not seem to affect the Par-1 directly. Instead, our results indicate that the molecular binding sites for Par-1, which are abundant and cause Par-1 accumulation, slowly delocalize upon PFC ablation while Par-1 turns over fast. Thus, the signal from the PFCs might act by reducing the mobility of these binding sites at the posterior, possibly through the regulation of tension at the posterior (Doerflinger et al., 2022).

Importantly, in this chapter, we show that *oskar* mRNA is lost shortly after Par-1 delocalizes. Therefore, the maintenance of Par polarity by the PFCs has a crucial functional role in determining the posterior pole of the future egg (Riechmann and Ephrussi, 2001). Although we observed the nucleation of microtubules at the posterior in some of the ablation experiments, we could also observe the loss of *oskar* mRNA in the absence of any detectable nucleation of microtubules. According to the current model of *oskar* localization, the inhibition of microtubule nucleation at the posterior by Par-1 prevents the removal of *oskar* mRNA by kinesin (Lu et al., 2018, 2020). Our results show that this inhibition is not sufficient to prevent *oskar* dissociation. Instead, PFCs are necessary to keep *oskar* anchored at the posterior, presumably through regulation of Par-1 localization and/or membrane tension.

4.7. Acknowledgements

I thank Ivo Telley for supervision, Jorge de-Carvalho for the initial help with experiments, and all members of the Telley lab for fruitful discussions. I acknowledge I. Gáspár and A. Ephrussi for suggestions on sample

preparation. I also thank the staff of the Fly Facility, the Advanced Imaging Facility (AIF), and the Technical Support Service at the Instituto Gulbenkian de Ciência (IGC). Finally, I thank Anne Ephrussi (EMBL Heidelberg), Daniel St. Johnston (The Gurdon Institute) and Eurico Morais-de-Sá (I3S Porto) for fly line donations, and The Bloomington Drosophila Stock Center for their services.

4.8. Bibliography

A. N. Becalska and E. R. Gravis. Bazooka regulates microtubule organization and spatial restriction of germ plasm assembly in the drosophila oocyte. *Developmental Biology*, 340:528–538, 2010.

R. Benton and D. St Johnston. Drosophila par-1 and 14-3-3 inhibit bazooka/par-3 to establish complementary cortical domains in polarized cells. *Cell*, 115:691–704, 2003a.

R. Benton and D. St Johnston. A conserved oligomerization domain in drosophila bazooka/par-3 is important for apical localization and epithelial polarity. *Current Biology*, 13:1330–1334, 2003b.

J. Chen, A.-C. Sayadian, N. Lowe, H. E. Lovegrove, and D. S. Johnston. An alternative mode of epithelial polarity in the drosophila midgut. *PLoS Biology*, 16:1–24, 2018.

J. de Carvalho, S. Tlili, L. Hufnagel, T. E. Saunders, and I. A. Telley. Aster repulsion drives short-ranged ordering in the drosophila syncytial blastoderm. *Development*, 149:1–13, 2022.

H. Doerflinger, R. Benton, I. L. Torres, M. F. Zwart, and D. St Johnston. Drosophila anterior-posterior polarity requires actin-dependent par-1 recruitment to the oocyte posterior. *Current Biology*, 16:1090–1095, 2006.

H. Doerflinger, N. Vogt, I. L. Torres, V. Mirouse, I. Koch, C. Nüsslein-Volhard, and D. St Johnston. Bazooka is required for polarisation of the drosophila anterior-posterior axis. *Development*, 137:1765–1773, 2010.

H. Doerflinger, V. Zimyanin, and D. St Johnston. The drosophila anterior-posterior axis is polarized by asymmetric myosin activation. *Current Biology*, 32:374–385, 2022.

H. M. Frydman and A. C. S. Howard. The receptor-like tyrosine phosphatase lar is required for epithelial planar polarity and for axis determination within drosophila ovarian follicles. *Development*, 128: 3209–3220, 2001.

B. Goldstein and I. G. Macara. Review the par proteins: Fundamental players in animal cell polarization. *Developmental Cell*, 13:609–622, 2007.

I. Gáspár, V. Sysoev, A. Komissarov, and A. Ephrussi. An rna-binding atypical tropomyosin recruits kinesin-1 dynamically to oskar mrnps. *The EMBO Journal*, 36:319–333, 2017.

C. Hoege and A. A. Hyman. Principles of par polarity in caenorhabditis elegans embryos. *Nature Reviews Molecular Cell Biology*, 14:315–322, 2013.

J.-R. Huynh, J. M. Shulman, R. Benton, and D. St Johnston. Par-1 is required for the maintenance of oocyte fate in drosophila. *Development*, 128:1201–1209, 2001.

D. Jia, Q. Xu, Q. Xie, W. Mio, and W.-M. Deng. Automatic stage identification of drosophila egg chamber based on dapi images. *Scientific Reports*, 6:1–12, 2016.

J. Jouette, A. Guichet, and S. B. Claret. Dynein-mediated transport and

membrane trafficking control par3 polarised distribution. *eLife*, 8:1–28, 2019.

C. F. Lang and E. Munro. The par proteins : from molecular circuits to dynamic self-stabilizing cell polarity. *Development*, 144:3405–3416, 2017.

N. Lowe, J. S. Rees, J. Roote, E. Ryder, I. M. Armean, G. Johnson, E. Drummond, H. Spriggs, J. Drummond, J. P. Magbanua, H. Naylor, B. Sanson, R. Bastock, S. Huelsmann, V. Trovisco, M. Landgraf, S. Knowles-Barley, J. D. Armstrong, H. White-Cooper, C. Hansen, R. G. Phillips, The UK Drosophila Protein Trap Screening Consortium, K. S. Lilley, S. Russell, and D. St Johnston. Analysis of the expression patterns, subcellular localisations and interaction partners of drosophila proteins using a pigp protein trap library. *Development*, 141:3994–4005, 2014.

W. Lu, M. Lakonishok, A. S. Serpinskaya, D. Kirchenbüechler, S. Ling, and V. I. Gelfand. Ooplasmic flow cooperates with transport and anchorage in drosophila oocyte posterior determination. *Journal of Cell Biology*, 217:3497–3511, 2018.

W. Lu, M. Lakonishok, R. Liu, N. Billington, A. Rich, M. Glotzer, J. R. Sellers, and V. I. Gelfand. Competition between kinesin-1 and myosin-v defines drosophila posterior determination. *eLife*, 9:1–25, 2020.

E. Morais-de-Sá, A. Mukherjee, N. Lowe, and D. St Johnston. Slmb antagonises the apkc / par-6 complex to control oocyte and epithelial polarity. *Development*, 141:2984–2992, 2014.

F. Motegi and G. Seydoux. The par network: Redundancy and robustness in a symmetry-breaking system. *Philosophical Transactions of the Royal Society B: Biological Sciences*, 368:1–11, 2013.

D. Nashchekin, A. Ribeiro Fernandes, and D. St Johnston. Patronin/shot cortical foci assemble the noncentrosomal microtubule array that specifies the drosophila anterior-posterior axis. *Developmental Cell*, 38: 61–72, 2016.

R. M. Parton, R. S. Hamilton, G. Ball, L. Yang, C. F. Cullen, W. Lu, H. Ohkura, and I. Davis. A par-1–dependent orientation gradient of dynamic microtubules directs posterior cargo transport in the drosophila oocyte. *The Journal of Cell Biology*, 194(1):121–135, 2011.

J. S. Poulton and W.-M. Deng. Dystroglycan down-regulation links egf receptor signaling and anterior-posterior polarity formation in the drosophila oocyte. *PNAS*, 103(34):12775–12780, 2006.

V. Riechmann and A. Ephrussi. Axis formation during drosophila oogenesis. *Current Opinion in Genetics and Development*, 11:374–383, 2001.

J. Schindelin, I. Arganda-Carreras, E. Frise, V. Kaynig, M. Longair, T. Pietzsch, S. Preibisch, C. Rueden, S. Saalfeld, B. Schmid, J.-Y. Tinevez, D. J. White, V. Hartenstein, K. Eliceiri, P. Tomancak, and A. Cardona. Fiji: an open-source platform for biological-image analysis. *Nature Methods*, 9:676–682, 2012.

J. M. Shulman, R. Benton, and D. St Johnston. The drosophila homolog of c. elegans par-1 organizes the oocyte cytoskeleton and directs oskar mrna localization to the posterior pole. *Cell*, 101:377–388, 2000.

A.-G. Tian and W.-M. Deng. Lgl and its phosphorylation by apkc regulate oocyte polarity formation in drosophila. *Development*, 135:463–471, 2008.

T. T. Weil, K. M. Forrest, and E. R. Gavis. Localization of bicoid mrna in late oocytes is maintained by continual active transport. *Developmental Cell*, 11:251–262, 2006.

R. Xi, J. R. McGregor, and D. A. Harrison. A gradient of jak pathway activity patterns the anterior-posterior axis of the follicular epithelium. *Developmental Cell*, 4(2):167–177, 2003.

V. Zimyanin, N. Lowe, and D. St Johnston. An oskar-dependent positive feedback loop maintains the polarity of the drosophila oocyte. *Current Biology*, 17:353–359, 2007.

V. L. Zimyanin, K. Belaya, J. Pecreaux, M. J. Gilchrist, A. Clark, I. Davis, and D. St Johnston. In vivo imaging of oskar mrna transport reveals the mechanism of posterior localization. *Cell*, 134:843–853, 2008.

5. Chapter 5: General Discussion

5.1. Brief historical overview: large-scale screens as the foundation of the field of *Drosophila* oocyte polarization and the signal that keeps escaping them

Large-scale genetic screens have been at the forefront of the analysis of body plan in the fruit fly since the late 1970s, when the now famous Heidelberg mutagenesis screen identified the genes involved in the patterning of the embryo (Nüsslein-Volhard and Wieschaus, 1980, 2016). These screens primarily focused on finding the zygotic lethal mutations. However, they also produced some mutants in which the flies would develop to adulthood, but the homozygous female offspring were sterile, suggesting that the mutation affects oogenesis. The work that followed up on these mutants showed that many of the mutations affect either anterior-posterior or the dorsal-ventral axis formation of the embryo. Thus, it became clear that the events occuring during oogenesis are involved in the establishment of the main body axes of the fly (Schüpbach and Wieschaus, 1986a,b; Lehmann and Nüsslein-Volhard, 1986; Nüsslein-Volhard et al., 1987; Schüpbach, 1987). Due to the female-sterile phenotype of these mutants, some of the first genes identified in the screen were named after the royal families that died out due to the lack of offspring - *tudor, staufen, vasa* and *valois* (Schüpbach and Wieschaus, 1986b; Schüpbach, 2019)

Since the initial discovery that the embryo inherits spatial information from the mother, the genetic screens have been crucial for studying the establishment of the fly body axes. Characterization of two mutants in which eggs lacked dorsal appendages - and were therefore named *gurken* (german for cucumber) and *torpedo* - led to the discovery that the communication between the germline and the soma is essential for the establishment of body axes. The analysis of mosaics in which either the

germline or the soma is mutant, while the other tissue is wild type, showed that *gurken* is needed in the germline, while *torpedo* is needed in the follicle cells to establish the dorsal-ventral axis (Schüpbach, 1987).

Some years later, it became possible to clone the genes, opening the door for molecular biology in higher organisms. This work revealed that *torpedo* encodes the *Drosophila* homolog of the EGF receptor (Price et al., 1989; Schejter and Shilo, 1989), while *gurken* encodes TGFα-like ligand (Neuman-Silberberg and Schupbach, 1993). Further advances in molecular biology, as well as developments in microscopy, allowed researchers to start visualizing the subcellular localization of proteins and mRNAs. These studies revealed that mRNAs or proteins derived from genes required for embryo polarization often show polarized distribution inside the oocyte. Thus, the field of oocyte polarization started to gain momentum.

Soon it became evident that the EGF pathway is necessary to induce the posterior follicle cell fate in the subset of follicle cells at the posterior of the egg chamber. If this step does not proceed correctly, the polarization of the oocyte is affected. This discovery led researchers to propose that the posterior follicle cells (PFCs) send a signal that polarizes the oocyte (González-Reyes and St Johnston, 1994; González-Reyes et al., 1995; Roth et al., 1995).

The following years brought further advances in the screening methods, enabling the identification of the genes beyond the reach of the traditional screens (St Johnston, 2002). These screens identified many genes necessary in the germline for the oocyte polarization downstream of the PFCs signal (Martin et al., 2003; Doerflinger et al., 2010). The characterization of the majority of these genes is still ongoing. These efforts recently identified di-phosphorylation of myosin II at the posterior of the oocyte as the earliest known downstream target of the PFCs signal (Doerflinger et al., 2022). However, nearly 30 years after the existence of

the polarizing signal from PFCs was proposed, its molecular identity remains beyond the reach of mutagenesis screens (Chen and Schüpbach, 2006; Pai et al., 2000; Merkle et al., 2020).

Two main reasons could explain why the mutagenesis screens have not identified the posterior signal. First, the gene that encodes the signal might play a role in the earlier stages of oogenesis, so that the mutants in this gene would not develop to the stage at which PFCs send the signal. Second, two redundant pathways might be involved in the transduction of the signal.

Recently, two gene expression screens have been carried out to identify the polarizing signal (Wittes and Schüpbach, 2019; Plygawko, 2020). Identifying the genes that are either under- or overexpressed in the PFCs compared to the other subtypes of follicle cells should provide a way to overcome the drawbacks of the mutagenesis screens mentioned earlier. However, the downside of gene expression screens is that they usually generate many hits, and deciding which hits to pursue is a daunting task. This might be the reason why these screens were not yet successful in identifying the signal.

5.2. Beyond the gene: use of micromanipulation techniques to probe the biological systems

In the work presented in this thesis, we attempted to study the polarization of an egg chamber - a system that has for many years been a playground for geneticists - by using micromanipulation techniques. Interestingly, some of the methods that we used predate large-scale genetic screens. In a time when genetic manipulations were very hard or even impossible, the use of micromanipulations provided a way to perturb and probe biological systems. Surgical ligations performed by Sander and Schubiger (Sander, 1971; Schubiger, 1976) inspired some of our experiments. At the time, the micromanipulation experiments were also carried out to probe the

architecture of chromosomes and spindles (Carlson, 1952; Nicklas and Staehly, 1967; Nicklas and Koch, 1969), while the aspiration techniques provided a way to measure the mechanical properties of the egg (Mitchison and Swann, 1954a,b).

However, by the end of the 20th century, mutagenesis screens started providing extensive lists of genes involved in many biological processes. As the cloning of genes became a trivial task, the characterization of mutants became the primary technique of cell and developmental biology. Therefore, micromanipulation techniques mainly fell out of fashion during the end of the 20th and the first decade of the 21st century. As the lists of candidate genes grew longer and longer, it became evident that knowing the genes involved in the process is often insufficient to uncover the underlying biological mechanisms. Therefore, in recent years, many laboratories started using micromanipulation techniques to complement genetic approaches.

Advances in microscopy and in precision of micromanipulations led to exciting insights into many biological processes. Ligation experiments helped reveal the mechanisms ensuring synchronous nuclear divisions in *Drosophila* embryos (Deneke et al., 2016). Microneedle manipulations uncovered mechanical forces in the spindle (Gatlin et al., 2010; Shimamoto et al., 2011; Takagi et al., 2019; Suresh et al., 2020). While micropipette aspiration was used to study cell mechanics and to measure the surface tension, pressure, and viscosity of cells and tissues (Maître et al., 2012, 2015). Even more recently, atomic force microscopy has provided unprecedented precision in measuring and manipulating the mechanical environment of cells in vivo (Koser et al., 2016; Barriga et al., 2018; Moreira et al., 2022).

We aimed to use micromanipulation techniques to study the long-standing question of anterior-posterior polarization of the oocyte during mid-oogenesis. As mentioned above, this question has been

extensively studied using traditional genetic approaches. However, egg chambers are the perfect system for micromanipulation. Their large size compared to other cells facilitates manipulations. In addition, egg chambers can be cultured under halocarbon oil, making them accessible to needles and pipettes.

In Chapter 2, we used ligation of egg chambers to show that Par polarity can be established and maintained when the communication between the oocyte and the nurse cells is cut off. These experiments also suggested that the PFCs play a crucial role in re-establishing polarity following perturbation and might be necessary for maintaining Par polarity throughout oogenesis. In Chapter 3, we confirmed this hypothesis using a micropipette to detach PFCs from the oocyte. In addition, detachment experiments suggested that the maintenance mechanism depends on mechanical contact between the oocyte and the PFCs. Although identification of the polarizing signal was never the goal of my Ph.D. work, I believe that these experiments provide novel insight into the nature of the signal, and help interpret the extensive list of candidate genes. I discuss this in more detail in the following section.

5.3. Revisiting the nature of the polarizing signal

The observation that the close contact between the PFCs and the oocyte is necessary to maintain the oocyte polarization is exciting in light of the results obtained in two recent screens mentioned above (Wittes and Schüpbach, 2019; Plygawko, 2020). One study found that the extracellular matrix (ECM) components are upregulated in the PFCs (Wittes and Schüpbach, 2019), while the other reported upregulation of actin-regulating genes (Plygawko, 2020). Both of these changes in expression could increase contact between the PFCs and the oocyte. As already discussed in Chapter 3, there is growing evidence suggesting the existence of crosstalk between cell-ECM and cell-cell adhesion (Mui1

et al., 2016). On the other hand, both cell-ECM and cell-cell adhesion depend on the interaction with the actin cytoskeleton (Bachir et al., 2017).

It remains to be determined if the contact between the PFCs and the oocyte is directly involved in polarization or if it only enables the transfer of the polarizing signal by keeping the cells close together.

The former mechanism acts in a four-cell stage *C. elegans* embryo, where anterior Pars are excluded from the membranes in contact with the neighboring cells (Nance and Priess, 2002). In this system, E-cadherin plays an active role in polarization by recruiting Rho GTPase activating protein PAC-1, which induces Par asymmetry (Anderson et al., 2008; Klompstra et al., 2015).

On the other hand, close contact between the PFCs and the oocyte might facilitate the transfer of the polarizing signal. In support of this mechanism, we show that ER membranes of the oocyte and the PFCs seem to be connected. In addition, previous studies showed increased endocytosis at the posterior of the oocyte and its role in the oocyte polarization (Tanaka and Nakamura, 2008; Vanzo et al., 2007; Jouette et al., 2019). This raises an exciting possibility that all follicle cells produce the signal, but only the ones where cell-cell contact is modified (i.e., PFCs) can deliver it. This might be the reason why the molecular nature of the signal has not been found in large-scale screens. Instead of focusing on small signaling molecules as potential candidates for the signal, more emphasis should be put on the characterization of adhesion molecules and molecules involved in intercellular trafficking. Interestingly, our ablation experiments show that the PFCs maintain the polarity with cell-size precision. Therefore, even if the cell-cell contact is only necessary to enable the transfer of the signal, the molecule that is transferred does not diffuse far away from the follicle cell that secrets it.

It is important to note that using null mutants to study the importance of contact between the oocyte and the PFCs is probably not the best

approach. The communication between the soma and the germline is crucial from the earliest phases of oogenesis (Merkle et al., 2020). Therefore, more acute or spatially-controlled ways of perturbing the genes or proteins possibly involved in establishing and maintaining contact will be needed. The use of *Drosophila melanogaster* as a model organism is especially advantageous in this case since the UAS/Gal-4 system provides a way to knock down the genes only in specific tissues. Therefore, it should be possible to knock-down genes of interest only in posterior follicle cells.

Interestingly, in both screening studies referenced above, the RNAi-induced knockdown of candidate genes showed the polarity phenotype. However, the CRISPR knockout did not reproduce these results. This could be due to either the off-targeting effects of interfering RNAs or genetic compensation (Rossi et al., 2015). The idea of genetic compensation could explain why the forward genetic screens keep failing to identify the polarizing signal. This reinforces the notion that acute ways of perturbing the genes or their products are the methods of choice to dissect the mechanism of PFCs to oocyte signaling. It also warns against relying solely on RNAi to study the effects of gene silencing, even if it is induced only in PFCs.

Fortunately, the availability of tools that enable the acute manipulation of proteins has been growing in the last decade. Optogenetics (Ryan et al., 2021), TEV protease system (Pauli et al., 2008), and the auxin-degron system (Nishimura et al., 2009) are just some of the techniques that have already been successfully used for acute protein degradation.

5.4. A novel view of Par antagonism in *Drosophila melanogaster* oocyte

The first downstream target of the polarizing signal is the establishment of Par polarity in the oocyte. At stage 9 of oogenesis, the localization of Par

proteins in the oocyte follows the rules established by the early studies in *C. elegans* zygote: Par-1 and Lgl localize to the posterior, while Bazooka, Par-6, and aPKC localize at the anterolateral cortex.

However, compared to the *C. elegans* zygote, which establishes the mutually exclusive Par domains within minutes after receiving the polarizing signal, the polarity of Par proteins in the oocyte is gradually established. While the first known signs of oocyte polarization in response to the PFCs signal - di-phosphorylation of myosin II (Doerflinger et al., 2022) and posterior enrichment of Par-1 (Doerflinger et al., 2006) - are visible already at stage 7, Bazooka is only excluded around 12 hours later during stage 9 (Doerflinger et al., 2010; Jouette et al., 2019).

A possible explanation of this observation is that a change in Bazooka, which occurs from stage 7 to stage 9, renders it susceptible to phosphorylation by Par-1. However, in Chapters 3 and 4, we show that Par-1 and Bazooka can colocalize even in later stages, which argues against this option.

Another possibility is that two different PFC signals, activated at different stages, regulate Par-1 and Bazooka localization in the oocyte. One is retaining Par-1 at the posterior, while the other excludes Bazooka. In support of this interpretation, we show that exclusion of Par-1 is faster than recruitment of aPKC, suggesting that exclusion of anterior Pars is insufficient to maintain Par-1 at the posterior. However, an important caveat of this analysis is that we are comparing the dynamics of an endogenously expressed aPKC (Chen et al., 2018) with that of overexpressed Par-1 (Huynh et al., 2001). Therefore, the analysis of endogenously tagged proteins is needed to confirm this observation. However, we also show that the patterns at which Bazooka is recruited and Par-1 removed from the posterior differ. While Bazooka is recruited in random patches, Par-1 is first excluded from the center of the cortex region that lost contact with PFCs, and extends towards the cortical

boundaries facing intact PFCs. This suggests that the recruitment of Bazooka and delocalizations of Par-1 following the ablation of PFCs occur by two distinct mechanisms.

Our observations might seem to contradict the current Par polarity model, according to which Bazooka recruits aPKC to exclude Par-1 (Doerflinger et al., 2010). However, it is important to note that we argue that the exclusion of aPKC from the posterior is insufficient to ensure the enrichment of Par-1. In contrast, previous work has shown the necessity of Bazooka (and to a less convincing extent aPKC) for Par-1 exclusion (Doerflinger et al., 2010).

Similarly, we show that Par-1 and Bazooka transiently colocalize at the posterior either following the ablation or in unperturbed stage 10B egg chambers. This is not in contradiction with previous evidence showing that Bazooka localizes all around the oocyte cortex in *par-1* mutants (Benton and St Johnston, 2003; Doerflinger et al., 2010). While previous work proved the necessity of Par-1 for the exclusion of Bazooka, our work shows the lack of sufficiency.

In sum, we argue that PFCs are necessary, in addition to anterior and posterior Par proteins, to maintain the polarity of the main-body axis in the oocyte. This argument could be further tested by ectopically recruiting Par-1 to the anterolateral cortex of the oocyte. To this end, either optogenetics (Guntas et al., 2015) or chemically induced recruitment to the membrane (Castellano and Chavrier, 2000) could give fresh insight. If our hypothesis is correct, ectopically localized Par-1 should not be sufficient to exclude Bazooka.

5.5. Bibliography

D. C. Anderson, J. S. Gill, R. M. Cinalli, and J. Nance. Polarization of the c. elegans embryo by rhogap-mediated exclusion of par-6 from cell contacts. *Science*, 320:1771–1774, 2008.

A. I. Bachir, A. R. Horwitz, W. J. Nelson, and J. M. Bianchini. Actin-based adhesion modules mediate cell interactions with the extracellular matrix and neighboring cells. *Cold Spring Harbor Perspectives in Biology*, 9: 1–19, 2017.

E. H. Barriga, K. Franze, G. Charras, and R. Mayor. Tissue stiffening coordinates morphogenesis by triggering collective cell migration in vivo. *Nature*, 554:523–527, 2018.

R. Benton and D. St Johnston. Drosophila par-1 and 14-3-3 inhibit bazooka/par-3 to establish complementary cortical domains in polarized cells. *Cell*, 115:691–704, 2003.

J. G. Carlson. Microdissection studies of the dividing neuroblast of the grasshopper, chortophaga viridifasciata (de geer). *Chromosoma*, 5:199–220, 1952.

F. Castellano and P. Chavrier. Inducible membrane recruitment of small gtp-binding proteins by rapamycin-based system in living cells. *Methods in Enzymology*, 325:285–295, 2000.

J. Chen, A.-C. Sayadian, N. Lowe, H. E. Lovegrove, and D. S. Johnston. An alternative mode of epithelial polarity in the drosophila midgut. *PLoS Biology*, 16:1–24, 2018.

Y. Chen and T. Schüpbach. The role of brinker in eggshell patterning. *Mechanisms of Development*, 123:395–406, 2006.

V. E. Deneke, A. Melbinger, M. Vergassola, and S. D. Talia. Waves of cdk1 activity in s phase synchronize the cell cycle in drosophila embryos article waves of cdk1 activity in s phase synchronize the cell cycle in drosophila embryos. *Developmental Cell*, 38:399–412, 2016.

H. Doerflinger, R. Benton, I. L. Torres, M. F. Zwart, and D. St Johnston. Drosophila anterior-posterior polarity requires actin-dependent par-1

recruitment to the oocyte posterior. *Current Biology*, 16:1090–1095, 2006.

H. Doerflinger, N. Vogt, I. L. Torres, V. Mirouse, I. Koch, C. Nüsslein-Volhard, and D. St Johnston. Bazooka is required for polarisation of the drosophila anterior-posterior axis. *Development*, 137:1765–1773, 2010.

H. Doerflinger, V. Zimyanin, and D. St Johnston. The drosophila anterior-posterior axis is polarized by asymmetric myosin activation. *Current Biology*, 32:374–385, 2022.

J. C. Gatlin, A. Matov, G. Danuser, T. J. Mitchison, and E. D. Salmon. Directly probing the mechanical properties of the spindle and its matrix. *Journal of Cell Biology*, 188:481–489, 2010.

A. González-Reyes and D. St Johnston. Role of oocyte position in establishment of anterior-posterior polarity in drosophila. *Science*, 266: 639–642, 1994.

A. González-Reyes, H. Elliott, and D. St Johnston. Polarization of both major body axes in drosophila by gurken-torpedo signalling. *Nature*, 375: 645–658, 1995.

G. Guntas, R. A. Halletta, S. P. Zimmerman, T. Williams, H. Yumerefendi, J. E. Bear, and B. Kuhlman. Engineering an improved light-induced dimer (ilid)for controlling the localization and activity ofsignaling proteins. *Proceedings of the National Academy of Sciences of the United States of America*, 112:112–117, 2015.

J.-R. Huynh, J. M. Shulman, R. Benton, and D. St Johnston. Par-1 is required for the maintenance of oocyte fate in drosophila. *Development*, 128:1201–1209, 2001.

J. Jouette, A. Guichet, and S. B. Claret. Dynein-mediated transport and

membrane trafficking control par3 polarised distribution. *eLife*, 8:1–28, 2019.

D. Klompstra, D. C. Anderson, J. Y. Yeh, Y. Zilberman, and J. Nance. An instructive role for c. elegans e-cadherin in translating cell contact cues into cortical polarity. *Nature Cell Biology*, 17:726–735, 2015.

D. E. Koser, A. J. Thompson, S. K. Foster, A. Dwivedy, E. K. Pillai, G. K. Sheridan, H. Svoboda, M. Viana, L. da F. Costa, J. Guck, C. E. Holt, and K. Franze. Mechanosensing is critical for axon growth in the developing brain. *Nature Neuroscience*, 19:1592–1598, 2016.

R. Lehmann and C. Nüsslein-Volhard. Abdominal segmentation, pole cell formation, and embryonic polarity require the localized activity of oskar, a maternal gene in drosophila. *Cell*, 47:141–152, 1986.

J.-L. Maître, H. Berthoumieux, S. F. G. Krens, G. Salbreux, F. Jülicher, E. Paluch, and C.-P. Heisenberg. Adhesion functions in cell sorting by mechanically coupling the cortices of adhering cells. *Science*, 338:253–256, 2012.

J.-L. Maître, R. Niwayama, H. Turlier, F. Nédélec, and T. Hiiragi. Pulsatile cell-autonomous contractility drives compaction in the mouse embryo. *Nature Cell Biology*, 17:849–855, 2015.

S. G. Martin, V. Leclerc, K. Smith-Litiere, and D. St Johnston. The identification of novel genes required for drosophila anteroposterior axis formation in a germline clone screen using gfp-staufen. *Development*, 130:4201–4215, 2003.

J. A. Merkle, J. Wittes, and T. Schüpbach. Signaling between somatic follicle cells and the germline patterns the egg and embryo of drosophila. *Current Topics in Developmental Biology*, 140:55–86, 2020.

J. M. Mitchison and M. M. Swann. The mechanical properties of the cell surface. i. the cell elastimeter. *Journal of Experimental Biology*, 31:443–460, 1954a.

J. M. Mitchison and M. M. Swann. The mechanical properties of the cell surface. ii. the unfertilized sea-urchin egg. *Journal of Experimental Biology*, 31:461–472, 1954b.

S. Moreira, J. A. Espina, J. E. Saraiva, and E. H. Barriga. A toolbox to study tissue mechanics in vivo and ex vivo. *Methods in Molecular Biology*, 2438:495–515, 2022.

K. L. Mui1, C. S. Chen, and R. K. Assoian. The mechanical regulation of integrin-cadherin crosstalk organizes cells, signaling and forces. *Journal of Cell Science*, 129:1093–1100, 2016.

J. Nance and J. R. Priess. Cell polarity and gastrulation in c. elegans. *Development*, 129:387–397, 2002.

F. S. Neuman-Silberberg and T. Schupbach. The drosophila dorsoventral patterning gene gurken produces a dorsally localized rna and encodes a tgfα-like protein. *Cell*, 75(1):165–174, 1993.

R. B. Nicklas and C. A. Koch. Chromosome micromanipulation. iii. spindle fiber tension and the reorientation of mal-oriented chromosomes. *The Journal of Cell Biology*, 43:40–50, 1969.

R. B. Nicklas and C. A. Staehly. Chromosome micromanipulation. i. the mechanics of chromosome attachment to the spindle. *Chromosoma*, 21: 1–16, 1967.

K. Nishimura, T. Fukagawa, H. Takisawa, T. Kakimoto, and M. Kanemaki. An auxin-based degron system for the rapid depletion of proteins in nonplant cells. *Nature Methods*, 6:917–922, 2009.

C. Nüsslein-Volhard and E. Wieschaus. Mutations affecting segment number and polarity in drosophila. *Nature*, 287:795–801, 1980.

C. Nüsslein-Volhard and E. Wieschaus. The heidelberg screen for pattern mutants of drosophila: A personal account. *Annual Review of Cell and Developmental Biology*, 32:1–46, 2016.

C. Nüsslein-Volhard, H. G. Frohnhöfer, and R. Lehmann. Determination of anteroposterior polarity in drosophila. *Science*, 238:1675–1681, 1987.

L.-M. Pai, G. Barcelo, and T. Schüpbach. D-cbl, a negative regulator of the egfr pathway, is required for dorsoventral patterning in drosophila oogenesis. *Cell*, 103:51–61, 2000.

A. Pauli, F. Althoff, R. A. Oliveira, S. Heidmann, O. Schuldiner, C. F. Lehner, B. J. Dickson, and K. Nasmyth. Cell-type-specific tev protease cleavage reveals cohesin functions in drosophila neurons. *Developmental Cell*, 14:239–251, 2008.

A. T. Plygawko. *Investigating the underlying mechanisms of axis formation in Drosophila melanogaster*. PhD thesis, University of Cambridge, 2020.

J. V. Price, R. J. Clifford, and T. Schüpbach. The maternal ventralizing locus torpedo is allelic to faint little ball, an embryonic lethal, and encodes the drosophila egf receptor homolog. *Cell*, 56:1085–1092, 1989.

A. Rossi, Z. Kontarakis, C. Gerri, H. Nolte, S. Hölper, M. Krüger, and D. Y. R. Stainier. Genetic compensation induced by deleterious mutations but not gene knockdowns. *Nature*, 524:230–233, 2015.

S. Roth, F. S. Neuman-Silberberg, G. Barcelo, and T. Schupbach. cornichon and the egf receptor signaling process are necessary for both anterior-posterior and dorsal-ventral pattern formation in drosophila. *Cell*, 81:967–978, 1995.

A. Ryan, J. Liu, and A. Deiters. Targeted protein degradation through fast optogenetic activation and its application to the control of cell signaling. *Journal of the American Chemical Society*, 143:9222–9229, 2021.

K. Sander. Pattern formation in longitudinal halves of leaf hopper eggs (homoptera) and some remarks on the definition of ”embryonic regulation”. *Wilhelm Roux Archiv für Entwicklungsmechanik der Organismen*, 167:336–352, 1971.

E. D. Schejter and B.-Z. Shilo. The drosophila egf receptor homolog (der) gene is allelic to faint little ball, a locus essential for embryonic development. *Cell*, 56:1093–1104, 1989.

G. Schubiger. Adult differentiation from partial drosophila embryos after egg ligation during stages of nuclear multiplication and cellular blastoderm. *Developmental Biology*, 50:476–488, 1976.

T. Schüpbach. Germ line and soma cooperate during oogenesis to establish the dorsoventral pattern of egg shell and embryo in drosophila melanogaster. *Cell*, 49:699–707, 1987.

T. Schüpbach. Genetic screens to analyze pattern formation of egg and embryo in drosophila: A personal history. *Annual Review of Genetics*, 53:1–18, 2019.

T. Schüpbach and E. Wieschaus. Germline autonomy of maternal-effect mutations altering the embryonic body pattern of drosophila. *Developmental Biology*, 113:443–448, 1986a.

T. Schüpbach and E. Wieschaus. Maternal-effect mutations altering the anterior-posterior pattern of the drosophila embryo. *Roux's Archives of Developmental Biology*, 195:302–317, 1986b.

Y. Shimamoto, Y. T. Maeda, S. Ishiwata, A. J. Libchaber, and T. M. Kapoor.

Insights into the micromechanical properties of the metaphase spindle. *Cell*, 145:1062–1074, 2011.

D. St Johnston. The art and design of genetic screens: Drosophila melanogaster. *Nature Reviews Genetics*, 3:176–188, 2002.

P. Suresh, A. F. Long, and S. Dumont. Microneedle manipulation of the mammalian spindle reveals specialized, short-lived reinforcement near chromosomes. *eLife*, 9:1–22, 2020.

J. Takagi, R. Sakamoto, G. Shiratsuchi, Y. T. Maeda, and Y. Shimamoto. Mechanically distinct microtubule arrays determine the length and force response of the meiotic spindle. *Developmental Cell*, 49:267–278, 2019.

T. Tanaka and A. Nakamura. The endocytic pathway acts downstream of oskar in drosophila germ plasm assembly. *Development*, 135:1107–1117, 2008.

N. Vanzo, A. Oprins, D. Xanthakis, A. Ephrussi, and C. Rabouille. Stimulation of endocytosis and actin dynamics by oskar polarizes the drosophila oocyte. *Developmental Cell*, 12:543–555, 2007.

J. Wittes and T. Schüpbach. A gene expression screen in drosophila melanogaster identifies novel jak/stat and egfr targets during oogenesis. *G3*, 9:47–60, 2019.

ITQB NOVA, Avenida da República, 2780-157 Oeiras, Portugal | Tel +351 214 469 100 | itqb.unl.pt